# GEOPHYSICAL MAPPING OF NEAR- SURFACE FEATURES ALONG IRUEKPEN - IFON HIGHWAY SOUTH-SOUTHERN, NIGERIA

**BY**

**Kesyton Oyamenda, OZEGIN**
**Matriculation Number: 124536**

**B. Sc (Hons) Applied Physics (Ekpoma), M.Sc. Physics (Ibadan)**

**A Dissertation in the Department of Physics Submitted to the Faculty of Sciences in partial fulfilment of the requirements for the Degree of**

**MASTER OF PHILOSOPHY**
**of the**
**UNIVERSITY OF IBADAN**

**APRIL, 2019**

## CERTIFICATION

This is to certify that this study was carried out by Ozegin K. Oyamenda under my supervision in the Department of physics, Faculty of Sciences, University of Ibadan, Ibadan, Nigeria.

---

Supervisor
Dr. A. A. Adetoyinbo
B. Sc., M. Sc., Ph.D. (Ibadan)
Department of Physics,
University of Ibadan, Ibadan, Nigeria.

## DEDICATION

This research work is dedicated to Almighty God for He has done it. I bless His Holy name.

**ACKNOWLEDGEMENT**

The success of this research work is largely attributable to the encouragement, unflagging support and guidance received from my supervisor Dr. A.A. Adetoyinbo. His friendly dispositions fostered the planning and execution of this research work. I remain highly indebted to you sir. I would like to express my profound gratitude to the authors of the books and published articles consulted during the thesis preparation especially Dr. P.A. Enikanselu of Department of Applied Geophysics, FUTA.

My profound gratitude to my Lovely spouse, Mrs. S. Ozegin and children for their understanding, tolerance and enormous supports for the family throughout the period of the research work. My sincere appreciation to other numerous contributors whose names could not be mention here.

Lastly, I thank the Almighty God for His guidance, protection and for assisting me with all that I needed for the successful completion of the research work.

**TABLE OF CONTENTS**


| | | |
|---|---|---|
| Title page | | i |
| Certification | | ii |
| Dedication | | iii |
| Acknowledgement | | iv |
| List of tables | | viii |
| List of figures | | ix |
| List of plates | | x |
| Abstract | | xi |
| **CHAPTER ONE: INTRODUCTION** | | |
| 1.1 | Background of the study | 1 |
| 1.2 | **S**cope of work | 2 |
| 1.3 | Aim and objectives | 3 |
| | 1.3.1 Aim | 3 |
| | 1.3.2 Objectives | 3 |
| 1.4 | Justification | 3 |
| 1.5 | Expected contributions to knowledge | 3 |
| **CHAPTER TWO: LITERATURE REVIEW** | | 5 |
| 2.1 | Introduction | 5 |
| 2.2 | Soil investigation for structural foundation design | 7 |
| | 2.2.1 Geophysical Investigation | 7 |
| | 2.2.2 Geotechnical Investigation | 7 |
| | 2.2.3 Geological investigation | 7 |
| 2.3 | Road failure classification | 7 |
| 2.4 | Highway structures | 14 |
| | 2.4.1 The embankment | 14 |
| | 2.4.2 The foundation beneath the embankment | 14 |
| | 2.4.3 The cutting | 14 |
| | 2.4.4 The highway pavement | 15 |
| 2.5 | Very Low Frequency Method | 15 |
| 2.6 | Data Presentation | 17 |
| 2.7 | Limitations | 18 |

2.8 Electrical Resistivity(ER) method 18
2.9 Generalized apparent resistivity equation 18
2.10 Vertical Electrode Sounding (VES) 20
2.11 Dar Zarrouk (D-Z) parameters 20
2.12 Electrical Resistivity Tomography 21
2.13 Field operation problems 22
2.13.1 Electrode Contact Resistance 22
2.13.2 Lateral inhomogeneity 22
2.13.3 Dip Effect 22
2.13.4 Leaking Cables 23
2.14 Electrical Resistivity Data Interpretation 23
2.14.1 Horizontal Electrical profiling (HEP) 23
2.14.2 Vertical Electrical Sounding (VES) 23
2.14.2.1 Empirical/semi-empirical technique 24
2.14.2.2 Analytic method 25
2.15 Model curve generation in resistivity 26
2.15.1 Hummel's Image Theory 26
2.15.2 Kernel Function Method 28
2.15.3 Linear Filter Theory 28
2.16 Ambiguity in VES Interpretation 29
2.61.1 Suppression 29
2.16.2 Equivalence 29
2.16.3 Dip Effect 29
2.17 Factors that Influence Resistivity 29
2.17.1 Degree of Mineralization 29
2.17.2 Temperature 30
2.17.3 Rock Texture 30
2.17.4 Porosity 30
2.17.5 Fluid salinity 30
2.17.6 Geologic processes 30
2.17.7 Permeability 30
2.18 Geographic Setting, Location, Access and Human Settlements 31
2.19 Topography, Climate and Vegetation 33
2.20 Local Geology 33

2.21 Specific Sites Studied 35

**CHAPTER THREE: MATERIALS AND METHODS OF STUDY**

3.1 Introduction 42

3.2 Geophysical Survey 42

3.2.1 Layout of the Site 42

3.4 Methods of Survey 43

3.3.1 Electromagnetic- Very Low Frequency (VLF) 43

3.3.2 Vertical Electrical Sounding (VES) 46

3.3.3 Electrical Resistivity Tomography (ERT) 48

**CHAPTER FOUR: RESULTS AND DISCUSSION**

4.1 Introduction 50

4.2 Data Interpretation 50

4.2.1 Qualitative Approach 50

4.2.2 Quantitative Approach 56

**CHAPTER FIVE: SUMMARY, CONCLUSION AND RECOMMENDATION(S)**

5.1 Summary 69

5.2 Conclusion and Recommendation 69

**REFERENCES** 71

**APPENDIX I:** Results of the VES curves at each of the Studied Locations 74

**APPENDIX II:** Electrical Resistivity VES Data 77

## LIST OF TABLES

Table 2.1: Effects of Geological Processes of the Resistivity of Rocks 30
Table 4.1a: VES interpretation Results from location 1 59
Table 4.1b: VES interpretation Results from location 2 60
Table 4.1c: VES interpretation Results from location 3 61
Table 4.4: Results from Dar Zarrouk parameters 63

## LIST OF FIGURES


Figure 2.1: Profile of the VLF-EM 17

Figure 2.2: Generalized electrode configuration. 18

Figure 2.3: The theory and application for the D-Z parameter in a geoelectrical column 21

Figure 2.4:Pseudo-section for combined H.P and VES 22

Figure 2.5: Lateral inhomogneities 22

Figure 2.6a**:** Moore's cumulative graph 24

Figure 2.6b: Apparent conductance graph 24

Figure 2.6c: Asymptotic graph 25

Figure 2.7: Partial curve matching 26

Figure 2.8: Positions of near image due to a source and sink 27

Figure 2.9: Location Base Map 31

Figure 3.1a: Field layout at location 1 at km 11 41

Figure 3.1b: Field layout at location 2 at km 14 41

Figure 3.1c Field layout at location 3 at km 24 42

Figure 3.3: Method of plotting Dipole- dipole data in a Pseudosection. 48

Figure 4.1a: VLF-EM Curves in locality 1. 50

Figure 4.1b: VLF-EM Curves in locality 2 52

Figure 4.1c: VLF-EM Curves in locality 3. 54

Figure 4.2a: Interpretation Model of Typical Class 1 type curves. 56

Figure 4.2b: Interpretation Model of Typical Class 2 type curve. 57

Figure 4.2c: Interpretation Model of Typical Class 3 type curves. 58

Figure 4.3a 2-D Modelling Double Dipole 1 65

Figure 4.3b 2-D Modelling Double Dipole 2 66

Figure 4.3c 2-D Modelling Double Dipole 3 67

## LIST OF PLATES

Plate 2.1: Alligator cracking. 9

Plate 2.2: Rutting at wheel path. 10

Plate 2.3: Potholes. 11

Plate 2.4: Ravelling 12

Plate 2.5: Block cracking 13

Plate 2.6: Geological Setting Showing beddings and Faults of the rock exposures 33

Plates 2.2a and 2.2b: Failed Section at Location 1 36

Plates 2.2c and 2.2d: Failed Section at Location 2 38

Plates 2.2e and 2.2f: Failed Section at Location 3 40

Plate 3.1:ABEM WADIinstrument 44

Plate 3.2:Field survey in progress using ABEMTerrameter (Resistivity Meter) 46

## ABSTRACT

The Iruekpen-Ifon road is of economic importance, linking several towns in Edo and Ondo States. However, the recurring failures of sections of the road had made it deplorable. There is dearth of information on the subsurface features that may be responsible for these failures. Hence, this study was designed to identify and characterise the subsurface features that may be responsible for the failures.

Three main sections of the 60 km Iruekpen-Ifon highway that have experienced recurring failures were identified. Very Low Frequency - Electromagnetic (VLF-EM) field data were taken in three traverses ($T_1$, $T_2$ and $T_3$) measuring 210 m, 600 m and 240 m at the sections. The VLF-EM data were processed and interpreted. Two electrical resistivity techniques; Vertical Electrical Sounding (VES) and 2-D Electrical Resistivity Tomography (ERT) were employed. In all, forty two (42) VES were carried out using Schlumberger configuration array with current electrode spacing varying from 1.00 to 100.00 m at locations 1, 2 and 3 having 7, 10 and 25 VES, respectively. The data were plotted on bi-logarithmic graph and were interpreted using partial curve matching with the aid of master curves. The outcome of these served as input for numerical iteration using appropriate software. The derived geoelectric parameters were used to generate the Dar Zarrouk second order parameters for the co-efficient of anisotropy ($\lambda$). A 2-D ERT using dipole-dipole electrode configuration with inter-station separation of 10 m and an expansion factor that varied from 1 to 5 was also carried out at the identified sections. The ERT data were processed and inverted to generate subsurface model beneath the sections.

The VLF-EM data presented positive anomalies which indicated presence of conductive subsurface features at 32.0 m, 160.0 m and 200. 0 m for $T_1$; 80.0 m, 175.0 m, 212.0 m, 245.0 m, 380.0 m, 420.0 m, 500.0 m and 550.0 m for $T_2$; 42.0 m, 102.0 m, 143.0 m, 169.0 m and 200.0 m for $T_3$ from the reference stations. The VES present resistivity distribution for locations 1, 2 and 3, which ranged from $1.0 - 1229.0\ \Omega$m with probed depth of 24.97 m; $1.0 - 2207\ \Omega$m with probed depth of 49.10 m; and $0.1 - 3236.0\ \Omega$m with probed depth of 24.97 m, respectively. The values of $\lambda$ ranged from $1.03 - 2.19$, with the relatively higher values $(1.03 - 1.80)$ suggesting that the subsurface rocks in these areas are intensely fractured. The geoelectric section delineated: the top section (lateritic/clayey sand) with resistivity values varying from $60.0 - 350.0\ \Omega$m and $0.0 - 4.0$ m in thickness; clay with characteristic low resistivity values ($1.0 - 100.0\ \Omega$m) and thickness of $4.0 - 14.0$ m.

The cause of the recurring failures on Iruekpen – Ifon highway is as a result of clay formation, underlain by highly fractured subsurface rocks environment.



**Keywords:** Subsurface resistivity, Pavement failure, Dar Zarrouk Parameter, Fracture

**Word count:** 448.

# CHAPTER ONE: INTRODUCTION

## 1.1 BACKGROUND OF THE STUDY

A road is a way on land between two places, which characteristically has been paved or otherwise improved to allow travel by some conveyance, including a horse, cart, or motor vehicle. Road that is available for use by the public may be referred to as public road or highway. Hence highway is a public road, especially a major road connecting two or more destinations. Any interconnected set of highways can be variously referred to as a highway system, a highway network or a highway transportation system. Interaction between highway and human activities are so pervasive that highway is considered a vital element in social-economic, growth and development of any nation.

In developed countries around the world, roads are constructed with in -depth facts acquired from geophysical, geological, geochemical and geotechnical investigations of the construction site. This is because, information obtained from these aforementioned play significant role in the design, stability, economical construction and maintenance of the roads. Such investigations are aimed at providing details with respect to topography of the area, lithology of the underlying rocks, soils and including groundwater conditions.

However, the performance of the Nigerian road sector has not been satisfactory despite its enormous potential for growth and development. The pitiable and deplorable state of our road infrastructure has impacted negatively on attempts to alleviate poverty in the country. The Nigeria inland water ways and railways are inefficient and inadequate, hence the heavy reliance of the nation's economy on road transportation. Unfortunately, the problems of terrible road network in Nigeria have developed into a thwarting (upsetting) stigma. Consequently, trillions of Nigerian currency has been put into highway development in the country. As at 2008 N1.38 trillion have been sunk into road construction, rehabilitation and expansion (CBN, 2010). Unfortunately, all these efforts do not seem to be yielding the desired results. The provision of efficient roads and transportation facilities are fundamentally important to the development of the nation as well as the well-being of its inhabitants. Nigeria roads need urgent attention considering that an average of fifty (50) persons die every day by road accident as claimed by a recent survey (Adewumi, 2009).

The road network is estimated at about 194,000 kilometers, with the Federal Government being responsible for about 17%, state government 16% and local Government 67% (Federal Ministry of Works and Housing, 2003). However, these roads, have been plagued by a number of problems due to the presence of discontinuities such as

pot holes, cracks, pavement failures, collapsed bridges and rutting making it intractable, expensive and exhausting to transport farm produce from rural to urban centres The annual loss due to bad roads is valued at eighty billion naira, while additional vehicle operating cost resulting from bad roads is valued at N53.8 billion bringing the total loss per annum to N133.8 billion (Federal Ministry of Works and Housing, 2003). These figures do not take into account the man-hour losses in traffic due to bad roads, other emotional and physical trauma undergone by people using the roads and the consequent loss in productivity.

The incessant failures and near-zero efficiency rehabilitation works on the roads have become a thing of common concern. While highway problems have become a common phenomenon as they are permanently on the increase, the problem seems to be more precarious on cut sections of roadways within the Precambrian Basement Complex areas of the country.

The ever-busy Iruekpen-Ifon highway is an important road in the south-south and western part of Nigeria as it links several towns in Edo and Ondo states. It has greatly contributed to the socio-economic development of the country as a whole, as it helps in the movement of materials. Three major segments of the road have witnessed perennial failure. These failed portions have been the cause of several disastrous human and material losses. The pattern of failure which had taken place on this highway can be broadly attributed to any or a combination of geophysical, geological, geochemical, geotechnical, design, construction and usage problem. However, both the stable and failed sections of this road fall within the same sedimentary terrain and have the same design, construction and usage capacity.

## 1.2 SCOPE OF WORK

The research largely focus on the challenge of developing a more rational and well-organized way (in terms of modelling) to geophysically investigate the state of Iruekpen-Ifon highway by assessing the physical parameters of the existing pavement. Before the commencement of the detail pavement evaluation, the entire road length was visually assessed and it is attempted to identify the types of failures occurred on the road surface. Based on the extent of failure observed from the visual investigation, an attempt was made to select three sections. The length traversed in the three localities is 1050 m (measuring 210 m, 600 m and 240 m at each section respectively).These sections were categorised as section 1(11Km) where relatively low damage is observed, section 3 (24Km) where intermediate damage is observed and section 2 (14Km) where extreme damage is observed.

## 1.3 AIM AND OBJECTIVES

### 1.3.1 AIM

The aim of the research is to use surface geophysics to investigate the heterogeneous near-surface materials responsible for highway failures along Iruekpen-Ifon road.

### 1.3.2OBJECTIVES

(i) To evaluate the longitudinal conductance and transverse resistance in the study area.

(ii) To determine and characterize the anisotropic properties of fractures in the failed portion.

(iii) To derive geoelectric parameters in terms of electrical resistivities and thickness that will aid in further identification of the depth to bedrock.

(iv) To establish the near surface features their engineering properties and implications.

(v) Delineation and identification of weak - zones and clay enriched water absorbing zones.

## 1.4 JUSTIFICATION

The pattern of failure which had taken place on this highway (Iruekpen-Ifon road) can be largely ascribed to one or a combination of geological, geotechnical incompetence of the soil carrying the sub-structure, design, inadequate pre-construction survey and usage problem. Taking cognisance of the disturbing effects of highway predicaments in recent years, it has become essential to experimentally investigate the major road (Iruekpen-Ifon) linking several towns in Edo and Ondo States.

## 1.5 EXPECTED CONTRIBUTIONS TO KNOWLEDGE

The success of the stated objectives would further assist to;

i. provide information on the likely cause(s) of the continuous failure of sections of the investigated highway.

ii. serve as a valuable guide to road engineers on their understanding of the causes of road failure and relevant information needed for rehabilitation or reconstruction.

iii. create scientific awareness on how optimally and effectively geophysical methods can be used to study the causes of road failure.

iv. serve as a veritable source of reference material for future researches using these techniques.

v. the existing information on the sub-surface geologic system in the area and deduce possible geologic materials which engender road failure and the depth at which they occur across the area.

# CHAPTER TWO: LITERATURE REVIEW

## 2.1 INTRODUCTION

According to Attewel and Farmer (1976), there are two main types of site investigation each conditioned by the type structure to be erected and may either be: (a) Foundation – simply compact – investigation or (b) Linear – extended – investigation. In the foundation investigation in which buildings, dams, bridges or docks are the structures, they exert large pressure on relatively confined areas; making the needed investigation give accurate and detailed picture of strata variation with depth to a stable load-bearing structure. In the linear investigation, involving highways, railways and tunnels, in which they exert smaller pressure over extensive areas, the strata sequence and groundwater levels need to be identified in order to avoid weak zones and prevent road problems.

Field observations and laboratory experiments carried out by Olorunfemi and Mesida (1987), opined that usage or design are not principally responsible for road failure. However influence of geology and geomorphology in the design and construction phases may not have been sufficiently considered or the problems could also be as a result of scarce information of the distinctiveness and behaviour of remaining soils with which our roads are constructed. The geological factors in road failures are in-situ and encompass the nature of soils and the near-surface geologic structures such as cavities, sink holes, fractures, faults, shear zones, fissues among others.

Olukoga (1990) studied the compaction of laterite soils around Osu, along the Ile-Ijesa road. The failure of the section studied of road was attributed to low specific gravity, Califonia Bearing Ratio (CBR) and high water absorption limit of the soil.

Jegede (2000) worked on a section of the F209 Highway pavement failures which manifested as potholes in Ikole-Ekiti area of southwestern Nigeria. It was concluded from geotechnical perspective, that the poor soil physical properties such as consistency limits, optimum moisture content and Califonia Bearing Ratio (CBR) have combined with lack of drainage channels to accelerate failure of pavement of the locality.

Akintorinwa *et al.,* (2010) from Geophysical Investigation of Pavement Failure inferred that the presence of undetected linear features, such as fractures and rock boundaries have been identified as the cause of pavement failure in the study area.

Adiat *et al.,* (2009) estimated the Relevance of Geophysics in Road Failures Investigation in a typical Basement Complex of Akure, South western Nigeria. Electrical resistivity and electromagnetic methods were used in evaluating the subsurface integrity of a 3 km stretch of road from Igbara-Oke to Ibuji in south western Nigeria. The results shown that road

pavement is founded on an incompetent (weathered) layer which account for the incessant failure being observed along the road.

Sellers *et al.,* (2010) worked on Electrical Resistivity as a tool to identify areas of progressive failure within UK infrastructure embankments. The results gathered from the field work show variation in temperature measured at 0.5 m below ground level is 6.5 $^{o}$C (9.7-16.2 $^{o}$C) between May and September. The temperature range at 0.5 m on the northern flank is 8.5 – 15.1 $^{o}$C between May and September which is approximately 1$^{o}$C lower than the southern flank. The values of resistivity identified vary from 10 to 542 Ωm. it implies from the study that winds coming from the north are generally colder than winds from other directions and the southern flank is protected from these cooling winds.

Fatoba *et al.,* (2013) worked on structural failure investigation using electrical resistivity (Schlumberger configuration) method, a case study of Amafor-Ihuokpala, Enugu South eastern Nigeria. The result shows the electrical resistivity survey for the structural failure investigation in the area indicates occurrence of two major geologic units made of clay/sandy clay and clay-shale formation from the ground surface to about 40 m depth.

Ibitomi *et al.,* (2014) worked on Geophysical Investigation of Pavement Failure on a portion of Okene-Lokoja Highway, North central Nigeria. The investigation involves the Very Low Frequency Electromagnetic (VLF-EM) and Electrical Resistivity methods. Clay, partly fractured bedrock and linear geological structures have been identified as the cause of pavement failure in the study area.

Falowo and Akintorinwa (2015) investigated the geophysical features of pavement failures along Akure-Ijare road, south western Nigeria. The investigation involves the Very Low Frequency Electromagnetic (VLF-EM) and Electrical Resistivity methods. From the results of the investigation, the causes of road failures in the studied roadway are heterogeneity and clayey nature of the subgrade material, lack of proper drainage at the road embankment and poor construction material.

## 2.2 SOIL INVESTIGATION FOR STRUCTURAL FOUNDATION DESIGN

The aim of soil investigation is to present a general portrayal of subsurface area on the desired scale and its thickness distribution. The drainage pattern and the topography of such area are also considered. Basically, there are three types of soil investigations, viz; Geophysical, Geotechnical and geological investigations.

### 2.2.1 Geophysical Investigation

Almost all engineering structures require the support of the ground. Thus, geophysics is of use in engineering practices in the following way: identify the sub-surface lithologies, resolve of depth to and nature of rock layer, delineation of geologic structures such as faults and joints, determination of soil strength in qualitative terms. It should be emphasized that massive engineering structures require a competent, load bearing and broad base support. However, geophysical investigations are limited bearing in mind the following: do not give bearing capacity, cannot predict the pattern of failure and do not determine the amount of settlement.

### 2.2.2 Geotechnical Investigation

The scope of geotechnical investigation in an engineering construction site is to know the following: specific gravity of solid particles, bulk density of the soil, mechanism of compaction and consolidation, distribution of the particles sizes etc. However, it is limited by the following: may not be accurate due to handling of the soil samples, do not determine the thickness of the weathered layer in areas of thick overburden, sampling may not be quantitative enough and boulder may be mistaken for bedrock.

### 2.2.3 **G**eological **I**nvestigation

The scope of geological investigation in an engineering construction site is to know the following: dip and strike directions, bearing capacity, identification of soil type and visibility study of possible outcrops. However geological investigations are limited by the following, viz; boulders may be mistaken for outcrop, cannot predict pattern of failure and cannot identify sub-surface lithologies.

## 2.3 ROAD FAILURE CLASSIFICATION

It is important to note that road failure is a foreseeable end result of man's actions and an expected observable fact as well, therefore failed portions can be categorised into different patterns depending on the failures observe. The following section provides

necessary information on the commonest types of pavement failures and their plausible cause.

(i) Alligator cracking

This can be seen as regular breaks appearing in chain of diminutive polygons akin to an alligator's skin (Plate 2.1). This could result from the weakness of repetitive heavy truck loads or ageing in combination with progressive loss of roadway thickness. It is possible with or without surface deformation.

(ii) Rutting

A rut is a long relatively deep distortion at wheel tracks mostly linked with thrusting the length of the highway (Plate 2.2). This is usually caused by intense loads sourced by deprived construction procedures, saturation, or asphalt mixtures of insufficient vigor.

(iii) Chuck holes (Potholes**)**

Chuck holes are holes of unevenly formed with diverse sizes. More often than result from wear or destruction of the wearing course, at times from the existence of foreign bodies in the surfacing (Plate 2.3).

(iv) Ravelling

This is as a result of gradual loss of roadway material. The likely cause may perhaps be disconnection of bituminous film from cohesive during stripping caused by dearth of bonding or ageing of surface due to differences in climatic and usage (Plate 2.4). Ravelling can also take place owing to the unpredictable distortion of the lower roadway layers.

(v)Shear failures (Block cracking)

This is block cracking leading to chipping of pavement surfacing and/or upheaval outside the tyre cracks with associated cracking. This could result from deficiency in cohesion and internal friction in pavement base structure due to ageing and fatigue (Plate 2.5).

Plate 2.1: Alligator cracking.

Plate 2.2: Rut.

Plate 2.3: Potholes

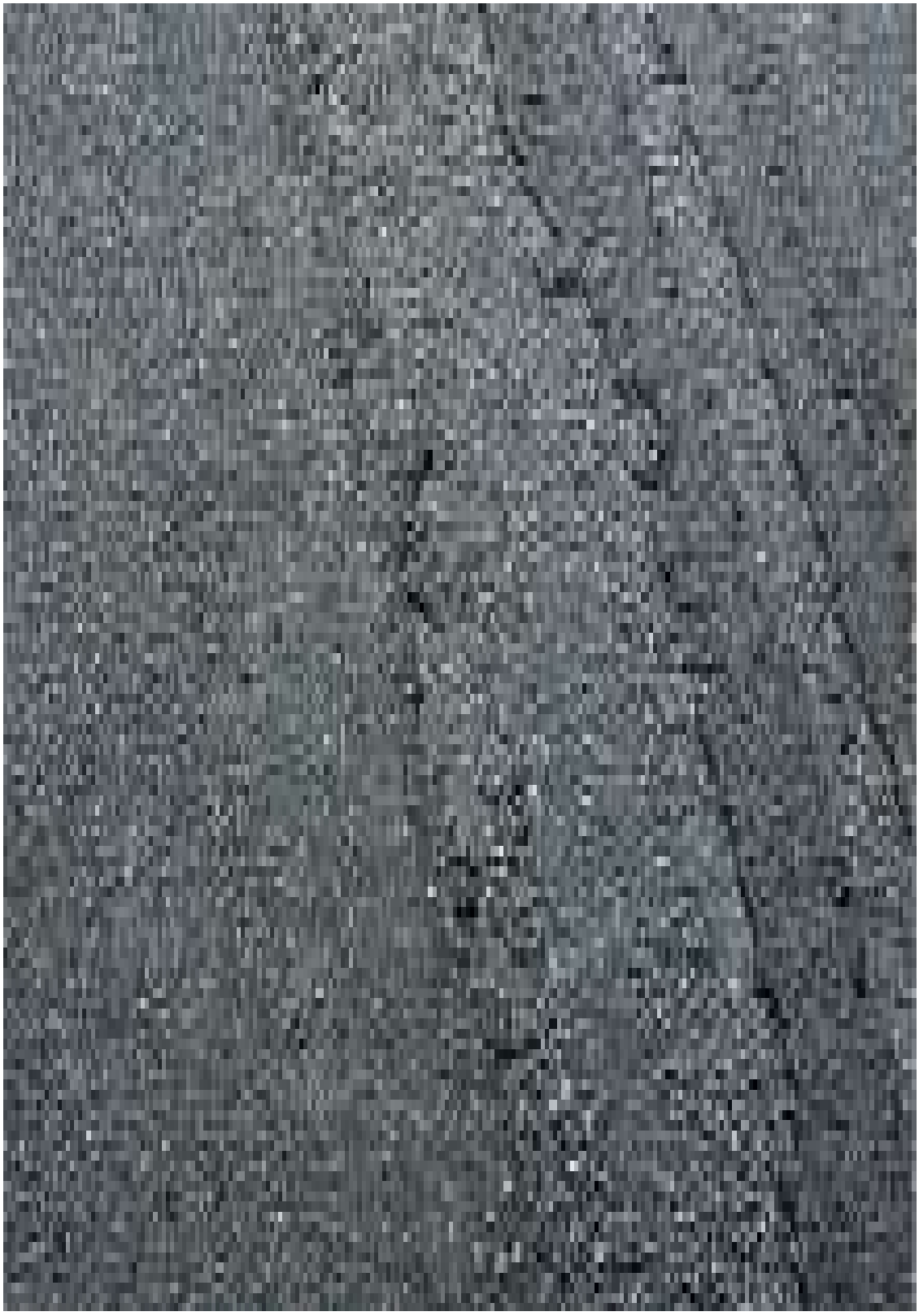

Plate 2.4: Ravelling

Plate 2.5: Block cracking

## 2.4 HIGHWAY STRUCTURES

The main structural elements involved in highway construction are as follows viz;

i. the embankment
ii. the foundation beneath the embankment
iii. the cutting
iv. the highway pavement.

**2.4.1 The embankment:** Highway embankment is the shoulder of the highway. When it is properly designed and constructed, it should possess stable slopes and should not settle to any extent. In its worst form, the slip of an embankment slope may result in the complete destruction of a length of highway. This is a rare occurrence. However, minor slip, in which the soil foundation of the highway moves outwards and downwards to a small extent, is quite common. These frequently occur where the highway has been constructed too close to the embankment, particularly as result of the widening of the highway.

**2.4.2 The foundation beneath the embankment:** The embankment requires a stable foundation in the same way as other structures. When the underlying soil consists of peat or soft clay, the weight of the embankment causes settlement due either to the consolidation of the foundation soil or, in extreme cases, the ultimate failure of the soil, in which a sudden settlement of the embankment is accompanied by the heaving of the ground at some distance from the toe of the embankment. Although it is not possible to prevent settlement occurring in the foundations of embankment, the period during which it occurs may be reduced sufficiently to enable movements to be completed before the final highway surfacing is constructed. This is achieved by the insertion of vertical sand drains in the foundation. These have the effect of reducing the path, and hence the time taken, for water to escape from the pores of the soil.

**2.4.3 The cutting:** Road cutting is a situation where a road is made to cut through hills. The structural consideration with a cutting is the stability of its slopes. The possibility of the occurrence of slip is greater with cutting than with embankments, since it is common with cuttings for water to seep towards the slopes under hydraulic gradients. Drainage measures are thus frequently required. Clays and other highly compressible soils are known to swell when an overburden pressure is removed, the effect being the reverse of the consolidation process. Highways constructed on clay cuttings where considerable weight of soil has been removed are liable to rise above their original level. Deleterious differential movement of a highway surface is particularly likely to occur at the junction of a clay cutting and fill, especially if the latter is poorly compacted.

**2.4.4 The highway pavement:** The pavement is the hard crust placed on the soil formation after the completion of the earthworks. It main functions are:-

i. To make available a even riding surface.

ii. To dispense the traffic loads over the soil formation sufficiently to prevent the soil from being over-stressed.

iii. To protect the soil formation from the undesirable effect of weather.

The characteristics of the pavement are thus reliant not only on the nature of the traffic but also on the properties of the soil on which the pavement is constructed. The main structural element of the highway pavement is the base and its function is to distribute the traffic loads. Broadly speaking, Highways are classified into two major groups, viz; flexible and rigid pavements.

## 2.5 VERY LOW FREQUENCY METHOD

The VLF method generally yields considerable EM anomalies, even over poor conductors such as sheared contacts, fracture zones, and faults. Hence, this method has been the most popular tool for the rapid mapping of near-surface geological structures (Parker, 1980; Phillips and Richards, 1975; Saydam, 1981; Sundararajan *et al.,* 2006). The VLF-EM technique is a passive method that uses radiation from ground-based military radio transmitters (used for navigation, of which there are about 42 worldwide) operating in the VLF band (15 - 30 kHz) as the primary EM field.

The VLF method's primary field source is the VLF radio signal broadcast by certain marine and air navigation systems. The signals are primarily used for marine and military navigations. The primary field - field of a vertical wire- are horizontal and theoretically tangential to circle concentric about the antenna mast. Transmitting station for VLF-EM prospecting is located in North America, Britain, England, Russia, Italy, France and Germany. Electromagnetic (EM) method is based on the principle of electromagnetic induction and makes use of coils to induce currents (primary current) flow in the ground and to detect the resultant (secondary) current. Electromagnetic Survey is usually done with two coils, one called the transmitter and the other the receiver. The secondary current is created by the anomalous subsurface medium which is usually a metallic conductor.

The propagation and attenuation of EM fields are best understood by the Maxwell's equations;

$$\nabla \times \mathrm{E} = -\frac{\partial \mathrm{B}}{\partial t} = \frac{-\mu \partial H}{\partial t} \qquad 2.1$$

$$\therefore \frac{-\partial B}{\partial t} = -\frac{\mu \partial H}{\partial t} \qquad 2.2$$

but

$$B = \mu H$$

$$\nabla \times H = J + \frac{\partial D}{\partial t} = J + \frac{\in \partial E}{\partial t} \qquad 2.3$$

$$D = \in E \qquad 2.4$$

where

E is Electric field Intensity (V/m)

B is the Magnetic Induction (Flux density) (Weber/$m^2$ or Tesla)

H is the Magnetic field Intensity (Ampere/m)

D is the Dielectric displacement current (Coloumb/m)

J is the Current Density (Ampere/$m^2$)

$\in$ is the Electric Permitivity = $8.854 \text{ X} 10^{-12}$ Farad/m

$\mu = 4\pi \text{X} 10^{-7}$ Henry/m

Defining an imaginary vector magnetic potential A in terms of B as;

$$\nabla \text{X} A = B \qquad 2.5$$

Combining 2.2 and 2.5 such that

$$E = \frac{-\partial A}{\partial t} \qquad 2.6$$

$$\frac{\partial}{\partial t}(\nabla XA) = \frac{-\partial B}{\partial t}$$

$$\nabla \text{X} \frac{-\partial A}{\partial t} = \frac{-\partial B}{\partial t}$$

But grad E

$$\nabla.E = 0$$

Hence $\nabla.A = 0$ 2.7

Taking the curl of 2.5

$$\nabla \text{X} \nabla \text{X} A = \nabla \text{X} B \qquad 2.8$$

$$\nabla(\nabla.\mathrm{A}) - \nabla.\nabla\ \mathrm{A} = \nabla \mathrm{XB}$$

$$-\nabla^2 \mathrm{A} = \nabla \mathrm{XB}$$

$$\nabla^2 \mathrm{A} = \mu(\nabla \mathrm{XH})$$

$$\nabla^2 \mathrm{A} = \mu\left(J + \frac{\in \partial E}{\partial t}\right)$$

$$\nabla^2 A = -\mu J - \mu \frac{\in \partial E}{\partial t} \qquad 2.9$$

but

$$\mathrm{E} \sim \mathrm{E}_o$$

$\nabla^2 A = -\mu J$ (similar to Poisson's Equation in gravity/magnetics) 2.10

$$A = \frac{\mu}{4\pi} \int_{vol} \frac{Idr}{r} \qquad 2.11$$

Where

$$r = \sqrt{x^2 + y^2 + z^2}$$

$$A = \mu / 4\pi \int_{vol} \frac{Idr}{r}$$

$$A = \frac{\mu}{4\pi} \oint \frac{Ids}{r}$$

## **2.6** DATA PRESENTATION

Field data are usually presented as profiles (Figure 2.1).

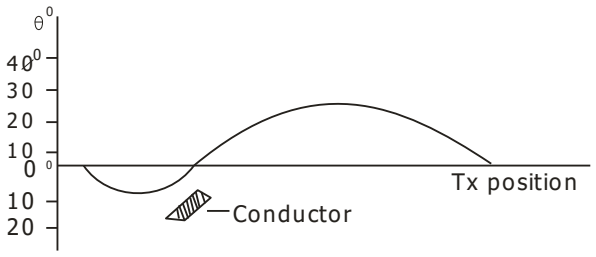


**Figure 2.1:** Profile of the VLF-EM method.

## 2.7 LIMITATIONS

1. Shallow depth of investigation due to high propagation frequency.
2. It is orientation dependent- The strike must be in the direction of the transmitter or at $45^0$ (The strike must be across the primary field). Poor coupling of conductor strike with available VLF transmitters may result in a low signal to noise ratio too small for an accurate measurement.
3. Suppression of signals from deeper targets of interest due to the presence of conductive overburdens which can by themselves generates significant VLF anomalies.
4. Susceptibility to Topographic variations.

## 2.8 ELECTRICAL RESISTIVITY(ER) METHOD

Resistivity methods utilise active sources of current which is passed into the earth through point electrodes called current electrodes and the potential measured at other electrodes called potential electrodes in the neighborhood of the current flow. This aids in the determination of an effective or apparent resistivity of the subsurface. The resistivity technique is at least theoretically superior to all other electrical methods because by using a controlled source of given dimensions, quantitative results are obtained. The mode of conduction is primarily electrolytic and minimally ionic (Telford et al., 1990).Resistivity evaluates the resistance of a given material to current flow and it is an intrinsic property of rocks. The principle underlying the resistivity method is embodied in Ohm's law, which states that the current density at a given point is proportional to the electric field intensity at that point. Thus, Ohm's law gives the relationship between current density J (amperes/m2) and electric field intensity E (volts/m) as: $J = \sigma E$ 2.12

Where σ is the conductivity of the medium and E is the gradient of a scalar potential U (volts)

## 2.9 GENERALIZED APPARENT RESISTIVITY EQUATION

Four electrodes are often utilized in electrical resistivity survey (Figure 2.2).

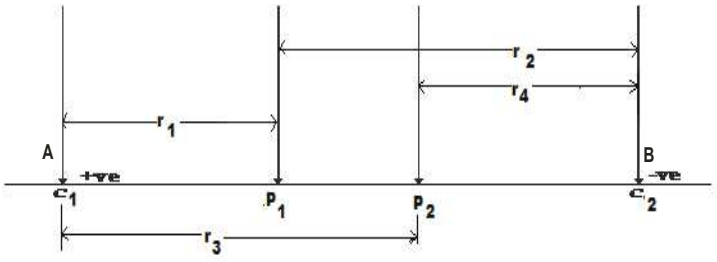


**Figure 2.2:** Generalised electrode configuration (Ozegin and Oseghale, 2012).

The potential $V_A$ at P is the sum of potential contribution $V_{11}$ and $V_{12}$ from the current source $C_1$ and the sink at $C_2$.

From figure 2.1, we get

The potential ($V_{11}$) at $P_1$ due to current at $C_1$ is given by;

$$V_{11}= \frac{I\rho}{2\pi r_1} \quad 2.13$$

The potential ($V_{12}$) at $P_1$ due to current at $C_2$ is given by;

$$V_{12} = \frac{I\rho}{2\pi r_2} \quad 2.14$$

the potential ($V_{21}$) at $P_2$ due to current at $C_1$ is given by;

$$V_{21} = \frac{I\rho}{2\pi r_3} \quad 2.15$$

the potential ($V_{22}$) at $P_2$ due to current at $C_2$ is given by

$$V_{22} = \frac{I\rho}{2\pi r_4} \quad 2.16$$

The sum of potential $V_A$ at $P_1$ due to current at $C_1$ and $C_2$ can be expressed as:

$$V_A = V_{11} + V_{12} = \frac{I\rho}{2\pi}\left(\frac{1}{r_1} - \frac{1}{r_2}\right) \quad 2.17$$

The sum of potential $V_B$ at $P_2$ due to $C_1$ and $C_2$ can be expressed as:

$$V_B = V_{21} + V_{22} = \frac{I\rho}{2\pi}\left(\frac{1}{r_3} - \frac{1}{r_4}\right) \quad 2.18$$

Thus, the potential difference $\Delta V$ between $P_1$ and $P_2$ is given by;

$$\Delta V = V_A - V_B$$

$$\Delta V = \frac{I\rho_1}{2\pi}\left(\frac{1}{r_1} - \frac{1}{r_2} - \frac{1}{r_3} + \frac{1}{r_4}\right) \quad 2.19$$

Hence the resistivity equation is expressed as;

$$\rho = \frac{2\pi\Delta V}{1}\left(\frac{1}{r_1} - \frac{1}{r_2} - \frac{1}{r_3} + \frac{1}{r_4}\right)^{-1} \quad 2.20a$$

or $$\rho = 2\pi R\left(\frac{1}{r_1} - \frac{1}{r_2} - \frac{1}{r_3} + \frac{1}{r_4}\right)^{-1} \quad 2.20b$$

## 2.10 VERTICAL ELECTRODE SOUNDING (VES)

The vertical electrical sounding measures vertical variations with respect to the centre of the array. It is employed when we are interested in identifying the layers that make up the Earth's crust.

It is necessary to execute this technique at several locations in an area, even when the main interest may be in lateral exploration, to establish reasonable electrode spacing for the lateral search. It is used in mining, environmental, engineering, hydrogeological, geothermal exploration among others. The array used include: Wenner, Schlumberger and sometimes dipole-dipole. The data are presented as depth sounding curves using the log-log paper: plotting $\rho_a$ against $^{AB}/2$ (Schlumberger) Or $^{AB}/3$ (Wenner).

## 2.11 DAR ZARROUK (D-Z) PARAMETERS

The concept of D-Z parameters was first introduced by (Mailet, 1974) to explain the problem of non-uniqueness in the interpretation of resistivity depth sounding curves.

In figure 3.3., T is the resistance normal to the face and S is the conductance parallel to the face for a unit cross section area, which plays an important role in resistivity soundings (Henriet, 1976). For a section consist of N fine letters with thickness $h_1$, $h_2$,...$h_n$ and resistivity $\rho_1,\rho_2,\ldots\rho_n$ for a block of unit square area and total thickness: $H = \sum_{i=1}^{N} h_i$

The values of S and T are set equal to those for an isotropic block with unit square area. Therefore, the longitudinal unit conductance (S) , will be :

$S = \sum_{i=1}^{N} \frac{h_i}{\rho_i}$ (Siemens) and the transverse unit resistance (T), will be: $T = \rho_i \; h_i$ (Ohm.m$^2$)

The longitudinal resistivity, $\rho_L$ =H/S and the transverse resistivity, $\rho_t$ = T/H

Generally, the co-efficient of the anisotropy is 1 and does not exceed 2 in most of the geological conditions (Zohdy *et al.,* 1974). Compact rock at shallow depth increases the coefficient of the anisotropy (Keller and Frischknecht, 1966). Hence, these areas can be associated with low porosity and permeability. The areas with 1.0 and less than 1.5 anisotropy values (high porosity and permeability) are considered as high groundwater potential zones (Rao *et al.,* 2003).The coefficient of anisotropy ($\lambda$) has been shown to have the same functional form as permeability anisotropy. Thus, a higher coefficient of anisotropy ($\lambda$ )implies higher - permeability anisotropy.

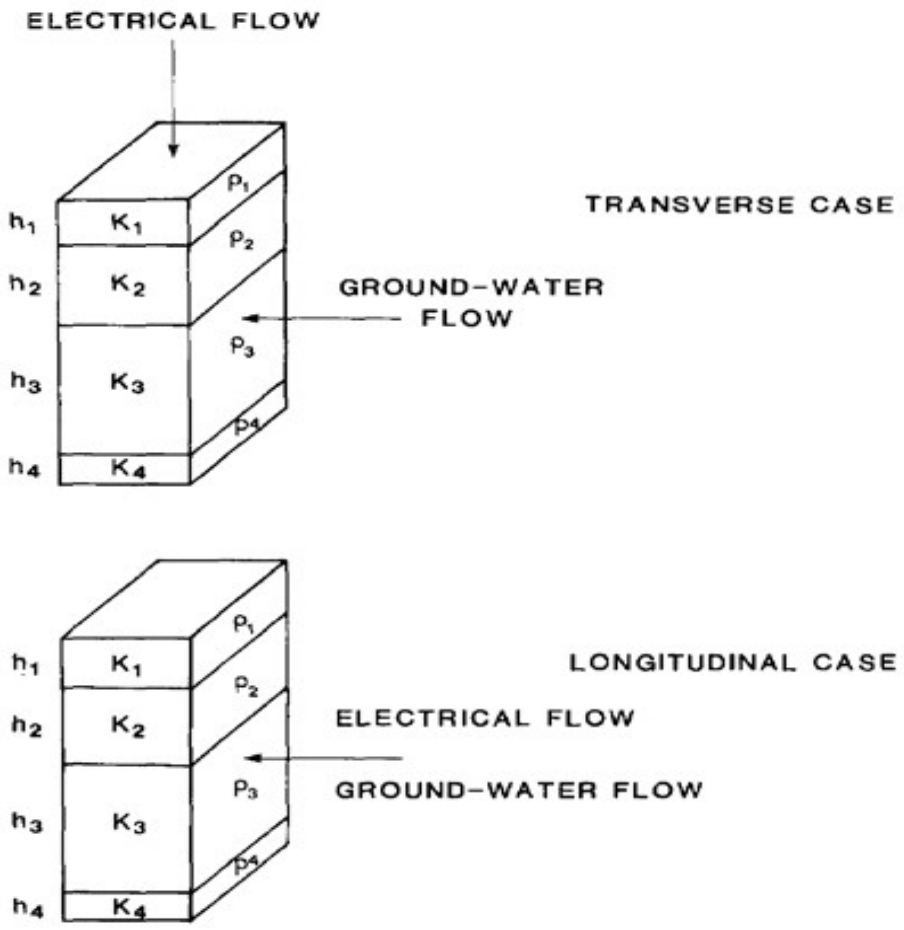


**Figure 2.3:** The theory and application for the D-Z parameter in a geoelectrical column.

## 2.12 ELECTRICAL RESISTIVITY TOMOGRAPHY

This technique enables us to measure variations in ground resistance along 2 directions- lateral and Vertical. Data acquisition is 2-Dimensional but in a vertical sense and can be inverted for the sake of accuracy. The array type employed is mainly the dipole-dipole configuration. Wenner and pole-dipole array can also be engaged. The station of measurement is the point of interception of two $45^0$ inclined lines (Figure 2.4). When the resistivity decreases towards the centre of the contour, we have sulphide ores and when it increases we have dolomite(Telford et al., 1990).This technique allows us to take a image of the near surface. The image could either be 2-D elongated or 3-D circular anomalies. The apparent depth of investigation is "0.250an"

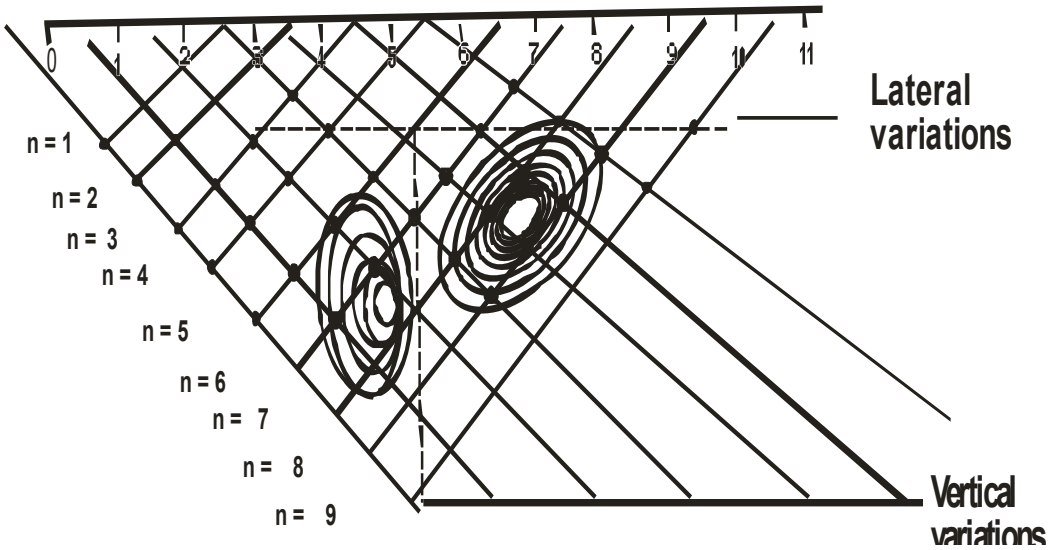


**Figure 2.4:** Pseudo-section for combined H.P and VES (Ozegin and Oseghale, 2012).

## 2.13 FIELD OPERATION PROBLEMS

### 2.13.1 **Electrode Contact Resistance**

This occurs due to dry or frozen ground. It can be solve by using multiple electrodes to reduce R and removing incoherent noise or by use of saline water solution around the electrodes.

### 2.13.2 **Lateral inhomogeneity**

Occurs from abnormal variation of resistivity called spike-shooting up or down above or below the normal signal (Figure 2.5). This can be corrected by mechanical smoothening.

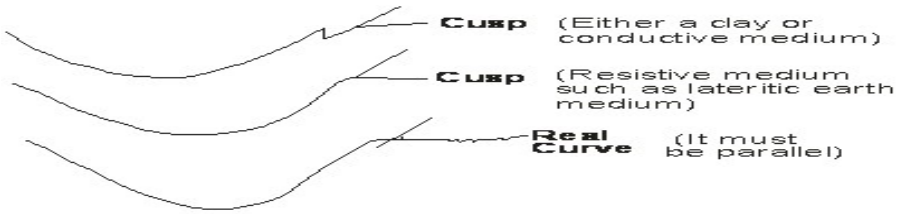


**Figure 2.5:** Lateral inhomogneities (Sharma, 1997).

### 2.13.3 **Dip Effect**

This occurs due to the presence of dipping layers or bed. When the dip of the bed is less than 10-25$^0$, there is no significant effect but when it is >25$^0$, the effect is significant. To determine the dip, $\rho_a$ should be measured in two horizontal directions.

2.13.4 **Leaking Cables**

Cultural and Geologic materials, such as buried cables, fences and topography are responsible for leaked cables.

## 2.14 ELECTRICAL RESISTIVITY DATA INTERPRETATION

### 2.14.1 Horizontal Electrical profiling (HEP)

Horizontal electrical profiling interpretation is primarily qualitative but can also be semi-quantitative and quantitative depending on the field result and survey objectives. Quantitative interpretation involves observation of profiles, maps and pseudo sections for anomaly patterns or signatures characteristic of the target of interest. Example such characteristics include;

(i) Observation of relatively low resistivities over water-bearing zones in typical basement formation or mineralization zone(s) within resistive host rock, saline water zones, military ordinances, impacted environment, water-saturated shear zones and faulted Basement Complex.

(ii) Observation of relatively high resistivities over dolerite dykes, basement intrusion, ridges, poorly conductive fluid saturated zones, concealed bunkers, sand and gravel deposits in clay among others.

The direction of elongation of the contour is usually the direction of the target and is obtained from maps.

Data obtained by dipole – dipole may be quantitatively interpreted as pseudo sections using models.

Two types of models can be employed:

i Forward Modeling - Comparison of field pseudosection with that of the theoretically generated model when they do not correlate, the data is iterated in order to have a maximum level of correlation.

ii Inverse modeling - Involves direct interpretation by imputing data obtained into software, to generate a pseudosection. It does not need an input or starting model but the raw data. It can be corrected when the geology of the area is known and assumes all data imputed are accurate. It can however be constrained to a particular accuracy.

### 2.14.2 VERTICAL ELECTRICAL SOUNDING (VES)

The VES interpretation can be qualitative and quantitative. It involves empirical/semi-empirical technique and analytic method.

2.14.2.1 EMPIRICAL/SEMI-EMPIRICAL TECHNIQUE

The empirical technique is an old technique and is adopted where there is no access to curves and computers but it is however obsolete. It can be employed when no high level of accuracy is desired.

The types include;

**(i) Moore's cumulative Technique**

It is applicable to Wenner array and is done by plotting

$\sum_{i=1}^{n} \rho_{ai}$ *Vs* $a$ (Figure 2.6a). n represents gathered data points.

a (m) = 1,2,3,4,5,8,12…

$\rho_a$ = 10, 15,35,26,35,32,50,78

i.e $\sum \rho_a$ = 10, 25, 60, 86, 111…

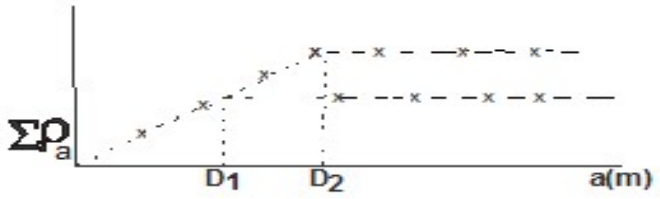


**Figure 2.6a:** Moore's cumulative graph (Parasnis, 1986)

Number of segments = Number of layers

Projection of interception of the segment into the x-axis gives the depth of the layer.

**Limitations**

**(a)** Does not give layer resistivity

**(b)** Not effective except when variation in values is constant and small with respect to layer thickness.

**(ii) Apparent conductance Technique.**

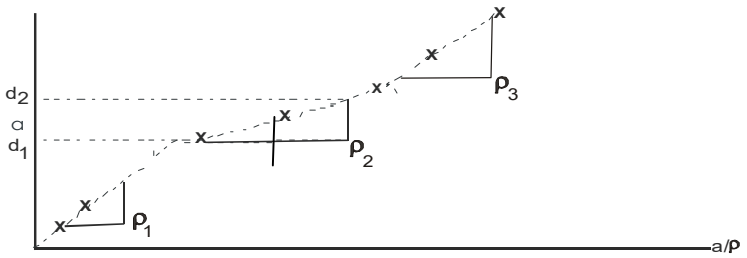


**Figure 2.6b:** Apparent conductance graph (Parasnis, 1986).

Taking the gradient (Figure 2.6b) gives the resistivities $\rho_{1,}\rho_{2,}\rho_{3}$ of the different layers. If the top soil layer is less than 1.5m thick, it will be difficult to map.

**(iii) Asymptotic Technique**

This method is specifically designed for 2-layer environment with the bottom layer resistivity infinite as illustrated in figure 2.6c.

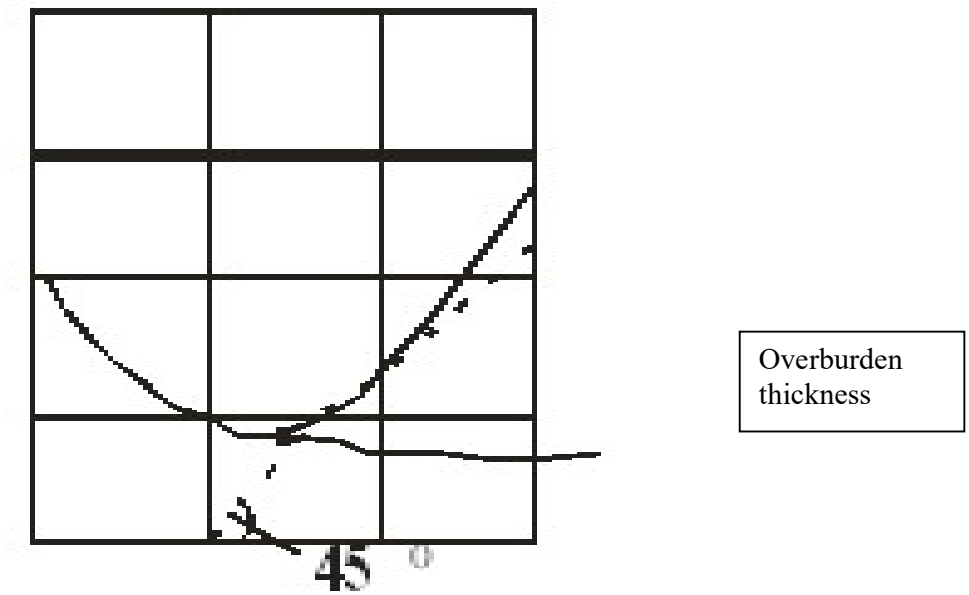


**Figure 2.6c:** Asymptotic graph.

2.14.2.2 ANALYTIC METHOD

This method involves partial curve matching complete curve Matching.

**i Partial Curve Matching**

This involves the use of two-layer curves and auxiliary curves. It involves matching them in segments. The asymptotic value of each segment is the resistivity of the segment (Figure 2.7).

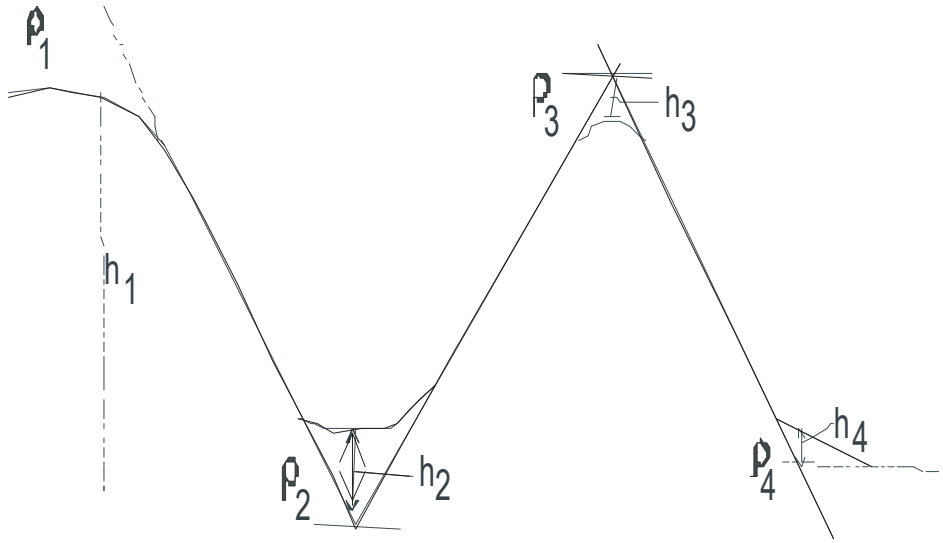


**Figure 2.7:** Partial curve matching (Ozegin and Oseghale, 2012).

**ii Complete curve Matching**

This has become obsolete, whatever is derived from it, is refined by forward modelling.

## 2.15 MODEL CURVE GENERATION IN RESISTIVITY

Three theories are available for model curve generation in Resistivity interpretation.

### 2.15.1 Hummel's Image Theory

Hummel (1929) and Lancaster-Jones (1930) applied the optical analogy to electrical currents to solve the two-layer boundary problem. The potential difference can be measured with the Wenner array.

From Figure 2.8 conditions are shown where a positive source and a negative sink at a finite distance apart represent the two current electrodes. A parallel plane surface is introduced at a distance below the ground so that a layer with resistivity $p_1$ is bounded by two semi-infinite media $p_o$ and $p_2$. The combined effect of the two boundaries in terms of reflection coefficients, k, produce an infinite series of images (known as Hummel image) so that the potential at any point on the surface is given by

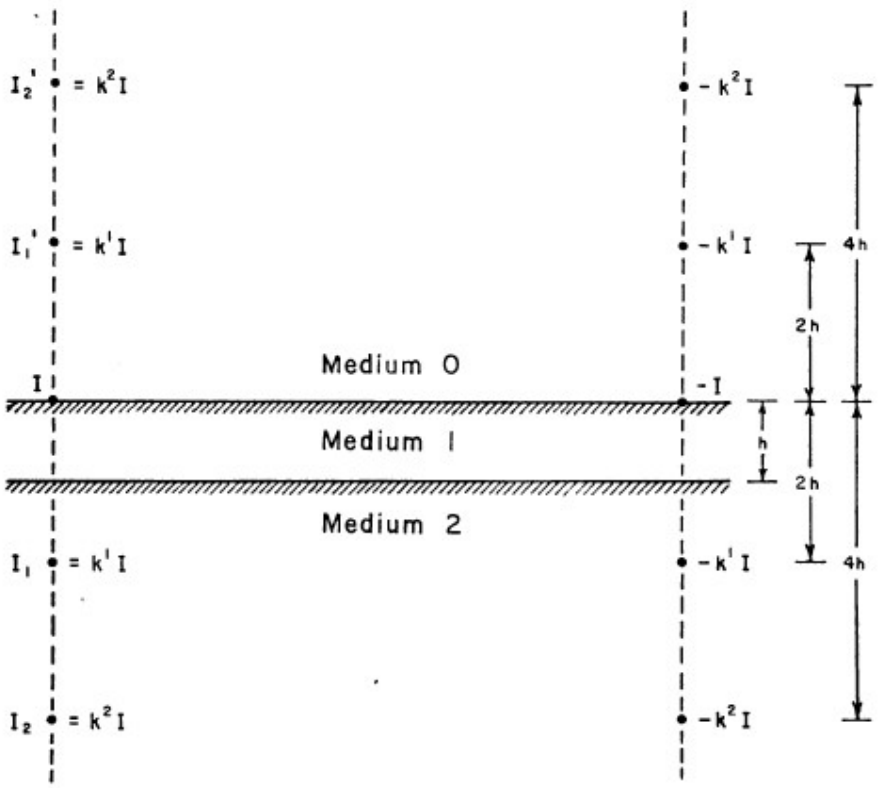


Figure 2.8: Positions of near image due to a source and sink

$$\Delta V = \frac{I\rho_1}{2\pi a}\left[1 + 4\sum_{n=1}^{\infty}\left(\frac{K^n}{\sqrt{1+\frac{4n^2h^2}{a^2}}} - \frac{K^n}{\sqrt{4+\frac{4n^2h^2}{a^2}}}\right)\right] \qquad 2.21$$

Then the apparent resistivity, $p_{wa}$, for a Wenner array can be expressed as

$$\rho_{wa} = \rho_1\left[1 + 4\sum_{n=1}^{\infty}\left(\frac{K^n}{\sqrt{1+\frac{4n^2h^2}{a^2}}} - \frac{K^n}{\sqrt{4+\frac{4n^2h^2}{a^2}}}\right)\right] \qquad 2.22$$

where a = equal electrode spacing, h = thickness of first layer .

2.15.2 Kernel Function Method

Computations of apparent resistivity using electrical resistivity image theory can be performed for multilayer structures, but the method is rather clumsy and tedious. However, using recurrence formulae (Kernel function) technique for calculations of the potential as well as the apparent resistivity can easily be executed. The general expression for the potential V at the surface over a series of horizontal layer is

$$\mathrm{V} = \frac{I\rho_1}{2\pi}\int_0^{\infty} K(\lambda)J_0(\lambda r)d\lambda \qquad 2.23$$

Where I is the strength of the current source, $\rho_1$ the resistivity of the first layer, $\lambda$ is a variable of integration, r the distance from the current source to the surface point where potential is measured. $J_0(\lambda r)$ the Bessel function of zero order whose behavior is known completely and $K(\lambda)$ is the 'kernel function' which is controlled by the resistivities and thicknesses of the layers. .

2.15.3 Linear Filter Theory

In present-day practice the calculations of the potential as well as the apparent resistivity are more easily executed using linear filtering technique. The linear filtering approach can

be effectively used to transform resistivity sounding data obtained with one type of electrode configuration into another Koefoed's (1979).

## 2.16 AMBIGUITY IN VES INTERPRETATION

### 2.61.1 Suppression

The suppression principle states that if a bed is very thin compared to those above and below, its effect on the sounding curve is insignificant unless its resistivity is extremely high or low.

### 2.16.2 Equivalence

Occurs in a three layer situation when $\rho_2$ is lower than $\rho_1$ or $\rho_2$ is greater than $\rho_1$ or $\rho_3$. It is typical of H- and K- type curve.

When $\rho_2 > \rho_1$ with different thickness for different layer models, the two curves will give the same curve provided the ratio of $h_2$ to $\rho_2$ is the same for both models. For longitudinal conductance,

$$(S) = h_2 / \rho_2 = h_2^I / \rho_2^I + h_2^{II} / \rho_2^{II} \qquad 2.24$$

and

Transverse Resistance

$$T = h_2 \rho_2 = h_2^I \rho^I{}_2 \quad (K\text{–type}). \qquad 2.25$$

To minimize the effect of equivalence and suppression, we need geological borehole information from logs.

### 2.16.3 Dip Effect

When the dip is $< 10^o$, the effect is minimal but when it is more than $10^o$; it may affect the interpretation result.

The double dipole configuration is more receptive toward dipping beds than the Schlumberger or Wenner array. To determine the dip, it is necessary to measure $\rho_a$ in two horizontal directions.

## 2.17 FACTORS THAT INFLUENCE RESISTIVITY

**2.17.1 Degree of Mineralization:** Resistivity decreases with increase in degree of mineralization because disseminated mineralization does not affect porosity. If the ore is

resistive, it will increase resistivity (e.g quartz), and if the ore is less resistive, the resistivity also decreases.

**2.17.2 Temperature:** The resistivity of fluids contained in rocks is influenced by temperature. The lower the temperature, the higher the resistivity. From Keller and Frishknecht, 1966:

$$\rho_t = \frac{\rho_{18}}{1+\alpha(t-18)} \qquad 2.26$$

where

$\rho_t$ = resistivity at temperature t

$\rho_{18}$ = reference resistivity at $18^0$c

$\alpha$ = temperature coefficient

t= temperature $0.25/^0$c

**2.17.3 Rock Texture**: A fine-grained rock has relatively low resistivity (e.g tuffs, volcanic ash, and clay). Coarse grained rock have high resistivity (e,g well sorted sandstones).

**2.17.4 Porosity:** The higher the porosity, the lower the resistivity and vice-versa because porous media retain a high amount of water due to it degree of compaction (e.g. clay minerals).

**2.17.5 Fluid salinity:** The higher the saturating fluid salinity (concentration), the higher the conductivity; the lower the resistivity and vice-versa (e.g. cyanide solution).

**2.17.6 Geologic processes:** They generally decrease resistivity of rocks with the exception of a few processes table 2.1.

Table 2.1: Effects of Geological Processes of the Resistivity of Rocks (Ward, 1990).

| **Geological Process** | **Effect on Electrical Resistivity** |
|---|---|
| Clay alteration | Decrease |
| Dissolution | Decrease |
| Faulting | Decrease |
| Jointing | Decrease |
| Salt-water intrusion | Decrease |
| Sharing | Decrease |
| Weathering | Decrease |
| Carbon precipitation | Increase |
| Induration | Increase |
| Recrystalisation | Increase |
| Silicification | Increase |
| Metamorphism | Increase or Decrease |

**2.17.7 Permeability:** Resistivity increases with permeability for fresh water contained clean sands.

## 2.18 GEOGRAPHIC SETTING, LOCATION, ACCESS AND HUMAN SETTLEMENTS.

The study area is bordered by Longitudes 5. 9262 and 5. 9884 $^{o}$E and Latitudes 6.8943 and 6.8209 $^{o}$N (Figure 2.9). It is also bounded by Ondo state to the West, Kogi State to the North and East, and to the South by Esan Central, Esan North-East, Esan South-East, Esan West and Uhumwode Local Government Area of Edo State respectively. It is also bounded by the River Niger to the East. The settlement pattern in the area is mainly the nucleated type and in few cases the linear settlement type with the towns, villages and hamlets closely separated and in most cases connected by poor roads. The major ethnic tribes in the area are Owan-speaking tribes and are in most cases mingled with other tribes which are a major feature of the traditional Nigerian setting.

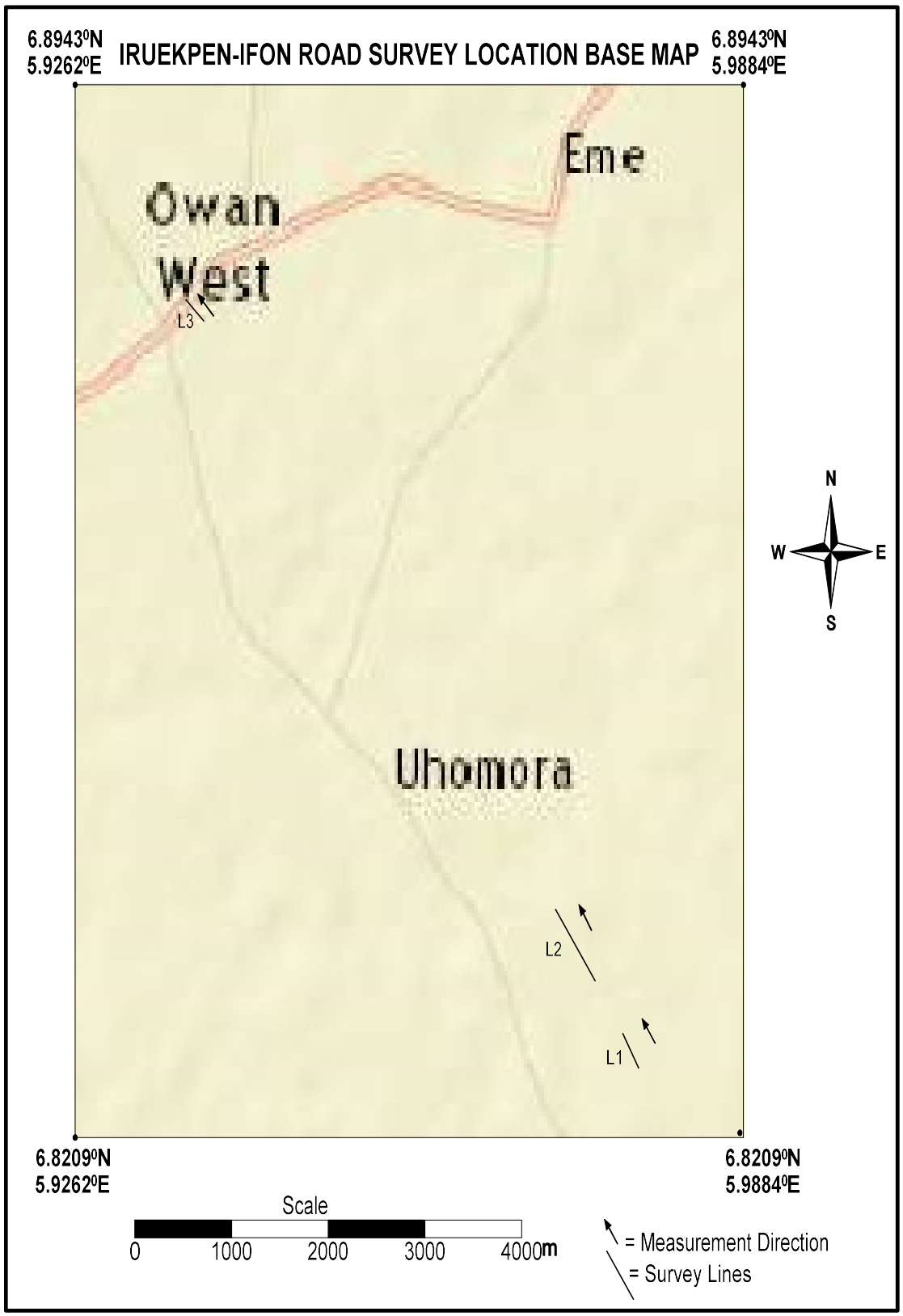


**Figure 2.9:** Location Base Map

## 2.19 TOPOGRAPHY, CLIMATE AND VEGETATION

The area is characterised by both steep and gently undulating terrains characterised by hills, plains. The elevation above sea level (EASL) across the area ranges between 160 and 376 m. The area is mainly drained by the River Niger located on the eastern part and other rivers serving as tributaries. They all form a network of dendritic drainage pattern and empty their waters into the Atlantic Ocean.

The area lies within the rainforest belt where the wet season occurs between April and October while the dry season between November and March. It also lies within the subequatorial climatic belt with a mean annual temperature range of $22^{O}C - 32^{O}C$ and an annual rainfall of over 1400 mm.

The vegetation type is the rainforest vegetation characterized by evergreen, broad-leaved trees, oil palm and rubber plantation to the southern parts and tall grass savannah with some trees to the northern parts. The crops found in the area are the cash crops (cocoa, oil palm and rubber), root crops (cassava and yams), cereals (maize and rice) and cane crops like sugar cane.

## 2.20 LOCAL GEOLOGY

The study area is underlain by Imo eusterine and marine shale. This is of grey-black shale ranked up into alternation of thin beds of fissile dirty-light shale and gypsum ranged 2 to 5cm. The section passes on into light yellow-brown sandy mudstone with lateral dissimilarity in facies from sandy mudstone to clay. The shale is by and large rigid at Uhonmora and the segment is of shale and intercalation of gypsum and shale in the direction of the top of the segment. On the other hand, the Ozalla segment of Imo Shale have no intercalation of gypsum bed amid shale instead it comprises mudstone, clay and shale (Plate 2.6). The two segments of Imo Shale in the environment show evidence of comparable distinctive attribute ferruginise nature contained by the sandy mudstone unit. This distinctive attribute in the environment increase the load transportation capability of the strata excepting for the region with facies discrepancy from ferruginised sandy mudstone to clay. The mudstone is well covered by means of imbedded clay clast.

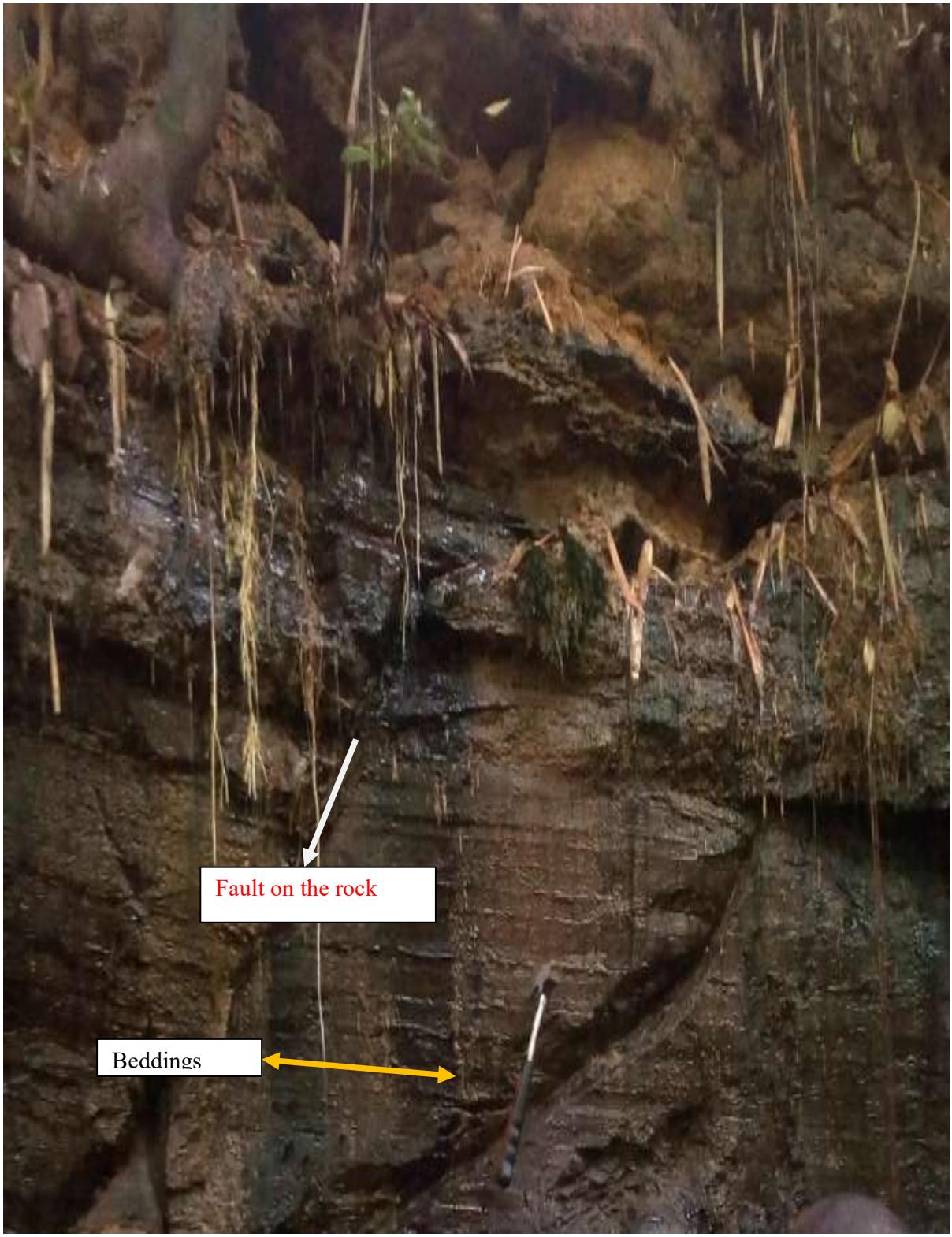


Plate 2.6: Geological Setting Showing beddings and Faults of the rock exposures.

## 2.21 SPECIFIC SITES STUDIED

A reconnaissance survey carried out along the Iruekpen/ Ifon highway in order to establish the failed portion. Three failed sections (plates 2.2a- 2.2f) were subsequently chosen with Iruekpen/Ozalla junction as the reference point (0.00 km).The length traversed in the three localities is 1050 m (measuring 210 m, 600 m and 240 m at each section respectively).

Plate 2.2a


Plates 2.2a and 2.2b: Failed Section at Location 1

Plate 2.2c


Plates 2.2c and 2.2d: Failed Section at Location 2

Plate 2.2e

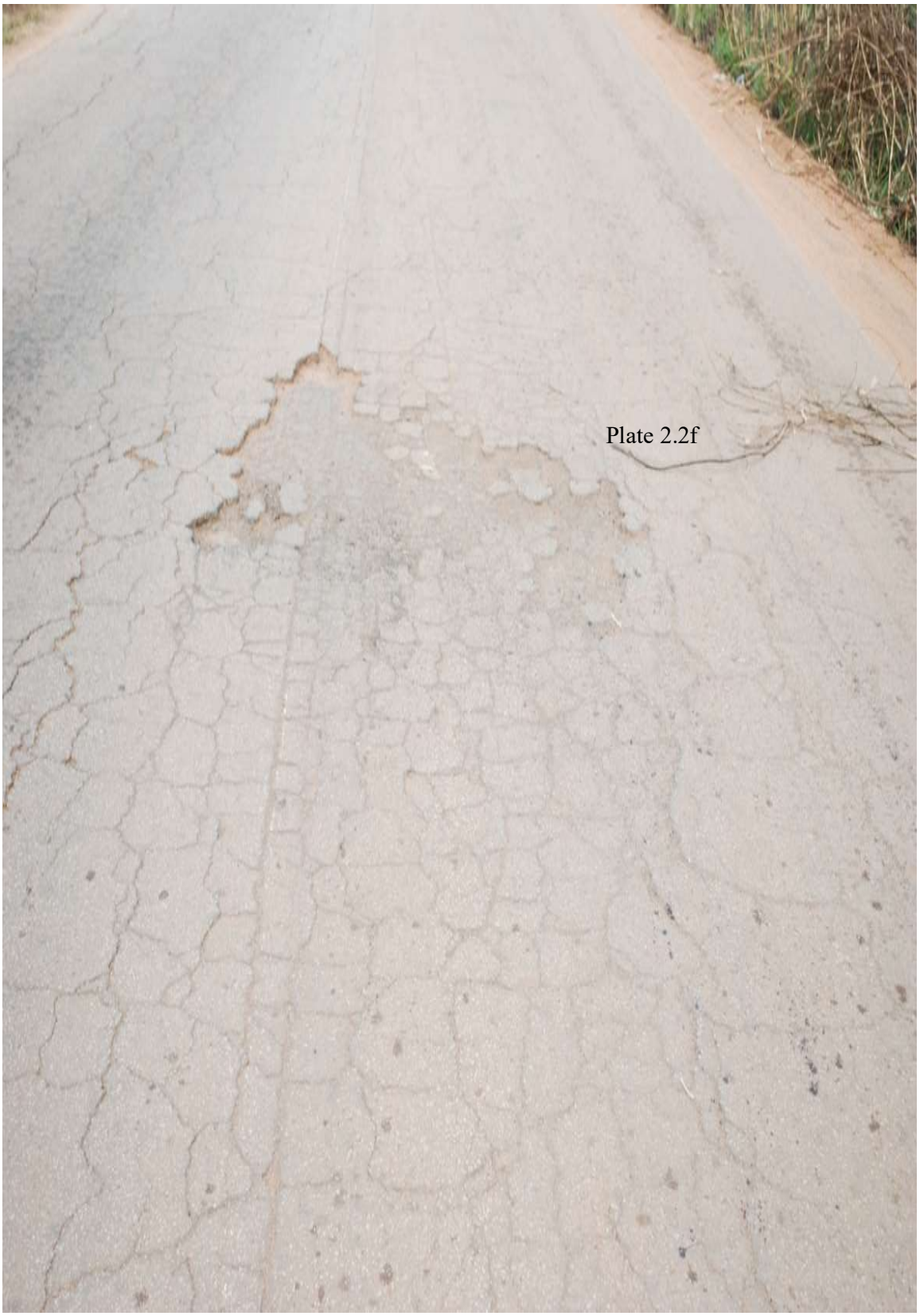


Plates 2.2e and 2.2f: Failed Section at Location 3

# CHAPTER THREE: MATERIALS AND METHODS OF STUDY

## 3.1 INTRODUCTION

The steps involved in the acquisition of geophysical data used in this research are discussed in this chapter. The methods of analysis of the data to generate the data sets required for the study are also outlined.

## 3.2 GEOPHYSICAL SURVEY

### 3.2.1 Layout of the site

One traverse was established in each of the localities taken as case study, parallel to the road pavement, which cut across the fairly stable and the failed segment of the localities (Figure 3.1). The direction of the traverses varies, depending on the orientation of the road. The length traversed in the three localities is 1050 m (measuring 210 m, 600 m and 240 m at each sections respectively).

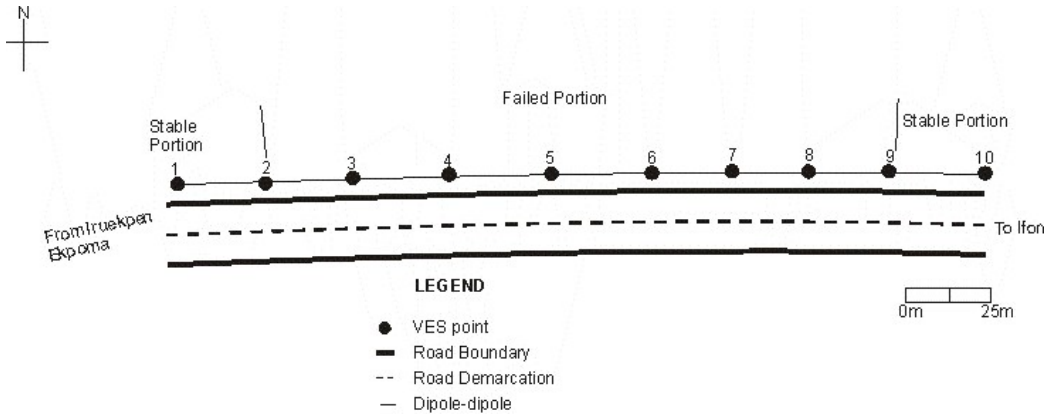


Figure 3.1a: Field layout at location 1 at km 11

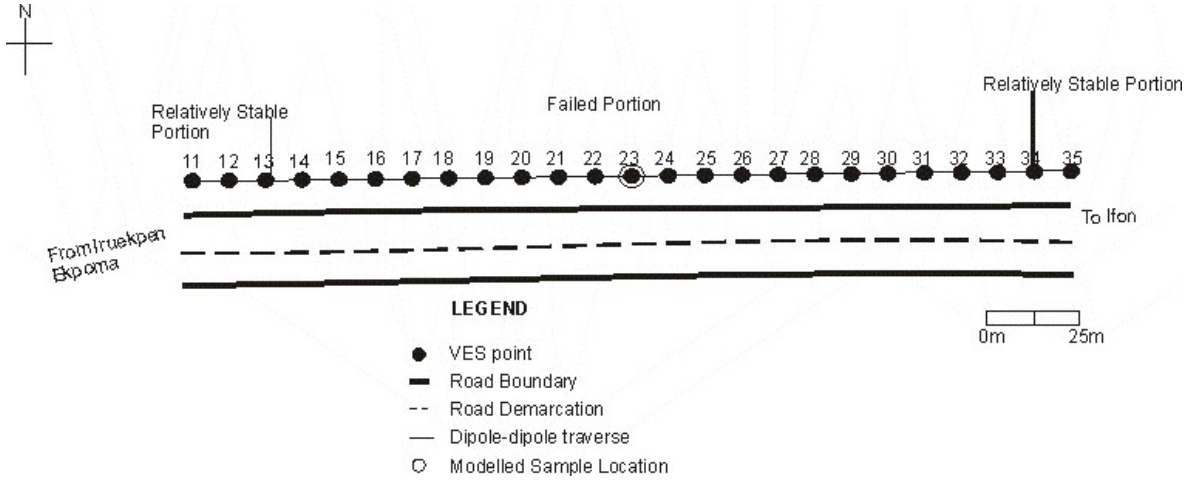


Figure 3.1b: Field layout at location 2 at km 14

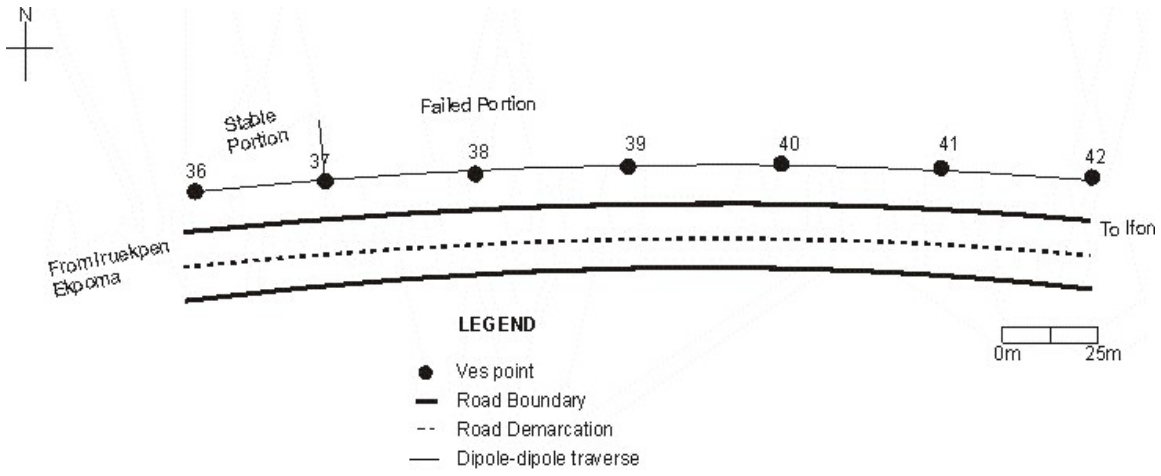


Figure 3.1c Field layout at location 3 at km 24

## 3.3 METHODS OF SURVEY

Two methods were adopted viz; Electromagnetic method- Very Low Frequency (VLF)and the electrical resistivity method (two field techniques used – VES using the Schlumberger configuration and 2-D electrical imaging using double dipole array).

### 3.3.1 ELECTROMAGNETIC- VERY LOW FREQUENCY (VLF)

Three traverses were carried out at locality 1, locality 2 and locality 3 with traverses which give a direct measure of ground conductivity measuring 210 m, 600 m and 240 m respectively at a mean separation of 10 m with signal strength of 13, frequency band 18.8 KHz. The investigation was done in the NE-SW orientation. Prospecting for these conductive zones was then carried out by systematically traversing the ground with the receiver unit alone, having the transmitter source signal at remote distance from the field.

The method is based on measurement of the secondary magnetic field induced in local conductors by primary electromagnetic fields generated by powerful military radio ABEM WADI transmitter in the very low frequency range. The ABEM WADI system is portable equipment mounted on a belt worn by the user as he transverses profiles at given intervals with the receiver and antenna held at right angles to each other while conductivity readings are taken(Plate 3.1a). It consists of the Hand – held controller unit, the Measuring unit with battery compartment and the Antenna unit. The hand-held controller unit contains a microcomputer, keyboard and screen where measurements are displayed and stored. The measuring unit contains the radio receiver with amplifier and other electronic circuitry from where information is sent to the in-built central processing unit and computerized printer.

The antenna is kept upright when the measurements are being taken for accuracy. ABEM WADI sends primary field waves into the subsurface which return with weak secondary magnetic fields that had been built around subsurface conductive geological structures which ultimately align in concentric lines around the ABEM WADI transmitting antenna. The WADI measures the field strength and phase displacement around geologic structure such as fault or shear zone in the bedrock. WADI instrument registered not only the filtered real part that is the part of the resulting field which is in phase with the primary field from the VLF transmitter, but also the imaginary part which is $90^{o}$ out of phase with the primary field. The WADI is sensitive to transmitters around the world and it automatically picks the most suitable. For induction to occur, the structure was aligned roughly towards the transmitter (Oluwafemi and Oladunjoye, 2013).


Plate 3.1:**ABEM WADI** instrument

### 3.3.2 VERTICAL ELECTRICAL SOUNDING (VES)

The VES technique was adopted because information on the variation of geophysical characteristics of the subsurface layers with depth was desired. The sounding stations were marked and pegged along the traverses in the location(s). The interval was chosen in view of the high degree of spatial resolution desired.

In the VES technique, vertical variations in the ground apparent resistivity are measured with respect to a fixed centre of array. The stepwise expansions of the electrode separations were undertaken parallel to the roadways at the road shoulder so as to avoid problems of high contact resistance that may arise when electrodes are driven into road pavement materials. Ten (10), twenty (25) and seven (7) sounding stations occupied at locations 1, 2, and 3 respectively. ABEM Resistivity Meter (plate 3.2) was used for resistivity data gathering. Highly sensitivity, easily carried, all-in-one resistivity instrument, which displays the internally computed resistance besides the display of the input current and the output voltage. The instrument was designed in such a way that it could measure these quantities over five cycles. This was done to make sure that the current was sufficiently commutated to avoid possible spurious signals from electrolytic polarization.

The current electrode spacing (AB/2) was varied from 1.00 to 100.00 m. The metal electrodes were driven into the ground with hammers to ensure good contact with the ground. The measurements were taken at all the stations with in-line arrangement of the electrodes with respect to the traverse lines and the apparent resistivity values were calculated.

Plate 3.2: Field survey in progress using ABEMTerrameter (Resistivity Meter)

### 3.3.3 ELECTRICAL RESISTIVITY TOMOGRAPHY (ERT)

The technique was adopted because information on the 2-D variation of geoelectrical characteristics of the subsurface layer was desired. The major limitation of the resistivity sounding method is that it does not take into account horizontal changes in the subsurface resistivity. A more accurate model of the subsurface is a two-dimensional (2-D) model where the resistivity changes simultaneously in the vertical direction, as well as in the horizontal direction along the survey line. In many situations, particularly for surveys over elongated geological bodies, the imaging technique gives a clearer picture of the cross-section of the body than what the vertical electrical sounding (VES) would do.

The inter-electrode spacing of 10 m was used while inter- dipole separation factor (n) was varied from 1 to 5 (Figure 3.3).

The receiving dipole was initially stationed at stations 3 and 4 (n=1) and subsequently moved to stations 4 and 5 (n=2), stations 5and 6 (n=3), stations 6 and 7 (n=4) and stations 7 and 8 (n=5). The transmitting dipole was moved to stations 2 and 3 and the expansion procedure repeated. The apparent resistivity values were calculated using $\pi a(n+1)\ (n+2)n$ as the geometric factor.

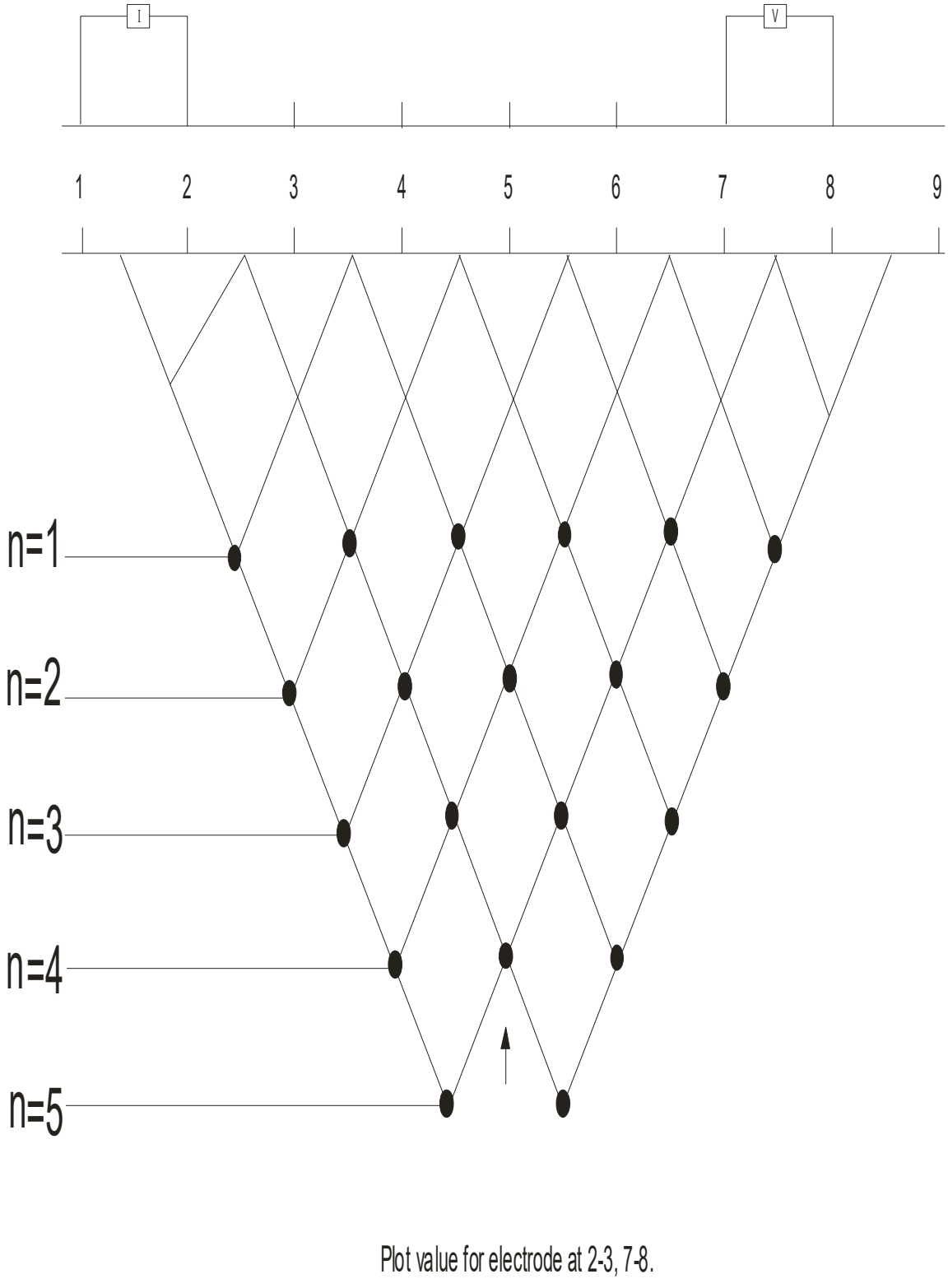


**Figure 3.3:** Method of plotting Dipole- dipole data in a Pseudosection.

# CHAPTER FOUR: RESULTS AND DISCUSSION

## 4.1 INTRODUCTION

The results of the processed data are in form of 2-D inversion models, curves, profiles, maps, geoelectric sections, pseudosections and graphs.

## 4.2 DATA INTERPRETATION

The procedure implemented for data interpretation are qualitative approach - involves graph examination of electromagnetic curves while quantitative approach - entails profundity computation of VES and Dar Zarrouk parameters.

### 4.2.1 QUALITATIVE APPROACH

The double plots of the raw real and filtered real components enable qualitative identification of the top of linear features i.e. points of coincident of crossovers and positive peaks of the real and filtered anomaly. From these plots (figures 4.1a to 4.1c), minor linear features suspected to be faults/fractured zones were identified which were used to pick points for VES survey after being processed using Graphic software, VELFAN 1.0. These suspected geological interfaces, delineated from the profiles, were shown occurring at varying distances on the profiles. These positive peaks mapped as fractures on the filtered real are zones of interest. High positive values indicate presence of conductive subsurface structures while low or negative values are indicative of resistive formations, (Sharma and Baranwal, 2005). The asymmetry of these conductive anomalies suggests that the conductive structures are dipping. Also, the anomaly patterns exhibit varying amplitudes, which are controlled by depth of the body to the surface, its geometry, and attitude.

The positive peak anomalies P1, P2, P3 and P4 on the filtered real curve, revealed vertical and/ or near vertical conductors (Figure 4.1a). These anomalies are 32.00 m, 160.00 m, 200.00 m and 280.00 m from the starting station (zero mark) of the survey profile. The P2 zone seems to be more conductive than P3 zone. Geologically, P3 and P4 probably indicates clay close to the surface while P2 might be clay filled fracture. P1 has low amplitude and fairly broad with, filtered imaginary almost of the same magnitude, indicative of a poor conductor.

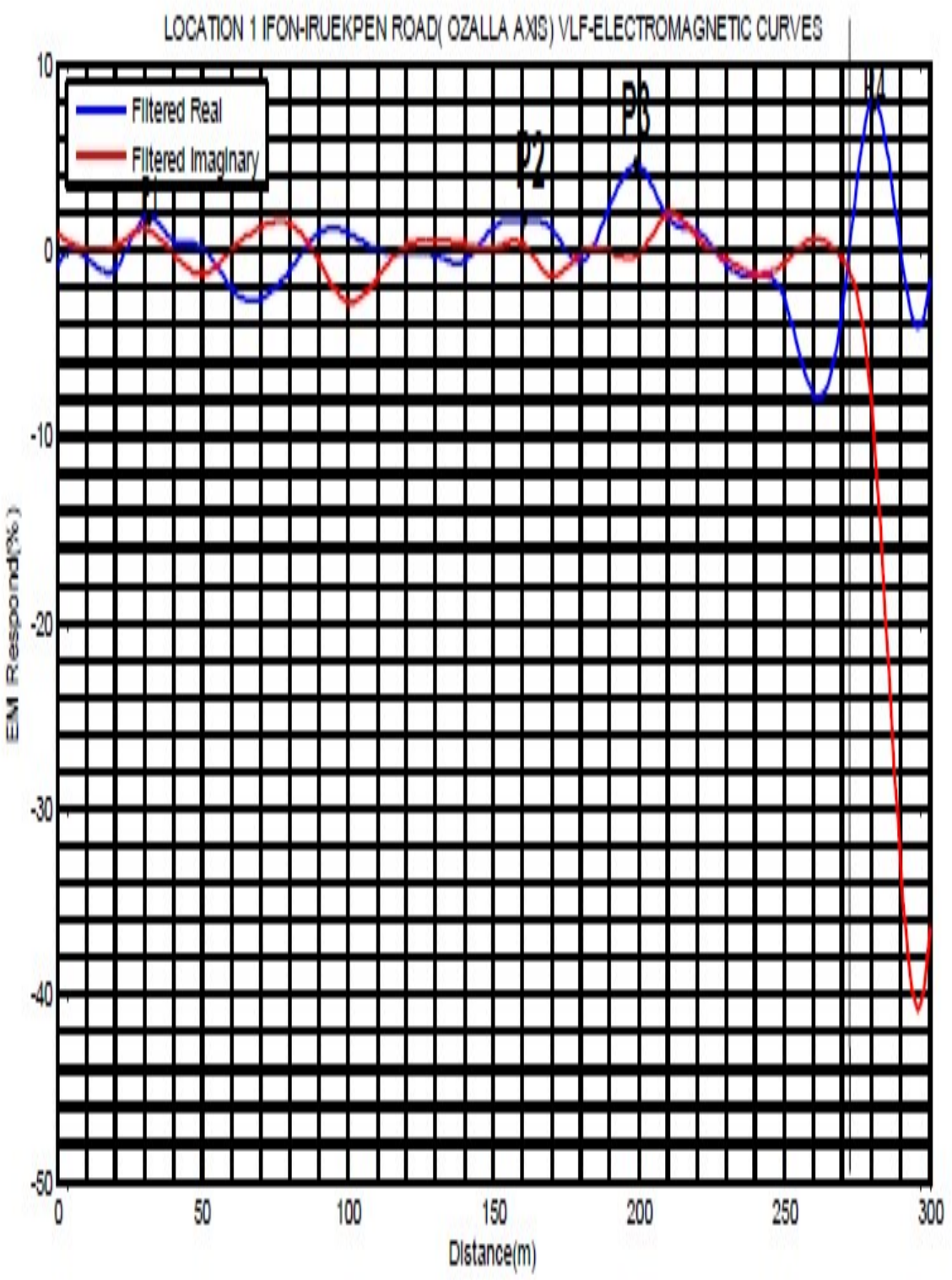


**Figure 4.1a:** VLF-EM Curves in locality 1.

In figure 4.1b**,** the filtered real curve indicates many dipping conductors with positive peaks. P1, P2, P3, P4, P5, P6, F1, F2 and F. These conductors are 80.00 m, 175.00 m, 212.00 m, 245.00 m, 380.00 m, 420.00 m, 500.00 m 522.00 m and 550.00 m from the starting station (zero mark) of the survey profile. The imaginary curves under P1 are below zero, and might be clay filled fracture.From the curve, fractures P2 and P3 are separated by distance of about 35.00 m , while P3 and P4 are separated by a distance of about 38.00 m. The imaginary curve under P2 is positive and almost of the same magnitude, and this is likely wet clay filled fracture, the imaginary curves under P3 and P4 are below zero, and these could be clay filled fractures. The imaginary curve under P5 is below zero, and this might be a clay filled fracture. The imaginary curve under P6 is below zero, and this could be a clay filled fracture. The anomalies F1 and F2 (amplitude doublet) have their tops at 500.00 m and 530.00 m (the features are separated by distance of 30.00 m) marks respectively on the profile. At greater depth, they blend together to form single broad anomaly indication. The imaginary curve under them is below zero, and this likely clay filled fractures. The imaginary curve under it is above zero, which probably indicate presence of clay in the fracture.

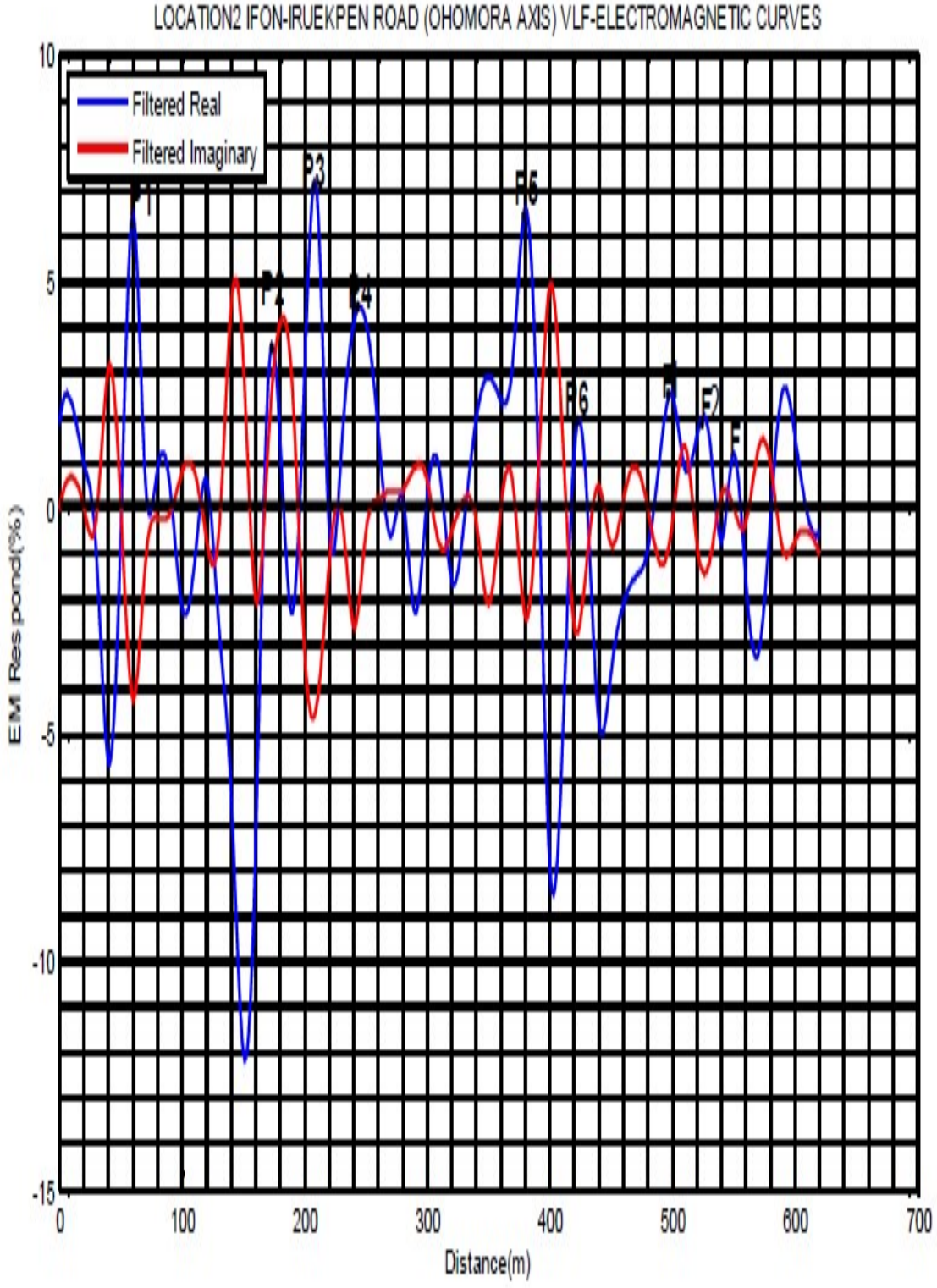


**Figure 4.1b:** VLF-EM Curves in locality 2

In figure 4.1c, the positive peaks anomalies P1, P2, P3 , P4 and P5 indicated on filtered real curve, show locations of vertical and/or near vertical conductors. These anomalies are 42.00 m, 102.00 m, 143.00 m, 169.00 m and 200.00 m from the starting station (zero mark) of the survey profile. The anomalies P3 and F4 (amplitude doublet) have their peaks at 145.00 m and 169.00 m (the features are separated by distance of 24.00 m marks respectively on the profile. The imaginary curve under P3 is below zero. It is likely clay fractures and that of P4 above zero almost of the same magnitude as the real, this fracture zone likely filled with wet clay. The imaginary curve under them is below zero, which probably indicate presence of clayin the fracture The imaginary curve under P1, P2 and P5 is below zero, which probably indicate presence of clay in the fracture.

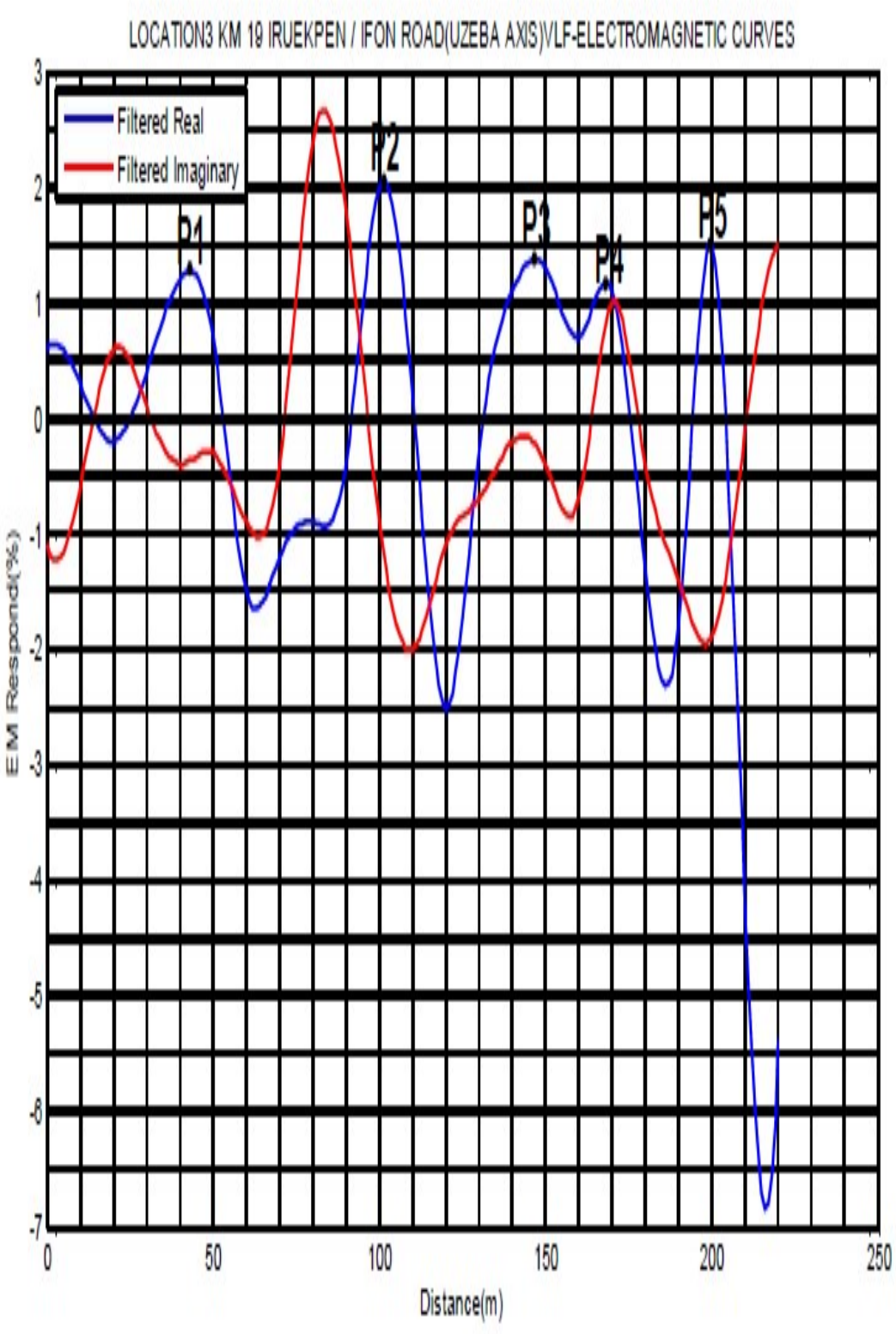


**Figure 4.1c:** VLF-EM Curves in locality 3.

### 4.2.2 QUANTITATIVE APPROACH

The interpretation of the VES curves at locations 1, 2 and 3 shows various layers; three to five layers. Nine classes of curve in the three locations were recognised, viz; K, HK, HKH, HKQ, Q, QH, QQ, QQH and QQQ. These curves types can be basically classified into three distinct classes as follows: CLASS 1: HK, HKH, and HKQ

CLASS 2: K and

CLASS 3: Q, QH, QQ, QQH and QQQ.

The curves in Class 1(HK, HKH, and HKQ) (Figure 4.2a) shows the succession of the subsurface layers starts with highly resistive topsoil followed by a more conductive horizon and then another less conductive layer underlines the latter this overlies the sandstone layer.

Figure 4.2a: Interpretation Model of Typical Class 1 type curves.

Type curve of Class 2 (K) (Figure 4.2b) is a typical of a succession of relatively low and high resistivity layer. Such is usually highly resistive lateritic hard pan underlies low resistivity clayey sand topsoil.

In the Class 3, (Q, QH, QQ, QQH and QQQ) (Figure 4.2c) type curves, the top soil may be subdivided into two horizons with the lower one being more conductive. This may be common in areas where there is regolith (transported material) in addition to the usual in situ saprolite. These class 2 type curves are symptomatic of a succession in which a more conductive clayey sand layer lies directly on the clay.

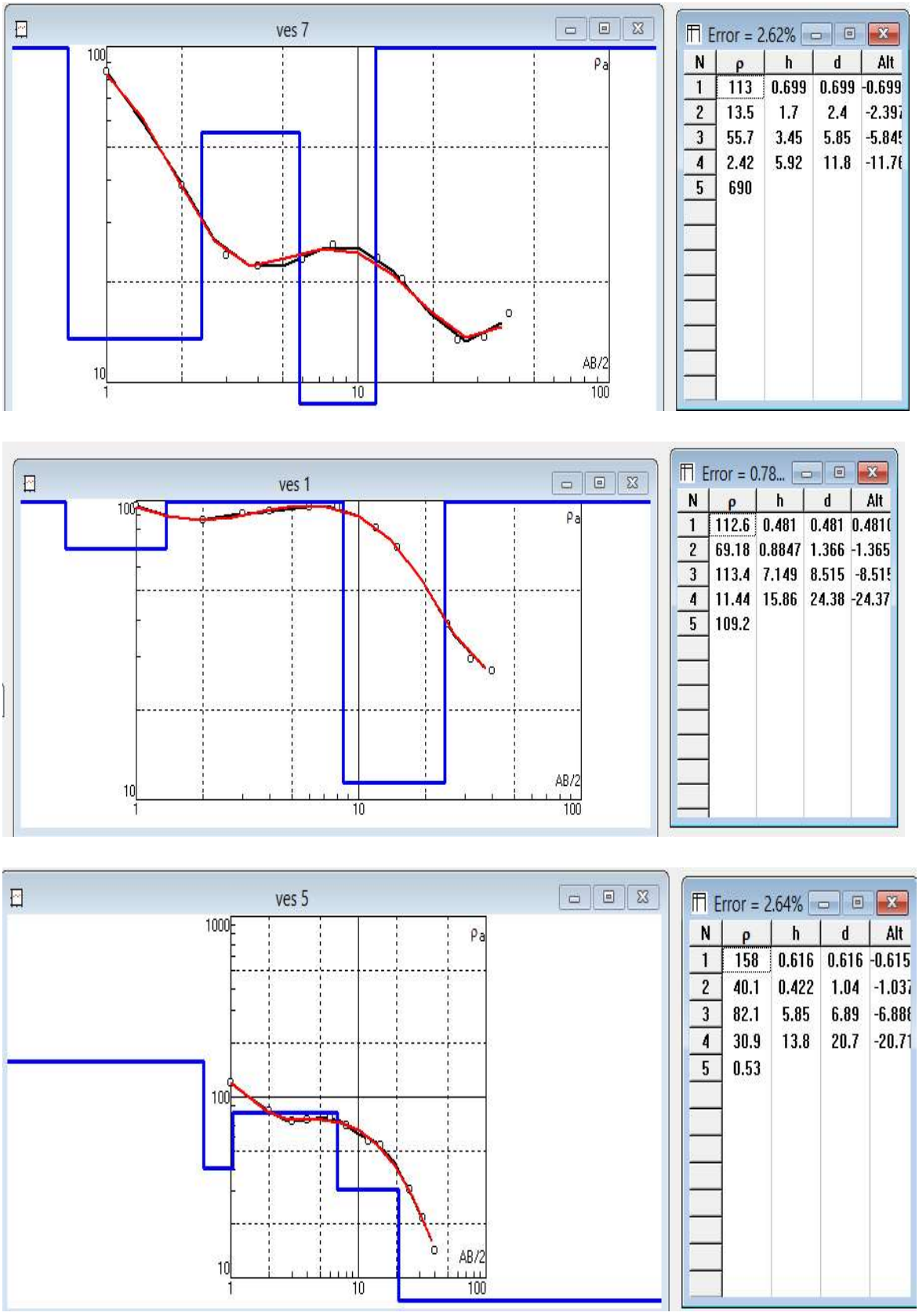


Figure 4.2a: Interpretation Model of Typical Class 1 type curve.

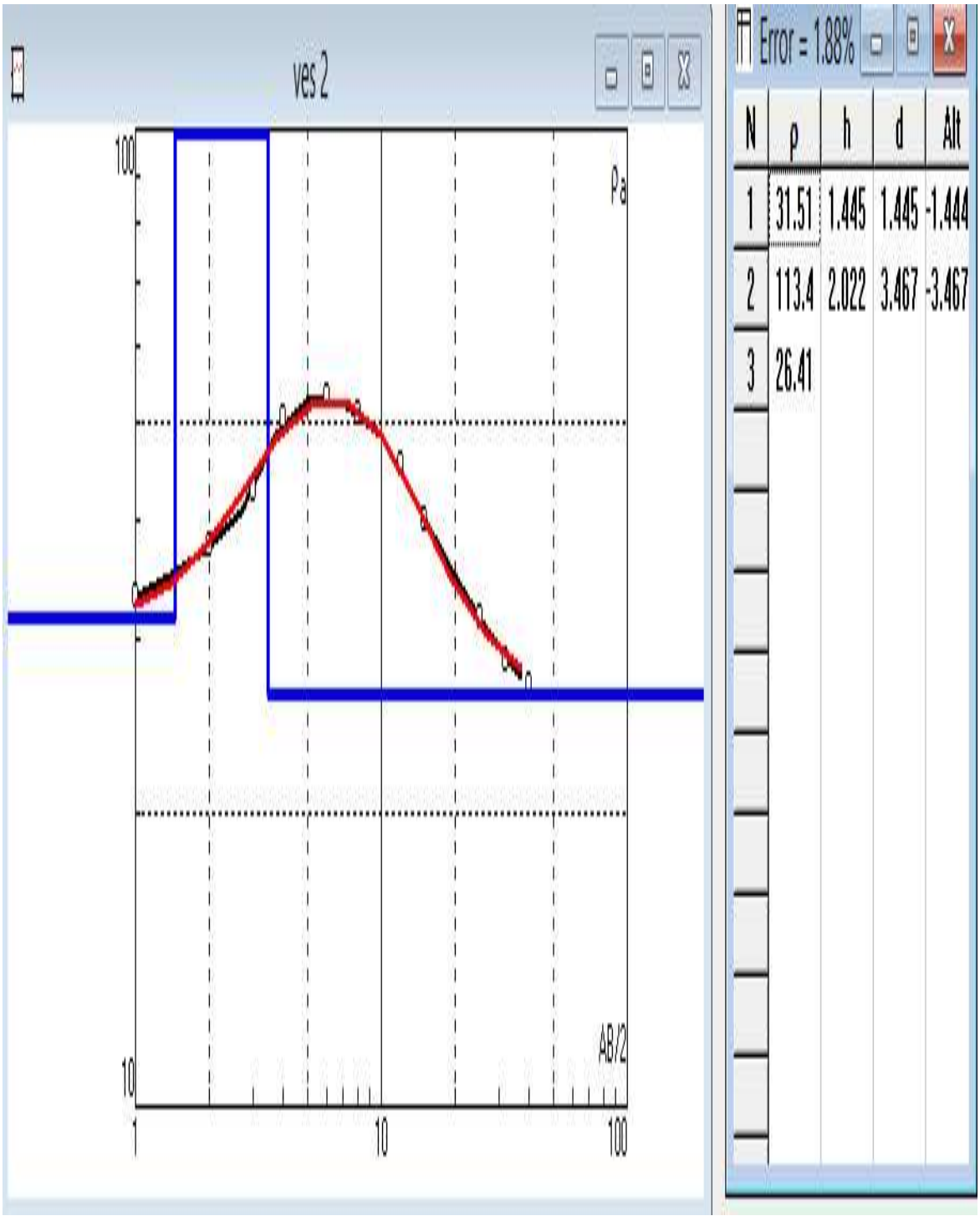


Figure 4.2b: Interpretation Model of Typical Class 2 type curve.


Figure 4.2c: Interpretation Model of Typical Class 3 type curves.

**Table 4.1a: VES interpretation Results from location 1**

| | | | LOCATION ONE | | | | | | | | | |
|---|---|---|---|---|---|---|---|---|---|---|---|---|
| | RESISTIVITY ρ (Ωm) | | | | | THICKNESS h (m) | | | | | DEPTH | CURVE |
| VES NO | $\rho_1$ | $\rho_2$ | $\rho_3$ | $\rho_4$ | $\rho_5$ | $h_1$ | $h_2$ | $h_3$ | $h_4$ | $h_5$ | (m) | TYPE |
| 1 | 113 | 69 | 113 | 11 | 109 | 0.48 | 0.89 | 7.15 | 16 | - | 24.38 | HKH |
| 2 | 32 | 113 | 26 | - | - | 1.45 | 2.02 | - | - | - | 3.47 | K |
| 3 | 87 | 41 | 108 | 31 | 4 | 0.6 | 0.84 | 2.02 | 17 | - | 20.01 | HKQ |
| 4 | 195 | 61 | 9 | 1224 | - | 0.66 | 8.6 | 9.48 | - | - | 18.7 | QH |
| 5 | 158 | 40 | 82 | 31 | 1 | 0.62 | 0.42 | 5.85 | 14 | - | 20.7 | HKQ |
| 6 | 32 | 89 | 18 | 62 | 4 | 1.44 | 2.02 | 4.86 | 12 | - | 20 | KHK |
| 7 | 113 | 14 | 56 | 2 | 690 | 0.7 | 1.7 | 3.45 | 5.9 | - | 11.8 | HK |
| 8 | 384 | 53 | 6 | 2 | 1 | 0.27 | 0.97 | 2.73 | 21 | - | 24.97 | QQQ |
| 9 | 382 | 120 | 4 | 8 | - | 0.56 | 1.34 | 11.9 | - | - | 13.72 | QH |
| 10 | 1229 | 221 | 14 | 1 | 129 | 0.44 | 1.43 | 4.16 | 9 | 5.8 | 20.8 | QQH |

**Table 4.1b: VES interpretation Results from location 2**

| | | LOCATION TWO | | | | | | | | | | |
|---|---|---|---|---|---|---|---|---|---|---|---|---|
| | RESISTIVITY ρ (Ωm) | | | | | THICKNESS h (m) | | | | | DEPTH (m) | CURVE TYPE |
| VES NO | $\rho_1$ | $\rho_2$ | $\rho_3$ | $\rho_4$ | $\rho_5$ | $h_1$ | $h_2$ | $h_3$ | $h_4$ | $h_5$ | | |
| 11 | 243 | 54 | 9 | 1 | 155 | 0.513 | 2.96 | 6.29 | 13.4 | - | 23.2 | QQH |
| 12 | 1285 | 114 | 23 | 3 | - | 0.239 | 2.12 | 5.24 | - | - | 7.6 | QQ |
| 13 | 806 | 104 | 26 | 5 | - | 0.413 | 2.41 | 7.19 | - | - | 10 | QQ |
| 14 | 497 | 68 | 21 | 2 | 99 | 0.443 | 2.356 | 6.004 | 16.4 | - | 25.2 | QQH |
| 15 | 145 | 38 | 12 | 2 | 1203 | 1.43 | 2.17 | 8.74 | 13.3 | - | 25.6 | QQH |
| 16 | 139 | 37 | 10 | 3 | 18 | 1.43 | 2.19 | 7.14 | 19.3 | - | 30.1 | QQH |
| 17 | 180 | 55 | 17 | 1 | - | 0.5007 | 1.852 | 9.634 | - | - | 11.9 | QQ |
| 18 | 2207 | 116 | 26 | 2 | - | 0.176 | 1.52 | 6.26 | - | - | 7.96 | QQ |
| 19 | 152 | 37 | 2 | 381 | - | 0.493 | 2.89 | 13 | - | - | 16.4 | QH |
| 20 | 187 | 47 | 4 | 36 | - | 0.501 | 2.76 | 33.1 | - | - | 36.4 | QH |
| 21 | 327 | 43 | 7 | 2 | 532 | 0.4038 | 1.383 | 5.474 | 9.56 | - | 16.32 | QQH |
| 22 | 314 | 41 | 7 | 2 | 178 | 0.3899 | 1.305 | 5.016 | 11.27 | - | 11.27 | QQH |
| 23 | 181 | 33 | 7 | 3 | - | 0.599 | 1.53 | 2.87 | - | - | 5 | QQ |
| 24 | 248 | 60 | 7 | 1 | 65 | 0.488 | 1.21 | 6.77 | 9.31 | - | 17.8 | QQH |
| 25 | 275 | 65 | 7 | 2 | 276 | 0.407 | 1.83 | 4.92 | 13 | - | 20.2 | QQH |
| 26 | 205 | 38 | 4 | 2 | 177 | 0.7045 | 2.385 | 5.753 | 10.42 | - | 19.26 | QQH |
| 27 | 217 | 54 | 8 | 2 | - | 0.5926 | 1.338 | 10.44 | - | - | 12.37 | Q |
| 28 | 404 | 81 | 10 | 0.1 | - | 0.6764 | 1.738 | 15.77 | - | - | 18.18 | Q |
| 29 | 499 | 80 | 2 | 14 | - | 0.445 | 1.797 | 3.61 | - | - | 6 | QH |
| 30 | 416 | 103 | 3 | 62 | - | 0.501 | 2.11 | 21.9 | - | - | 24.5 | QH |
| 31 | 294 | 79 | 8 | 1 | 323 | 0.299 | 1.99 | 5.52 | 7.52 | - | 7.8 | QQH |
| 32 | 89 | 31 | 2 | 282 | - | 1.43 | 3.16 | 16.6 | - | - | 21.8 | Q |
| 33 | 397 | 35 | 3 | - | - | 0.777 | 4.18 | - | - | - | 4.96 | Q |
| 34 | 419 | 54 | 14 | 4 | 0.2 | 0.528 | 2.45 | 8.21 | 4.36 | - | 49.1 | QQ |
| 35 | 320 | 105 | 12 | 1 | 11 | 0.206 | 1.98 | 11.3 | 13 | 22.5 | 48.8 | QQHK |

**Table 4.1c: VES interpretation Results from location 3**

| LOCATION THREE | | | | | | | | | | | | |
|---|---|---|---|---|---|---|---|---|---|---|---|---|
| | RESISTIVITY ρ (Ωm) | | | | | THICKNESS h (m) | | | | | DEPTH | CURVE |
| VES NO | $\rho_1$ | $\rho_2$ | $\rho_3$ | $\rho_4$ | $\rho_5$ | $h_1$ | $h_2$ | $h_3$ | $h_4$ | $h_5$ | (m) | TYPE |
| 36 | 2435 | 274 | 28 | 4 | - | 0.687 | 1.77 | 4.52 | - | - | 5.48 | QQ |
| 37 | 733 | 122 | 16 | 0.1 | - | 1.54 | 1.51 | 18.3 | - | - | 21.4 | QQ |
| 38 | 626 | 48 | 12 | 0.3 | 53 | 0.727 | 1.63 | 5.9 | 10.6 | - | 18.8 | QQ |
| 39 | 200 | 34 | 7 | 247 | - | 0.427 | 2.31 | 28.7 | - | - | 31.5 | QH |
| 40 | 258 | 32 | 8 | 102 | - | 0.437 | 2.61 | 33.7 | - | - | 36.8 | QH |
| 41 | 1714 | 49 | 15 | 6 | 0.2 | 0.162 | 1.07 | 5.32 | 19.5 | - | 26 | QQQ |
| 42 | 210 | 71 | 6 | 2 | 1444 | 0.299 | 1.258 | 10.85 | 12.53 | - | 24.93 | QQH |

**DAR ZARROUK PARAMETERS**

Table 4.2 shows co- efficient of anisotropy (λ) values ranged from of 1.03 to 2.19. However, from 1.03 to 1.80ofthe $\lambda$ values defines the near surface rocks in these areas are intensely fractured; these prevent the contacts (in terms of lithology) and enhance high swelling potential which can easily result to failed portion in the studied location.

The lower coefficient of anisotropy ($\lambda$) means lower - permeability anisotropy similarly, the higher coefficient of anisotropy ($\lambda$) means higher - permeability anisotropy for the reason that coefficient of anisotropy ($\lambda$) has been shown to have the same functional form as permeability anisotropy.

## Table 4.2: Results from Dar Zarrouk parameters

| VES NO | TOTAL RESISTANCE (T) | TOTAL CONDUCTANCE (S) | CO-EFFICIENT OF ANISOTROPY (λ) |
|---|---|---|---|
| 1 | 115.400 | 0.017 | 1.030 |
| 2 | 274.730 | 0.063 | 1.200 |
| 3 | 87.310 | 0.027 | 1.070 |
| 4 | 654.080 | 0.144 | 1.050 |
| 5 | 114.210 | 0.015 | 1.240 |
| 6 | 226.130 | 0.068 | 1.130 |
| 7 | 102.790 | 0.128 | 1.510 |
| 8 | 153.280 | 0.019 | 1.380 |
| 9 | 376.840 | 0.013 | 1.150 |
| 10 | 851.870 | 0.007 | 1.290 |
| 11 | 284.500 | 0.057 | 1.160 |
| 12 | 548.800 | 0.019 | 1.360 |
| 13 | 583.520 | 0.024 | 1.310 |
| 14 | 380.820 | 0.036 | 1.310 |
| 15 | 289.810 | 0.067 | 1.220 |
| 16 | 279.800 | 0.070 | 1.210 |
| 17 | 190.990 | 0.037 | 1.120 |
| 18 | 564.750 | 0.013 | 1.610 |
| 19 | 181.870 | 0.081 | 1.240 |
| 20 | 223.410 | 0.061 | 1.140 |
| 21 | 191.510 | 0.033 | 1.420 |
| 22 | 175.930 | 0.033 | 1.420 |
| 23 | 158.910 | 0.050 | 1.330 |
| 24 | 193.620 | 0.022 | 1.220 |
| 25 | 230.880 | 0.030 | 1.170 |
| 26 | 235.050 | 0.066 | 1.280 |
| 27 | 200.850 | 0.028 | 1.220 |
| 28 | 414.040 | 0.023 | 1.280 |
| 29 | 380.380 | 0.026 | 1.290 |
| 30 | 425.750 | 0.022 | 1.160 |
| 31 | 245.120 | 0.026 | 1.110 |
| 32 | 225.230 | 0.118 | 1.120 |
| 33 | 454.770 | 0.121 | 1.500 |
| 34 | 353.530 | 0.047 | 1.370 |
| 35 | 273.820 | 0.020 | 1.060 |
| 36 | 2212.630 | 0.008 | 1.530 |
| 37 | 1313.040 | 0.015 | 1.430 |
| 38 | 533.340 | 0.035 | 1.840 |
| 39 | 163.940 | 0.070 | 1.240 |
| 40 | 196.270 | 0.083 | 1.330 |
| 41 | 330.100 | 0.022 | 2.190 |
| 42 | 150.450 | 0.019 | 1.090 |

## 2-D ELECTRICAL IMAGING

The 2D inversion results for the data sets have been presented in the form of 2D geoelectrical pseudosection (Figures 4.3a - 4.3c). Although, there are matching between the 2D and VES results in the general trends of increasing and decreasing resistivity values, some details can be observed only in the VES results particularly at a depth beyond 12 m. This is due to the fact that depth of investigation is deeper in the VES results.

The double dipole profiling which involves the combination of horizontal profiling and vertical electrical sounding was espoused as a means of mapping vertical discontinuities characteristic of joints, fractures and faults zones. The double dipole field data were processed using 'ZONDRES for Window' software.

The dipole-dipole pseudosections and the 2-D resistivity structure at locality 1 are shows in (Figure 4.3a), the topsoil ranges from a depth of 0.0 to 4.0 m beneath the surface and compose of a varying resistivity materials(60.0 to 96.0Ωm) suspected to be clayey sand filling materials. The second geoelectric layer extends from a depth of 4.0 to about 14.0 m with resistivity range from 1.0 to 60.00Ωm predominantly made up of clay material. The depth range of this material between lateral distances of 0 to 230.00 m is about 0.0 to 14.0 m and between 240.00 to 250.00 m is about 0.0 to 5.0 m. This shows a nearly uniform layer filled with clay along this traverse have varying thickness and depth. This layer is unfavourable to the foundation of engineering structure along this traverse.

The dipole-dipole pseudosections (field and theoretical) and 2-D resistivity structure at location 2 are shows in Figure, 4.5b. The 2-D resistivity structure shows a subsurface sequence with very thin topsoil which is virtually unrepresented on the 2-D resistivity structure, a nearly uniform layer filled entire structure with clay with resistivity1.0 to 50.0Ωm at depth ranged 0.0 – 14 m.

In the 2D resistivity section along Traverse 3 (Figure 4.3c),reveals the topsoil ranges from a depth of 0.0 to 4.0 m beneath the surface and compose of a varying resistivity materials(100.0 to 350.0Ωm) suspected to be lateritic/clayey sand filling materials. The second geoelectric layer extends from a depth of 4.0 to 14.0 m with resistivity range from 1.0 to 100.0Ωm predominantly made up of clay material. The depth range of this material between lateral distances of 0.0 to 48.0 m is about 0.0 to 14.0 m and between 50.00 to 170.00 m is about 0.0 to 14.0 m. This shows that the clay material along this traverse have varying thickness and depth. This layer is inimical to the foundation of engineering structure along this traverse.

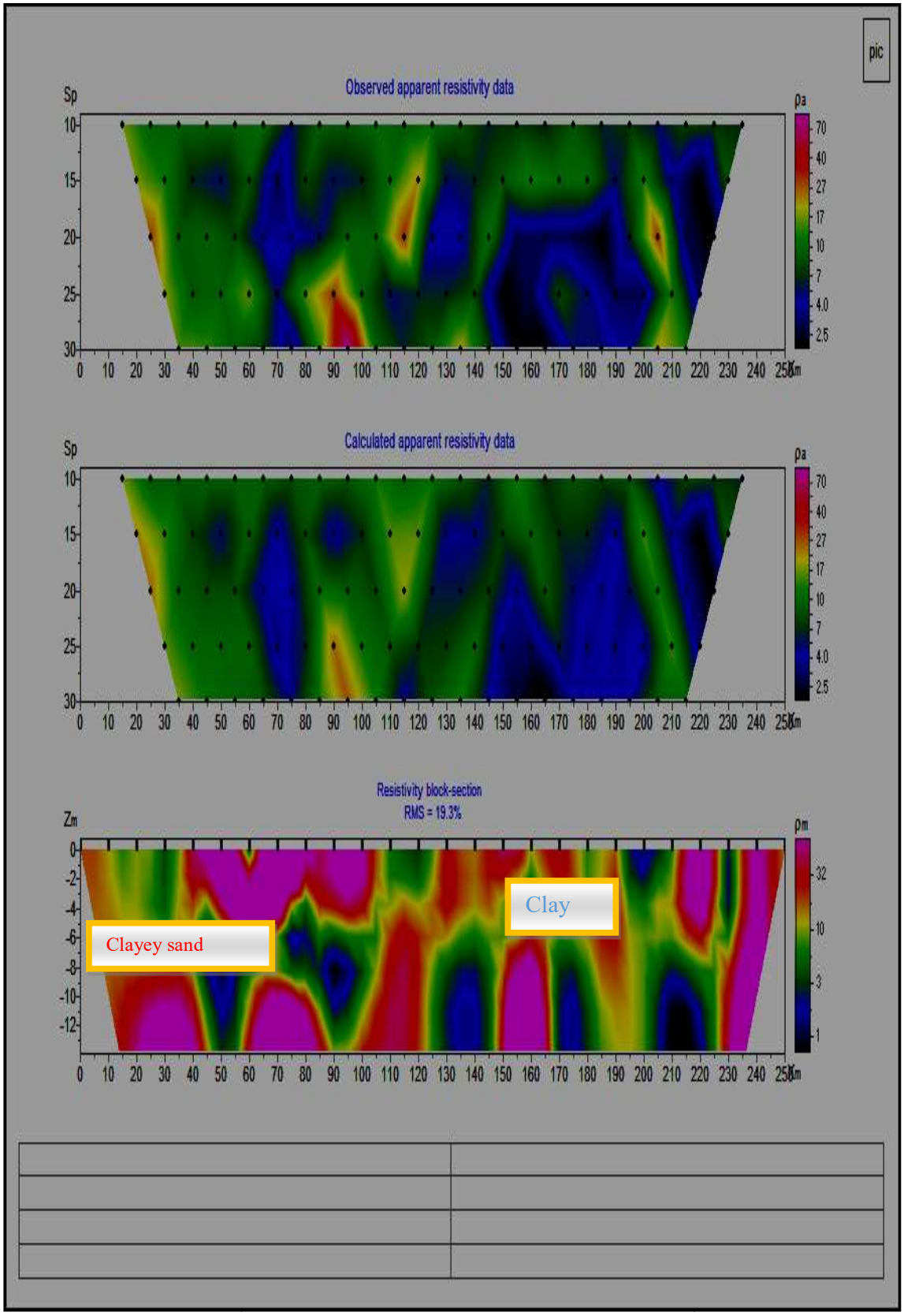


Figure 4.3a 2-D Modelling of Double Dipole 1

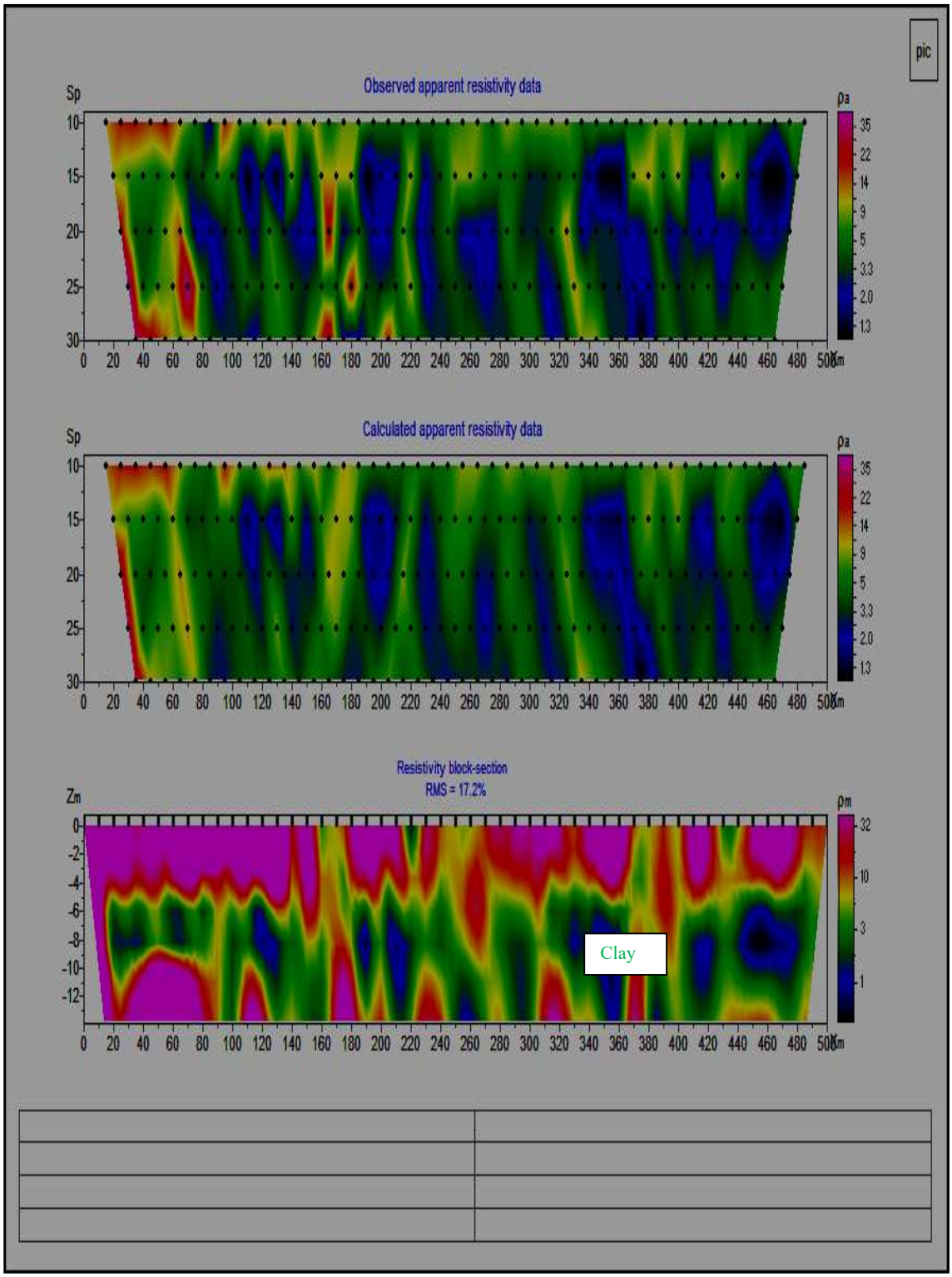


Figure 4.3b 2-D Modelling of Double Dipole 2

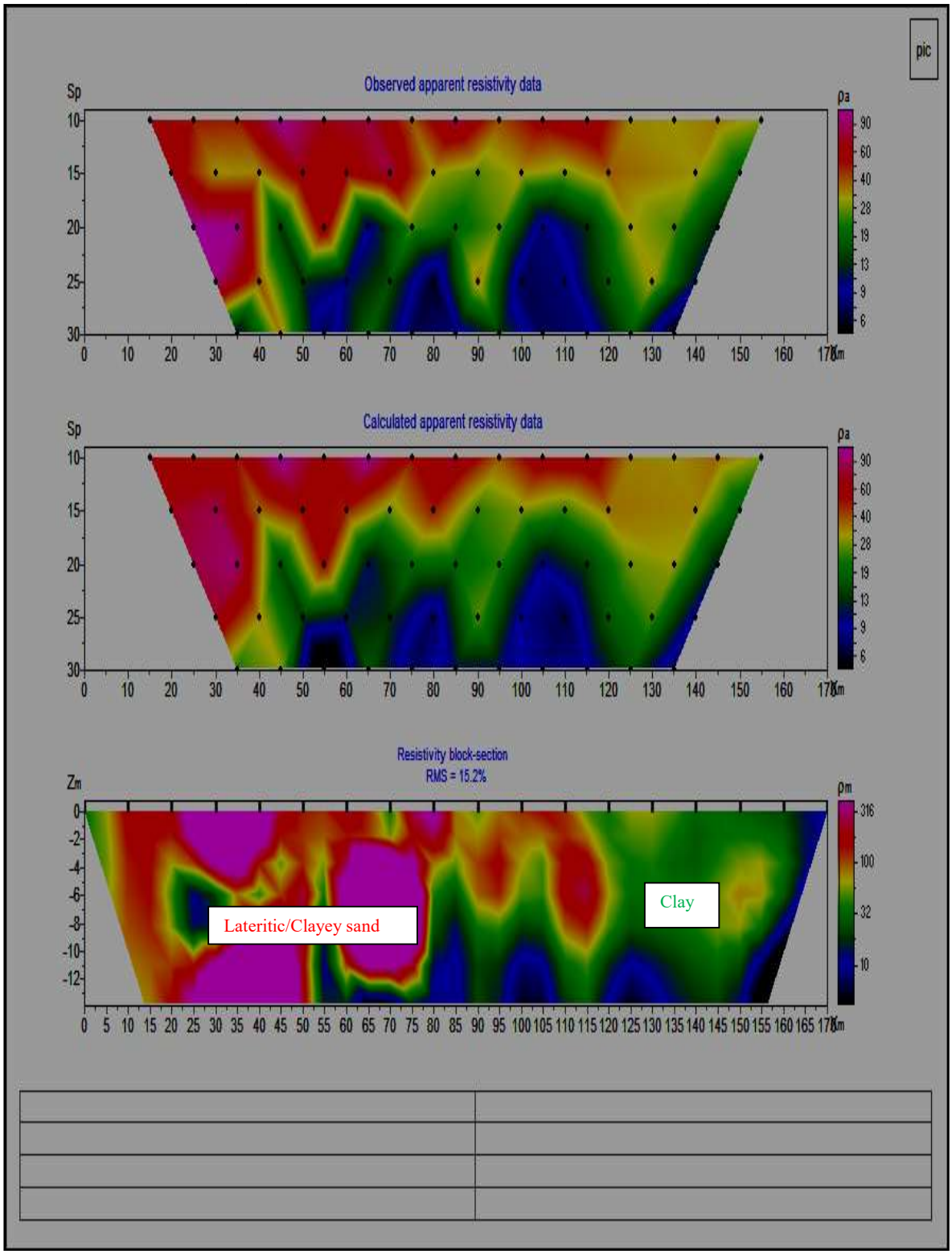


Figure 4.3c 2-D Modelling of Double Dipole 3

## CHAPTER FIVE: SUMMARY, CONCLUSION AND RECOMMENDATION(S)

## 5.1 SUMMARY

An engineering geophysical investigation using electromagnetic method and electrical resistivity method integrated with dar Zarrouk parameters were used to identify and characterise features responsible for road pavement failure along the Ireukpen-Ifon highway in Edo State southsouth Nigeria. Three failed locations (including stable portions) were selected for the study. The results of the geophysical investigation were presented as profiles, field curves, tables, pseudo-cross sections. The studied highway is underlain by the tertiary-recent sediments of the southsouth Nigeria. Generally, the geoelectric sounding delineates three geoelectric/geologic substratum layers at the studied area. The layers comprise the topsoil(laterite/clayey sand), clay and subsurface rocks.

The topsoil segment generally varies in composition from clayey and laterite with resistivity values varying from 60.0 to 350.0 Ωm and thickness between 0.0 to 4.0m.Clay layers with resistivity values ranging from 1.0 to100.0 Ωm and the thickness between 4.0to 14.0m. The coefficient of ($\lambda$)has been shown to have the same functional form as permeability anisotropy. Thus, a higher coefficient of anisotropy ($\lambda$) implies higher - permeability anisotropy. The values λranged from 1.03 to 2.19. The relatively higher values of $\lambda$ (1.03 to 1.80) suggesting that the subsurface rocks in these areas are intensely fractured and more permeable. These clearly limit the lithological contacts and enhance high swelling potential which might be responsible for the road pavement failures in the studied area.

## 5.2 CONCLUSION AND RECOMMENDATION

From locations 1, 2 and 3 of the studied area, it can be concluded that the possible cause of highway pavement failures is as result of clay formation, underlain by highly fractured subsurface rocks environment.

Clay topsoils with characteristic low layer resistivity (less than 100 Ωm) have the propensity of engrossing water as a result of severe fracture hence show evidence of soaring swelling potential and fail under forced passage of load stress which consequently produces a translational failure. Unwarranted cut into the conductive water engrossing clayey sand substratum that is montmorillonite (clay that undergoes spreading out and tightening by virtue of change in moisture contents). This was observed at locality 1. Potential to degrade the pavement material is the presence of water (permanent or seasonal)

in the road environment may have a far more adverse effect on the road formation than salts present in the water. This is clearly seen in locality 2.

The result of the study shows the need for the application of detailed geophysical investigation in pre-construction feasibility study of highway roads and would therefore recommend that a comprehensive geophysical investigation should be undertaken at all the failed segments noted to have defiled several rehabilitations efforts to allow for proper identification of the causes of the failure.

## REFERENCES


Adewumi, R. (2009). Nigeria Road: Roadmap to progress. Unpublished Ph.D Thesis, Newcastle University, UK.

Adiat, K.A.N., Adelusi, A.O. and Ayuk, M.A. (2009). Relevance of Geophysics in Road Failures Investigation in a Typical Basement Complex of South-western Nigeria. *The Pacific Journal of Science and Technology.* 10(1), 528 – 539.

Akintorinwa, O.J., Ojo, J.S. and Olorunfemi, M.O. (2010). Geophysical Investigation of Pavement Failure in a Basement Complex Terrain of south western Nigeria". Pacific Journal of Science and Technology.11 (2), 649-663.

Attewel, P.B. and Farmer, I.W. (1976). Principles of Engineering Geology first edition, Chapman and Hall, A Halstel Press Book London. 112-460.

Falowo, H andAkintorinwa, T (2015). Geophysical investigation of pavement failures along Akure-Ijare Road, Southwestern Nigeria. *Journal of Applied Geology and Geophysics Research* 3(6), 45-54.

Fatoba J. O., Salami B. M. and Adesida A. (2013). Structural failure investigation using electrical resistivity method: A case study of Amafor Ihuokpala, Enugu, Southeastern Nigeria. *Journal of Geology and Mining Research 5(8),* 208-215.

Federal Ministry of Works and Housing, (2003). Task Force for Road Maintenance.

Henriet, J.P. (1976). Direct application of the Dar Zarrouk parameters in groundwater surveys. Geophysical Prospecting, 24(2), 344-353.

Hummel, J. N., (1929). Der scheinbare spezifische Widerstand bei vier pIan-parallelen Schichten: Zeitschr. *Geophysik.* 5, (5-6), 228-238.

Ibitomi, M.A., Fatoye, F.B and Onsachi J.M. (2014). Geophysical Investigation of Pavement Failure on a Portion of Okene-Lokoja Highway, North Central Nigeria. *Journal of Environment and Earth Science.* 4(13), 44-50.

Jegede, G (2000). Effect of soil properties on pavement failure along the F209 highway at Ado-Ekiti, Southwestern Nigeria. Journal of Construction and Building Materials. 14, 311-315.

Keller, G. V. and Frischknecht, F. C. (1966). Electrical methods in geophysical prospecting, Pergamon Press Inc., Oxford. 179-187.

Koefoed, O. (1979). Geosounding Principles: Resistivity Measurements, in Methods in Geochemistry and Geophysics, 14A Elsevier, New York, 276.

Lancaster-Jones, E., 1930, The earth-resistivity method of electrical prospecting: *Mining Mag.,* 42(6) 352-355.

Maillet, R. (1974). The fundamental equations of electrical prospecting. Geophysics, 12(4),529-556.

McNeill, J. D., and Labson, V. F. (1991). Geological mapping using VLF radio fields. In: Nabighian, M.C. (Ed.), *Geotechnical and Environmental Geophysics, Review and Tutorial*, 1, Society of Exploration, Tulsa, 191–218.

Olorunfemi, M.O. and E.A. Mesida, (1987).Engineering Geophysics and its application in Engineering Site Investigation-(case study from Ile-Ife area). *The Nigerian Engineer,* 22(2), 57-66.

Olukoga, O.A. (1990). Highway geotechnical characteristics of some compacted laterites soils around Osun, Ile- Ife – Ilesha road, Nigeria. Unpublished B.Sc. thesis, Dept. of Civil Engineering Obafemi Awolowo University, Ile-Ife.

Oluwafemi, O., and Oladunjoye, M. A**.** (2013). Integration of Surface Electrical and Electromagnetic Prospecting Methods for Mapping Overburden Structures in Akungba-Akoko, Southwestern Nigeria. *International Journal of Science and Technology* 2(1)*,* 122-147.

Ozegin, K.O and Oseghale, A.O. (2012).Fundamentals of active methods of geophysical prospecting. In: Osemenikhian, J.E.A. (ed). Oshio kings concepts computers, Benin city, Nigeria, 34-78.

Parasnis, D. S. (1986): Principles of Applied Geophysics 4th edition, Chapman and Hall, London.

Parker, M.E.(1980). VLF electromagnetic mapping for strata-bound mineralization near Aberfeldy, Scondland. Trans. Inst. Min. Metall. Sect. B 89, B123-B133.

Phillips, W.J., Richards, W.E.(1975). A study of the effectiveness of the VLF method for the location of narrow mineralized zones. Geoexploration 13, 215-226.

Rao JP, Rao SB, Rao JM, Harikrishna P (2003). Geo-electrical data analysis to demarcate groundwater pockets and recharge zones in Champavathi River Basin, Vizianagaram District, Andhra Pradesh. *J. Indian Geophys. Union* 7(2), 105-113.

Saydam, A.S.(1981). Very low frequency electromagnetic interpretation using tilt angle and ellipticity measurements. *Geophysics* 46, 1594-1606.

Sellers, R., Dixon, N., Dijkstra T.A., Gunn, D.A., Chambers, J.E., Jackson, P.D. and Hughes, P. (2010). Electrical Resistivity as a tool to identify areas of progressive failure within UK infrastructure embankments. In: *IAEG Congress 2010, Auckland, New Zealand,* EAGE.

Sharma, P. V. (1997): Environmental and Engineering Geophysics Cambridge University Press.

Sundararajan, N., Ramesh Babu, V., Shiva Prasad, N., Srinivas, Y. (2006). VLFPROS- a Matlab code for processing of VLF-EM data. *Comput. Geosci*. 32, 1806 - 1813.

Telford, W. M., Geldert, L.P. and Sheriff, R. E. (1990): Applied Geophysics (Second Edition) Cambridge University Press, Cambridge England.

Ward, S.H., (1990). Resistivity and induced polarization methods. In: Ward, S.H. (Ed.), Geotechnical and Environmental Geophysics. *Investigations in Geophysics* No. 5. SEG, USA, pp. 169–189.

Zohdy A.A.R, Eaton G.P., Mabey, D.R. (1974). Application of surface geophysics to groundwater investigations: Techniques of water resources investigations of the United Geophysical Survey Book. United States Government Printing Office, Washington DI, P. 116.

# APPENDIX II

ELECTRICAL RESISTIVITY VES DATA

Location 1

| AB/2 | RESISTIVITY (Ohm-m) | | | | | | | | | |
|---|---|---|---|---|---|---|---|---|---|---|
| | V1 | V2 | V3 | V4 | V5 | V6 | V7 | V8 | V9 | V10 |
| 1 | 80 | 42 | 94 | 152 | 74 | 83 | 113 | 181 | 647 | 570 |
| 2 | 72 | 47 | 73 | 95 | 51 | 61 | 46 | 86 | 209 | 404 |
| 3 | 82 | 54 | 75 | 73 | 45 | 48 | 33 | 46 | 87 | 155 |
| 4 | 77 | 68 | 73 | 62 | 46 | 44 | 25 | 25 | 41 | 85 |
| 6 | 75 | 68 | 68 | 61 | 48 | 38 | 14 | 12 | 13 | 30 |
| 6 | 81 | 59 | 81 | 58 | 43 | 36 | 23 | 14 | 14 | 38 |
| 8 | 87 | 60 | 75 | 56 | 44 | 35 | 30 | 7 | 7 | 13 |
| 12 | 69 | 45 | 57 | 42 | 36 | 31 | 52 | 9 | 8 | 6 |
| 15 | 54 | 45 | 49 | 35 | 34 | 27 | 35 | 10 | 4 | 13 |
| 15 | 65 | 51 | 48 | 46 | 38 | 26 | 19 | 10 | 5 | 8 |
| 25 | 33 | 40 | 37 | 29 | 16 | 19 | 12 | 5 | 54 | 2 |
| 32 | 25 | 28 | 18 | 24 | 10 | 17 | 11 | 2 | 6 | 2 |
| 40 | 23 | 34 | 20 | 42 | 7 | 8 | 20 | 1 | 4 | 7 |
| 40 | 27 | 27 | 16 | 34 | 14 | 8 | 16 | 1 | 6 | 7 |
| 65 | | | | | | | | | | 3 |
| 100 | | | | | | | | | | 4 |

# Location 2

| | RESISTIVITY (Ohm-m) | | | | | | | | | | | | | | | | | | | | | | | | |
|---|---|---|---|---|---|---|---|---|---|---|---|---|---|---|---|---|---|---|---|---|---|---|---|---|---|
| AB/2 | V11 | V12 | V13 | V14 | V15 | V16 | V17 | V18 | V19 | V20 | V21 | V22 | V23 | V24 | V25 | V26 | V27 | V28 | V29 | V30 | V31 | V32 | V33 | V34 | V35 |
| 1 | 165 | 135 | 198 | 184 | 148 | 142 | 108 | 106 | 118 | 112 | 131 | 127 | 125 | 123 | 132 | 124 | 207 | 202 | 261 | 205 | 120 | 91 | 184 | 164 | 130 |
| 2 | 83 | 75 | 76 | 71 | 116 | 112 | 61 | 60 | 62 | 59 | 45 | 43 | 55 | 54 | 66 | 63 | 102 | 100 | 104 | 102 | 75 | 77 | 84 | 63 | 101 |
| 3 | 59 | 98 | 54 | 50 | 93 | 90 | 45 | 49 | 44 | 42 | 26 | 25 | 29 | 29 | 52 | 49 | 56 | 54 | 65 | 70 | 59 | 69 | 38 | 36 | 96 |
| 4 | 54 | 53 | 48 | 42 | 62 | 59 | 42 | 41 | 38 | 36 | 18 | 17 | 19 | 18 | 38 | 35 | 36 | 35 | 44 | 49 | 50 | 50 | 40 | 31 | 90 |
| 6 | 40 | 32 | 34 | 31 | 37 | 35 | 25 | 25 | 23 | 22 | 9 | 9 | 12 | 11 | 18 | 17 | 19 | 18 | 24 | 22 | 24 | 31 | 17 | 22 | 49 |
| 6 | 38 | 31 | 45 | 42 | 40 | 38 | 27 | 27 | 24 | 23 | 11 | 10 | 9 | 9 | 16 | 15 | 20 | 19 | 22 | 24 | 21 | 30 | 21 | 24 | 51 |
| 8 | 25 | 20 | 30 | 28 | 23 | 29 | 19 | 18 | 16 | 15 | 8 | 8 | 6 | 6 | 9 | 8 | 10 | 9 | 10 | 13 | 12 | 16 | 15 | 15 | 19 |
| 12 | 6 | 5 | 22 | 20 | 14 | 14 | 14 | 14 | 5 | 5 | 5 | 5 | 8 | 8 | 5 | 4 | 10 | 10 | 5 | 4 | 6 | 9 | 7 | 15 | 15 |
| 15 | 9 | 7 | 11 | 10 | 10 | 9 | 8 | 8 | 5 | 5 | 4 | 4 | 4 | 4 | 9 | 7 | 8 | 7 | 7 | 5 | 4 | 4 | 4 | 9 | 11 |
| 15 | 9 | 7 | 16 | 15 | 14 | 14 | 14 | 13 | 7 | 7 | 5 | 5 | 3 | 3 | 4 | 3 | 12 | 11 | 10 | 7 | 6 | 7 | 5 | 10 | 11 |
| 25 | 4 | 13 | 6 | 5 | 7 | 6 | 3 | 3 | 4 | 4 | 5 | 4 | 2 | 2 | 5 | 5 | 9 | 9 | 9 | 3 | 2 | 6 | 3 | 5 | 22 |
| 32 | 3 | 2 | 4 | 4 | 5 | 5 | 2 | 2 | 5 | 4 | 5 | 5 | 2 | 1 | 5 | 4 | 6 | 6 | 11 | 3 | 3 | 3 | 2 | 5 | 9 |
| 40 | 5 | 3 | 7 | 6 | 8 | 8 | 1 | 1 | 5 | 5 | 6 | 6 | 3 | 3 | 4 | 4 | 2 | 2 | 12 | 6 | 3 | 4 | 3 | 4 | 3 |
| 40 | 4 | 3 | 7 | 6 | 7 | 7 | 2 | 2 | 5 | 5 | 6 | 6 | 3 | 3 | 6 | 6 | 3 | 3 | 10 | 6 | 3 | 4 | 3 | 5 | 5 |
| 65 | | | | | | | | | | | | | | | | | | | | | | | | | 6 |
| 100 | | | | | | | | | | | | | | | | | | | | | | | | | 3 |

Location 3

| AB/2 | RESISTIVITY (Ohm-m) | | | | | | |
|---|---|---|---|---|---|---|---|
| | V1 | V2 | V3 | V4 | V5 | V6 | V7 |
| 1 | 1010 | 616 | 505 | 80 | 104 | 71 | 97 |
| 2 | 559 | 540 | 245 | 35 | 38 | 44 | 56 |
| 3 | 239 | 384 | 79 | 26 | 27 | 34 | 35 |
| 4 | 144 | 216 | 34 | 21 | 23 | 23 | 16 |
| 6 | 58 | 94 | 23 | 22 | 17 | 16 | 11 |
| 6 | 65 | 93 | 23 | 19 | 19 | 20 | 13 |
| 8 | 25 | 40 | 14 | 10 | 12 | 17 | 10 |
| 12 | 11 | 17 | 10 | 8 | 10 | 14 | 7 |
| 15 | 18 | 14 | 4 | 4 | 15 | 11 | 7 |
| 15 | 18 | 14 | 4 | 12 | 15 | 11 | 18 |
| 25 | 3 | 12 | 1 | 6 | 13 | 16 | 4 |
| 32 | 4 | 11 | 1 | 6 | 12 | 6 | 3 |
| 40 | 4 | 5 | 1 | 10 | 12 | 5 | 4 |
| 40 | 4 | 6 | 1 | 12 | 11 | 4 | 6 |
| 65 | | | | | | | 15 |
| 100 | | | | | | | 97 |

# APPENDIX I

RESULTS OF THE VES CURVES AT EACH OF THE STUDIED LOCATIONS

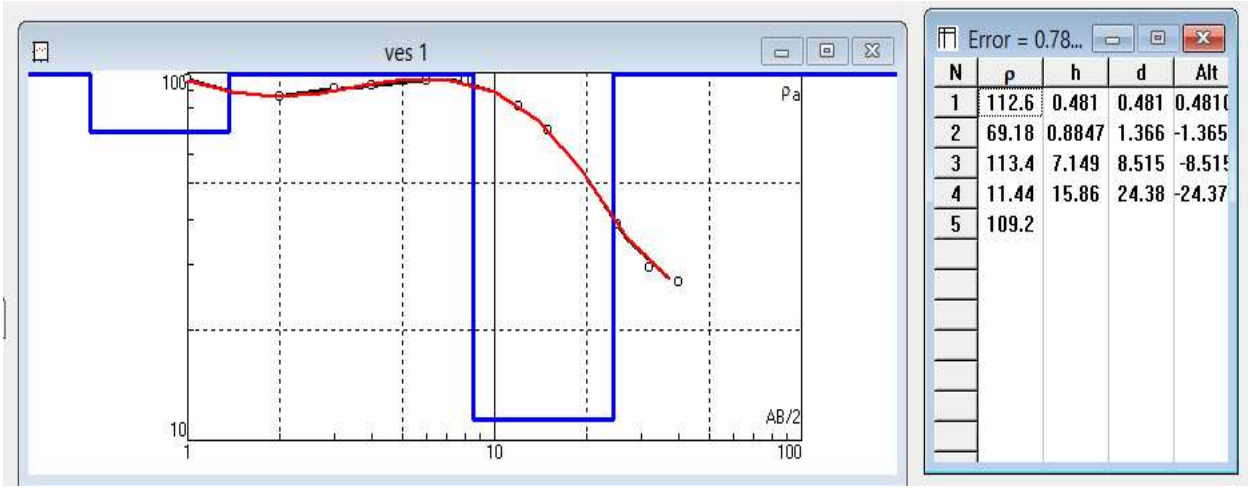


Error = 0.78...

| N | ρ | h | d | Alt |
|---|---|---|---|---|
| 1 | 112.6 | 0.481 | 0.481 | 0.481( |
| 2 | 69.18 | 0.8847 | 1.366 | -1.365 |
| 3 | 113.4 | 7.149 | 8.515 | -8.515 |
| 4 | 11.44 | 15.86 | 24.38 | -24.37 |
| 5 | 109.2 | | | |

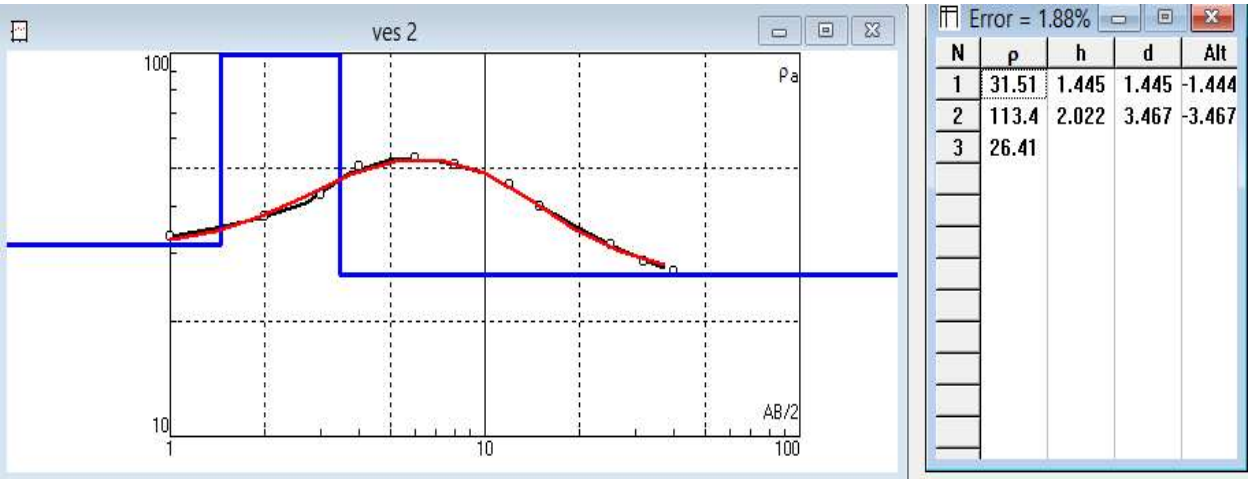


Error = 1.88%

| N | ρ | h | d | Alt |
|---|---|---|---|---|
| 1 | 31.51 | 1.445 | 1.445 | -1.444 |
| 2 | 113.4 | 2.022 | 3.467 | -3.467 |
| 3 | 26.41 | | | |

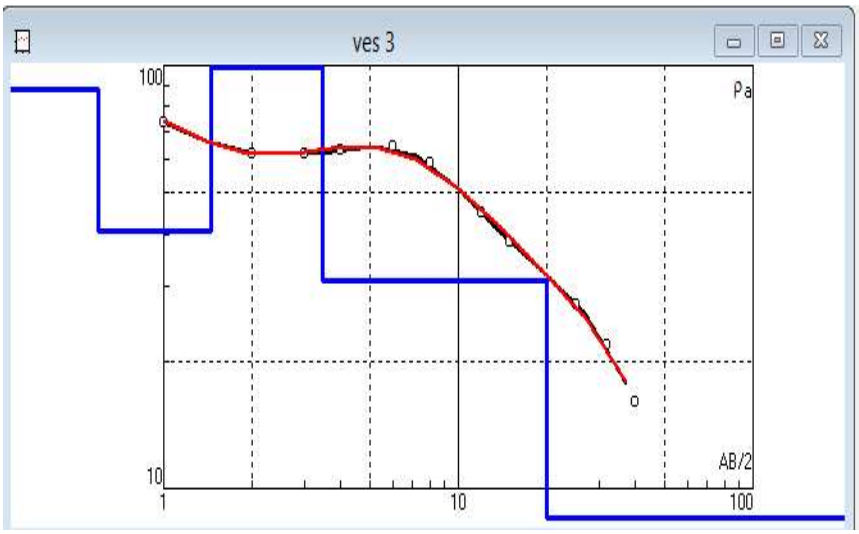


Error = 1.32%

| N | ρ | h | d | Alt |
|---|---|---|---|---|
| 1 | 87.49 | 0.6 | 0.6 | -0.6 |
| 2 | 40.62 | 0.8417 | 1.442 | -1.441 |
| 3 | 107.8 | 2.022 | 3.464 | -3.464 |
| 4 | 31.04 | 16.55 | 20.01 | -20.01 |
| 5 | 4.306 | | | |

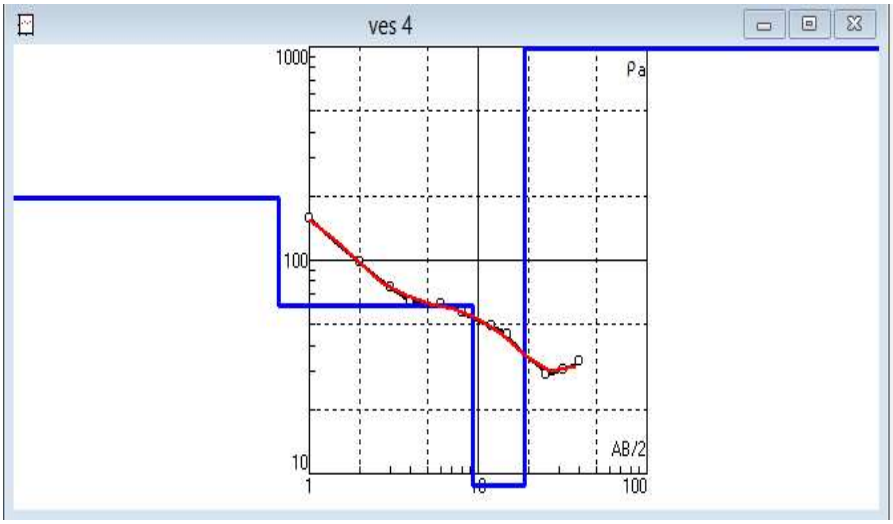


Error = 2.31%

| N | ρ | h | d | Alt |
|---|---|---|---|---|
| 1 | 195 | 0.664 | 0.664 | -0.663 |
| 2 | 61.4 | 8.6 | 9.27 | -9.266 |
| 3 | 8.84 | 9.48 | 18.7 | -18.75 |
| 4 | 1224 | | | |

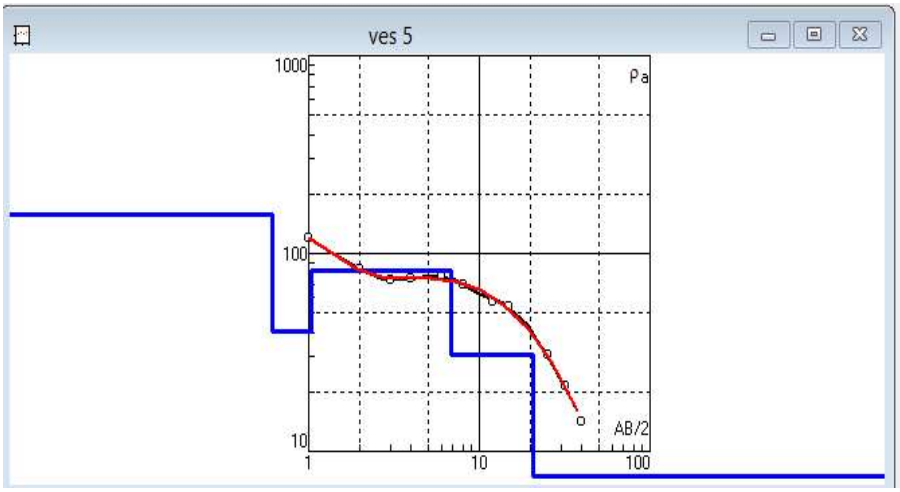


Error = 2.64%

| N | ρ | h | d | Alt |
|---|---|---|---|---|
| 1 | 158 | 0.616 | 0.616 | -0.615 |
| 2 | 40.1 | 0.422 | 1.04 | -1.037 |
| 3 | 82.1 | 5.85 | 6.89 | -6.888 |
| 4 | 30.9 | 13.8 | 20.7 | -20.71 |
| 5 | 0.53 | | | |

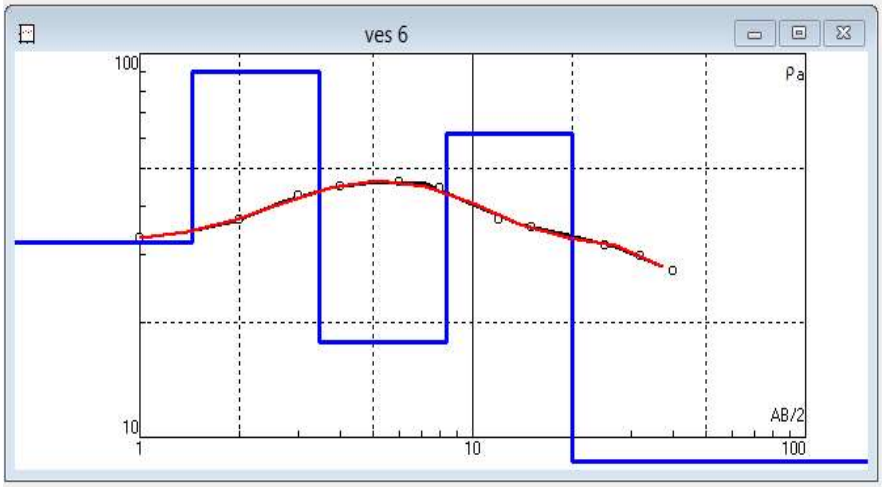


Error = 0.84...

| N | ρ | h | d | Alt |
|---|---|---|---|---|
| 1 | 32.09 | 1.443 | 1.443 | -1.443 |
| 2 | 89.46 | 2.022 | 3.466 | -3.465 |
| 3 | 17.77 | 4.859 | 8.325 | -8.325 |
| 4 | 61.94 | 11.68 | 20 | -20.00 |
| 5 | 3.76 | | | |

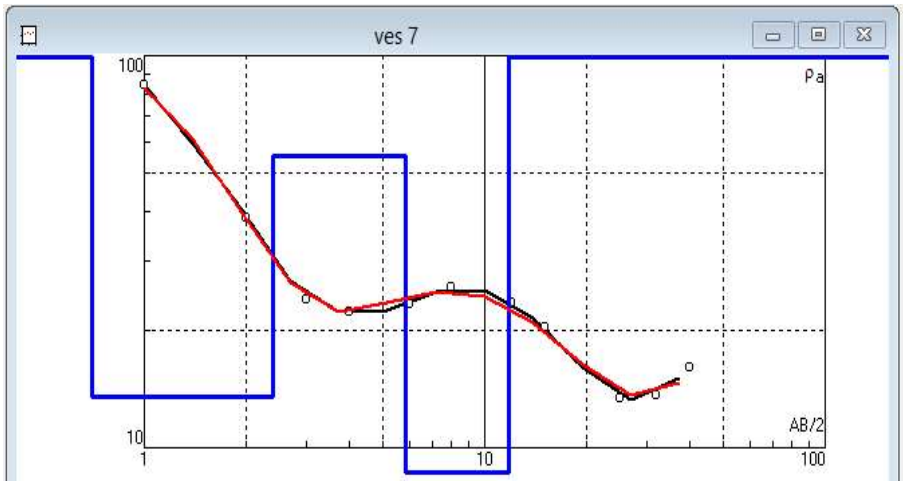


Error = 2.62%

| N | ρ | h | d | Alt |
|---|---|---|---|---|
| 1 | 113 | 0.699 | 0.699 | -0.699 |
| 2 | 13.5 | 1.7 | 2.4 | -2.397 |
| 3 | 55.7 | 3.45 | 5.85 | -5.845 |
| 4 | 2.42 | 5.92 | 11.8 | -11.76 |
| 5 | 690 | | | |

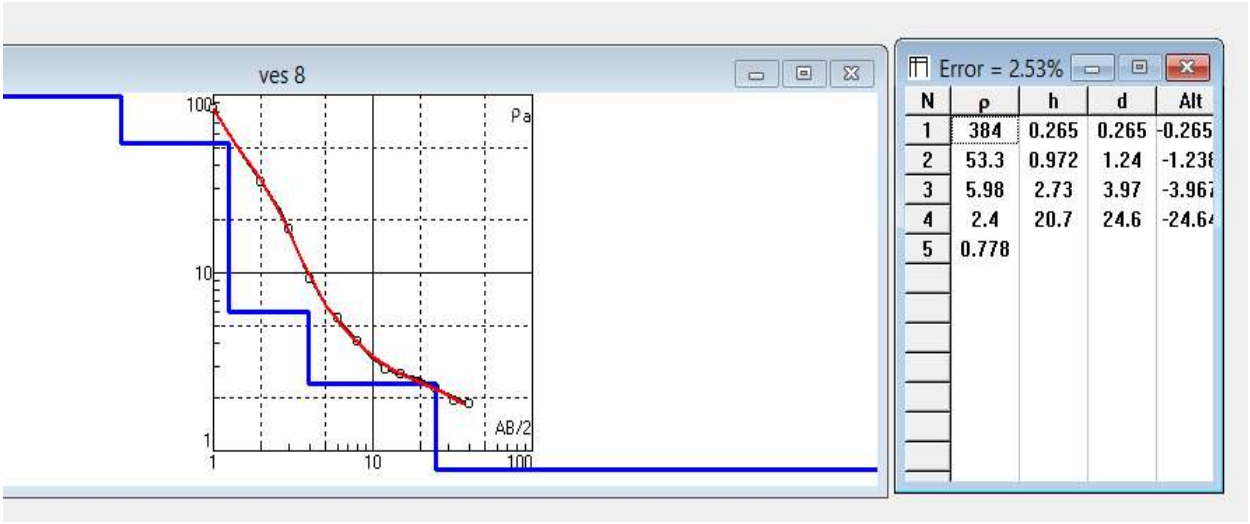


Error = 2.53%

| N | ρ | h | d | Alt |
|---|---|---|---|---|
| 1 | 384 | 0.265 | 0.265 | -0.265 |
| 2 | 53.3 | 0.972 | 1.24 | -1.23 |
| 3 | 5.98 | 2.73 | 3.97 | -3.96 |
| 4 | 2.4 | 20.7 | 24.6 | -24.6 |
| 5 | 0.778 | | | |

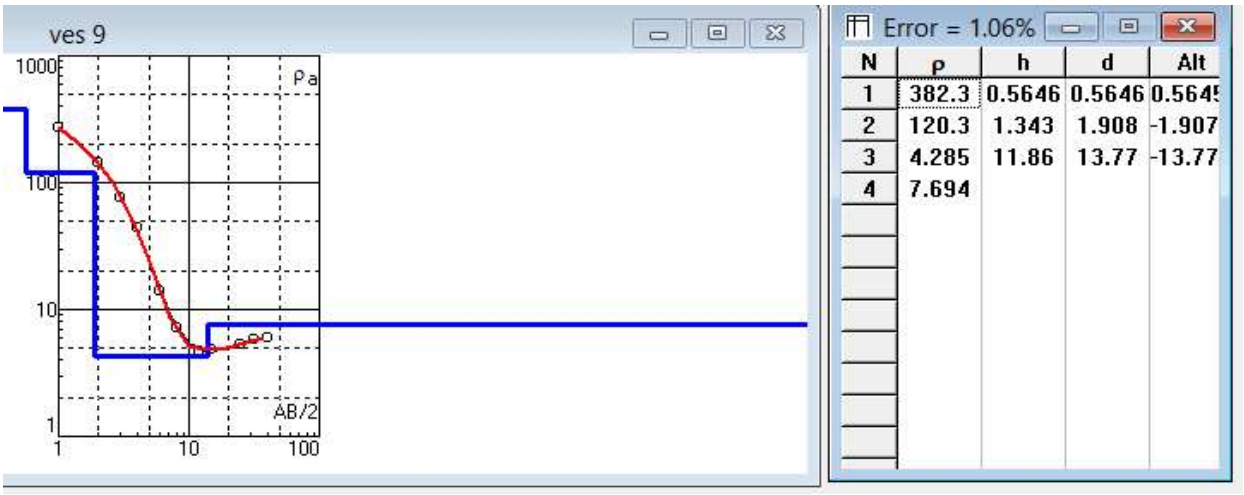


Error = 1.06%

| N | ρ | h | d | Alt |
|---|---|---|---|---|
| 1 | 382.3 | 0.5646 | 0.5646 | 0.564 |
| 2 | 120.3 | 1.343 | 1.908 | -1.907 |
| 3 | 4.285 | 11.86 | 13.77 | -13.77 |
| 4 | 7.694 | | | |


Error = 2.92%

| N | ρ | h | d | Alt |
|---|---|---|---|---|
| 1 | 1229 | 0.436 | 0.436 | -0.436 |
| 2 | 221 | 1.43 | 1.87 | -1.869 |
| 3 | 14.1 | 4.16 | 6.03 | -6.027 |
| 4 | 1.41 | 8.96 | 15 | -14.99 |
| 5 | 129 | 5.82 | 20.8 | -20.81 |
| 6 | 0.136 | | | |

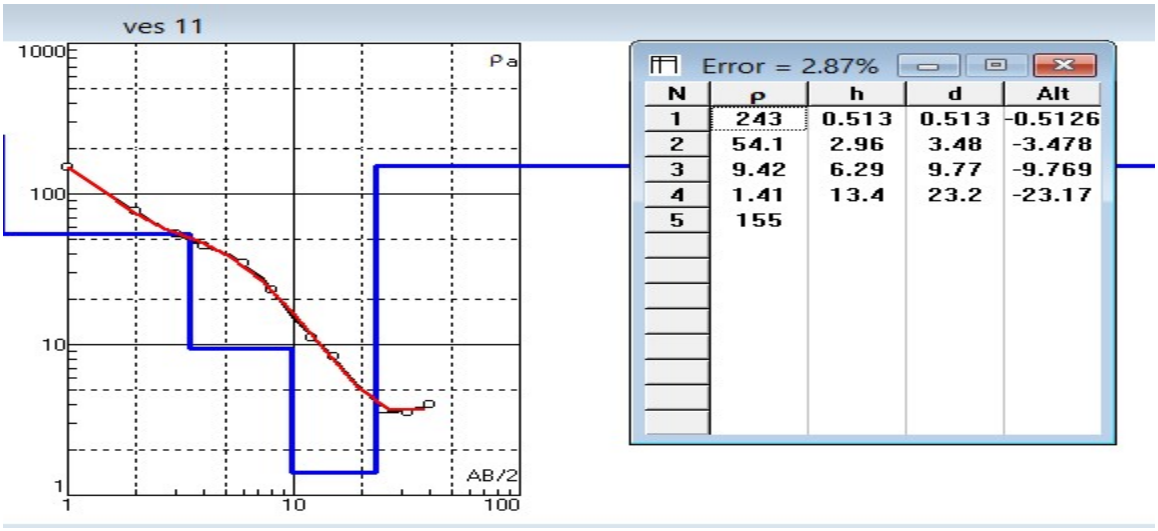


Error = 2.87%

| N | ρ | h | d | Alt |
|---|---|---|---|---|
| 1 | 243 | 0.513 | 0.513 | -0.5126 |
| 2 | 54.1 | 2.96 | 3.48 | -3.478 |
| 3 | 9.42 | 6.29 | 9.77 | -9.769 |
| 4 | 1.41 | 13.4 | 23.2 | -23.17 |
| 5 | 155 | | | |

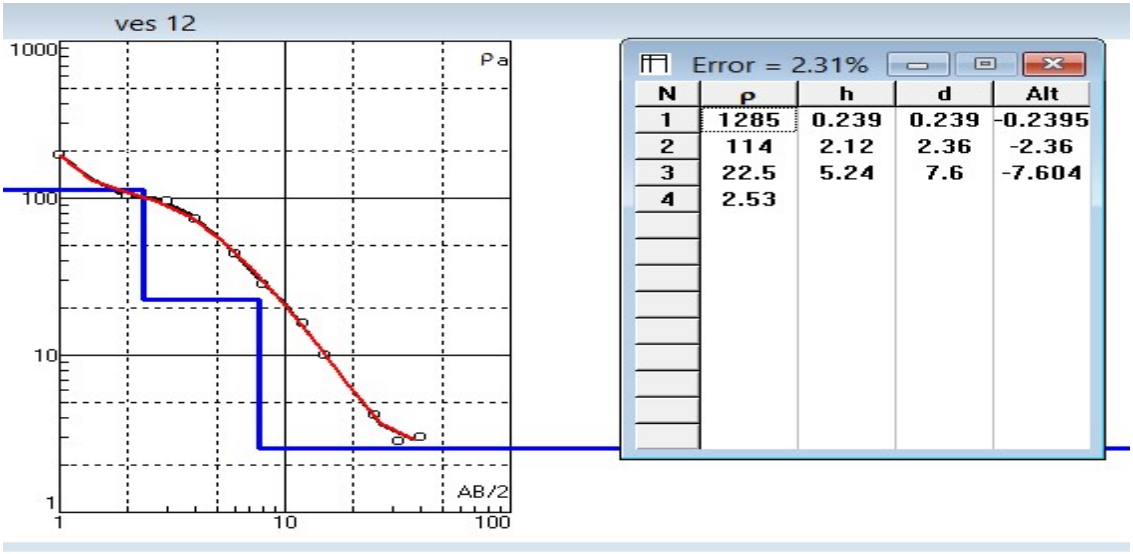


Error = 2.31%

| N | ρ | h | d | Alt |
|---|---|---|---|---|
| 1 | 1285 | 0.239 | 0.239 | -0.2395 |
| 2 | 114 | 2.12 | 2.36 | -2.36 |
| 3 | 22.5 | 5.24 | 7.6 | -7.604 |
| 4 | 2.53 | | | |

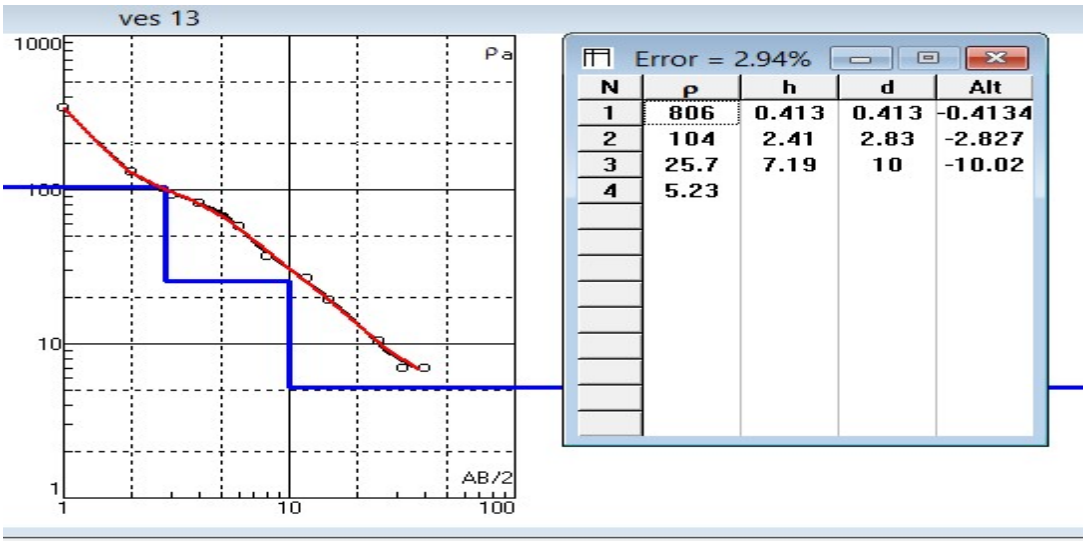


Error = 2.94%

| N | ρ | h | d | Alt |
|---|---|---|---|---|
| 1 | 806 | 0.413 | 0.413 | -0.4134 |
| 2 | 104 | 2.41 | 2.83 | -2.827 |
| 3 | 25.7 | 7.19 | 10 | -10.02 |
| 4 | 5.23 | | | |

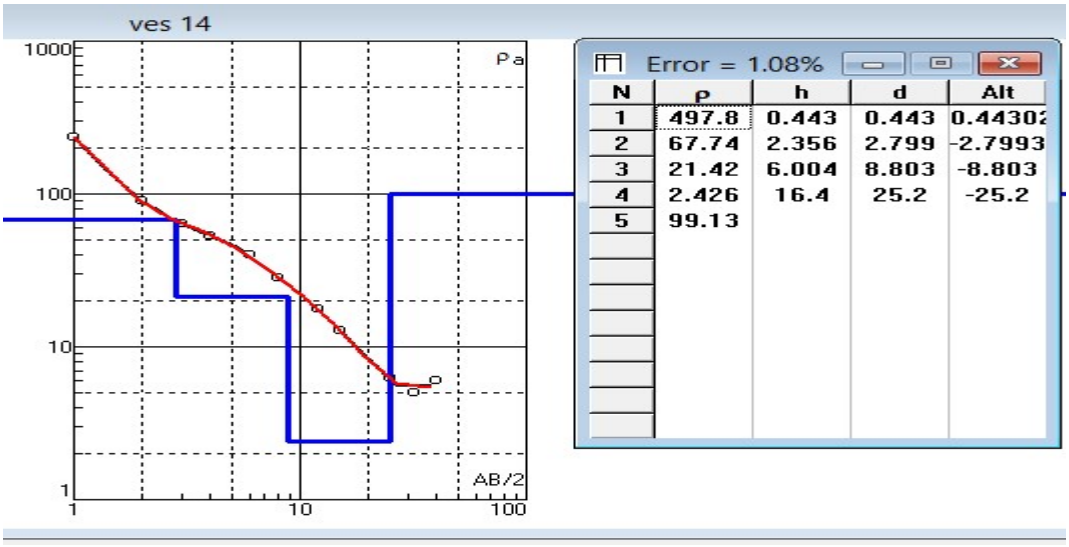


Error = 1.08%

| N | ρ | h | d | Alt |
|---|---|---|---|---|
| 1 | 497.8 | 0.443 | 0.443 | 0.44302 |
| 2 | 67.74 | 2.356 | 2.799 | -2.7993 |
| 3 | 21.42 | 6.004 | 8.803 | -8.803 |
| 4 | 2.426 | 16.4 | 25.2 | -25.2 |
| 5 | 99.13 | | | |

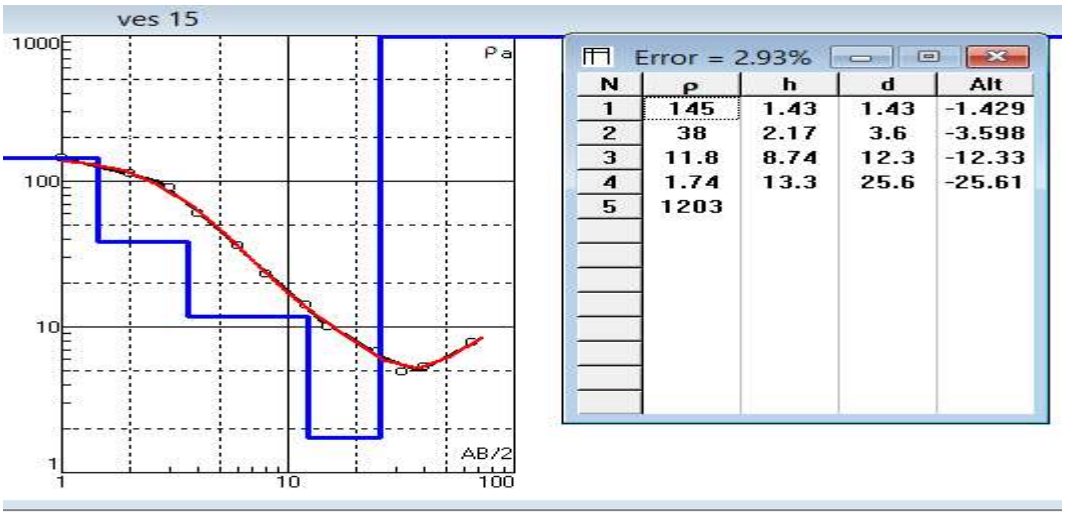


Error = 2.93%

| N | ρ | h | d | Alt |
|---|---|---|---|---|
| 1 | 145 | 1.43 | 1.43 | -1.429 |
| 2 | 38 | 2.17 | 3.6 | -3.598 |
| 3 | 11.8 | 8.74 | 12.3 | -12.33 |
| 4 | 1.74 | 13.3 | 25.6 | -25.61 |
| 5 | 1203 | | | |

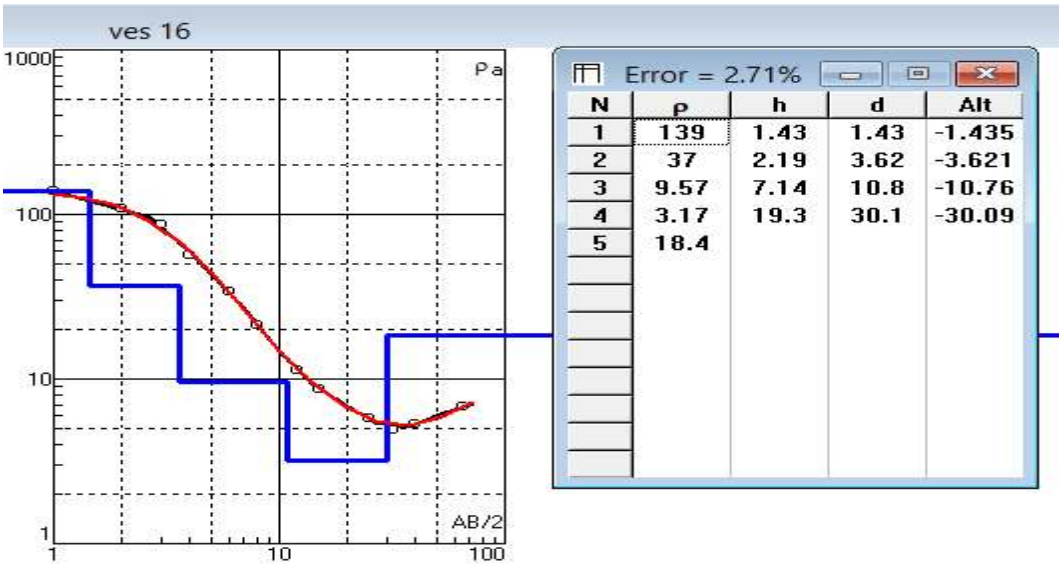


Error = 2.71%

| N | ρ | h | d | Alt |
|---|---|---|---|---|
| 1 | 139 | 1.43 | 1.43 | -1.435 |
| 2 | 37 | 2.19 | 3.62 | -3.621 |
| 3 | 9.57 | 7.14 | 10.8 | -10.76 |
| 4 | 3.17 | 19.3 | 30.1 | -30.09 |
| 5 | 18.4 | | | |

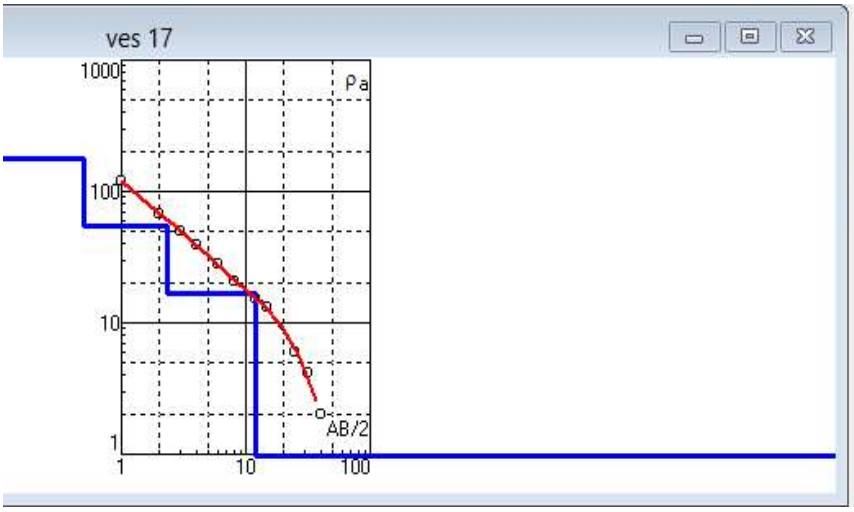


Error = 1.67%

| N | ρ | h | d | Alt |
|---|---|---|---|---|
| 1 | 179.7 | 0.5007 | 0.5007 | 0.5007 |
| 2 | 54.92 | 1.852 | 2.352 | -2.352 |
| 3 | 16.6 | 9.634 | 11.99 | -11.98 |
| 4 | 0.9712 | | | |

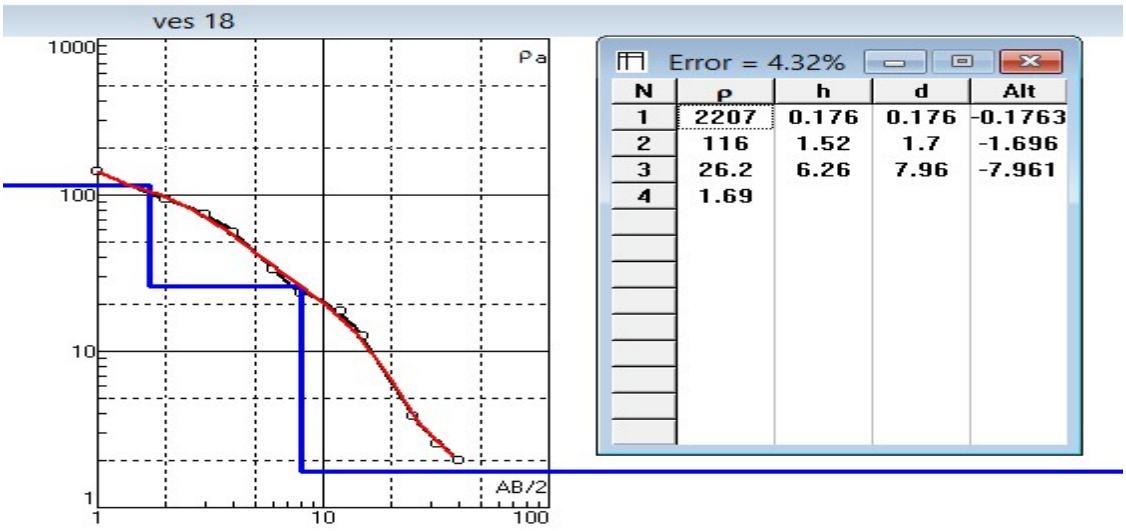


| N | ρ | h | d | Alt |
|---|---|---|---|---|
| 1 | 2207 | 0.176 | 0.176 | -0.1763 |
| 2 | 116 | 1.52 | 1.7 | -1.696 |
| 3 | 26.2 | 6.26 | 7.96 | -7.961 |
| 4 | 1.69 | | | |

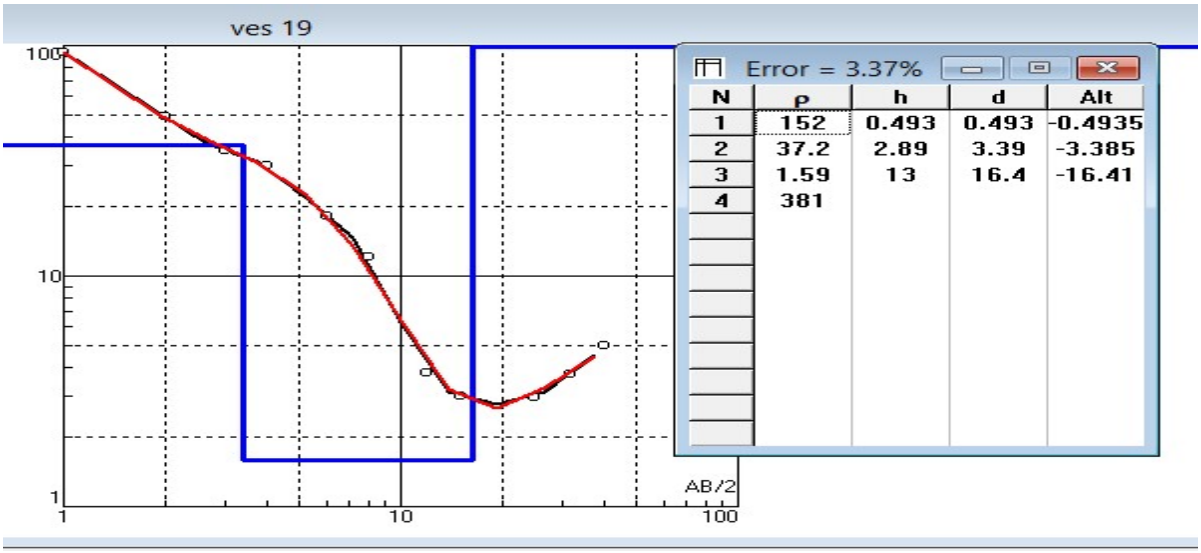


| N | ρ | h | d | Alt |
|---|---|---|---|---|
| 1 | 152 | 0.493 | 0.493 | -0.4935 |
| 2 | 37.2 | 2.89 | 3.39 | -3.385 |
| 3 | 1.59 | 13 | 16.4 | -16.41 |
| 4 | 381 | | | |

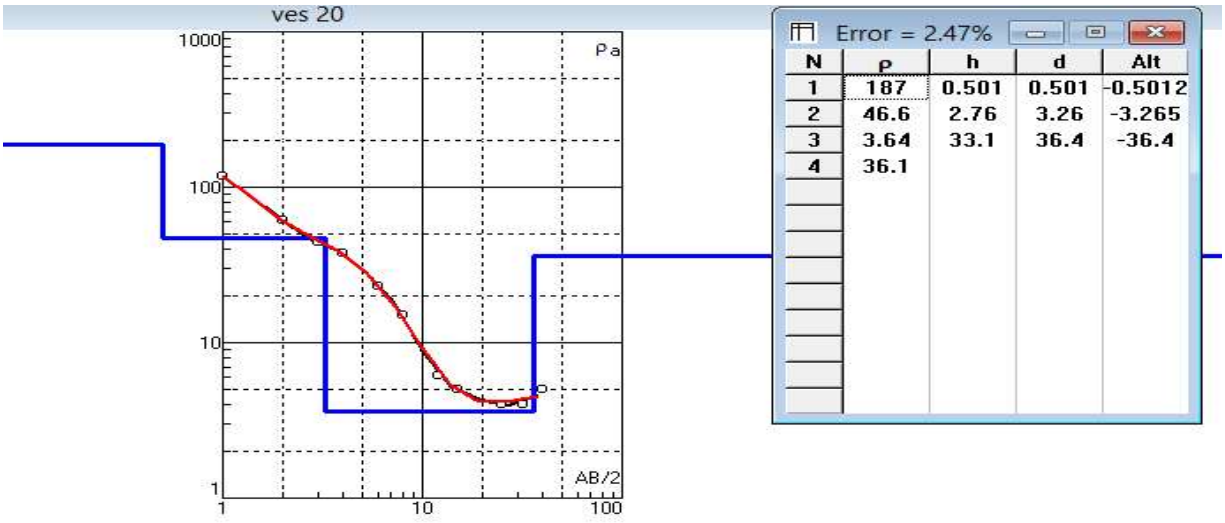


Error = 2.47%

| N | ρ | h | d | Alt |
|---|---|---|---|---|
| 1 | 187 | 0.501 | 0.501 | -0.5012 |
| 2 | 46.6 | 2.76 | 3.26 | -3.265 |
| 3 | 3.64 | 33.1 | 36.4 | -36.4 |
| 4 | 36.1 | | | |

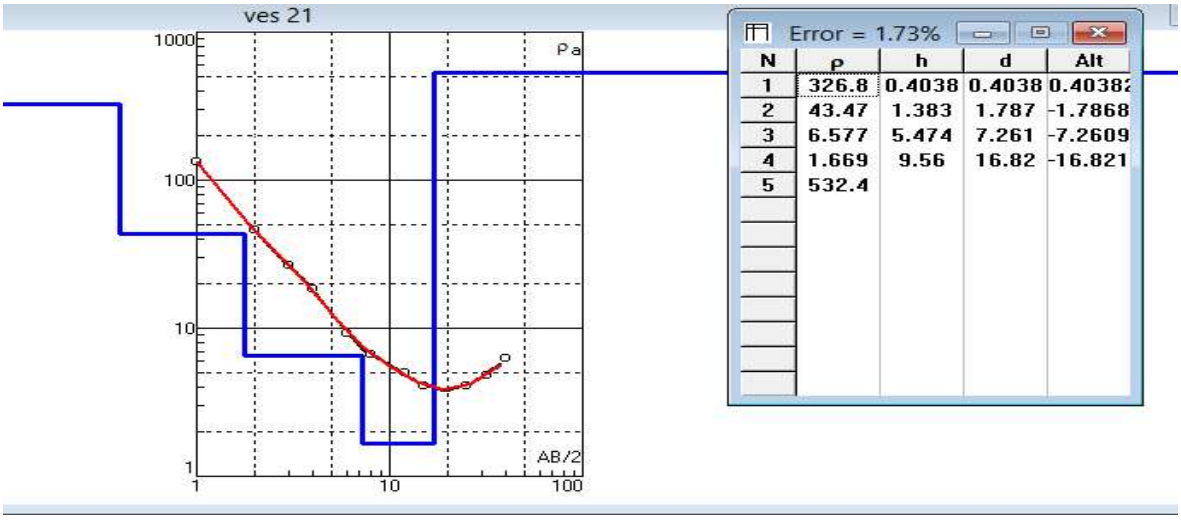


Error = 1.73%

| N | ρ | h | d | Alt |
|---|---|---|---|---|
| 1 | 326.8 | 0.4038 | 0.4038 | 0.40382 |
| 2 | 43.47 | 1.383 | 1.787 | -1.7868 |
| 3 | 6.577 | 5.474 | 7.261 | -7.2609 |
| 4 | 1.669 | 9.56 | 16.82 | -16.821 |
| 5 | 532.4 | | | |

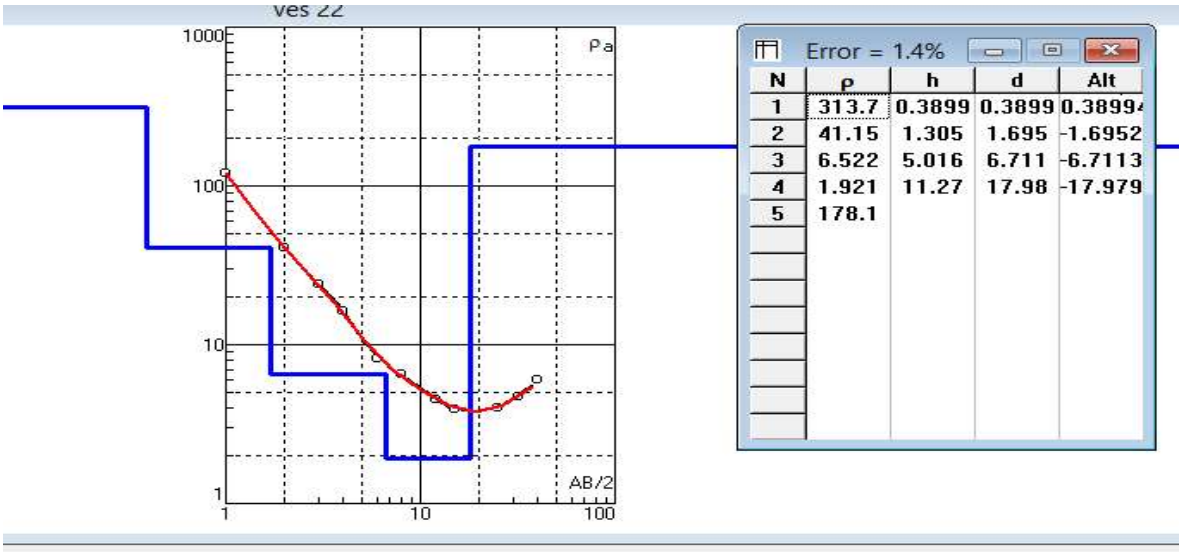


Error = 1.4%

| N | ρ | h | d | Alt |
|---|---|---|---|---|
| 1 | 313.7 | 0.3899 | 0.3899 | 0.3899 |
| 2 | 41.15 | 1.305 | 1.695 | -1.6952 |
| 3 | 6.522 | 5.016 | 6.711 | -6.7113 |
| 4 | 1.921 | 11.27 | 17.98 | -17.979 |
| 5 | 178.1 | | | |

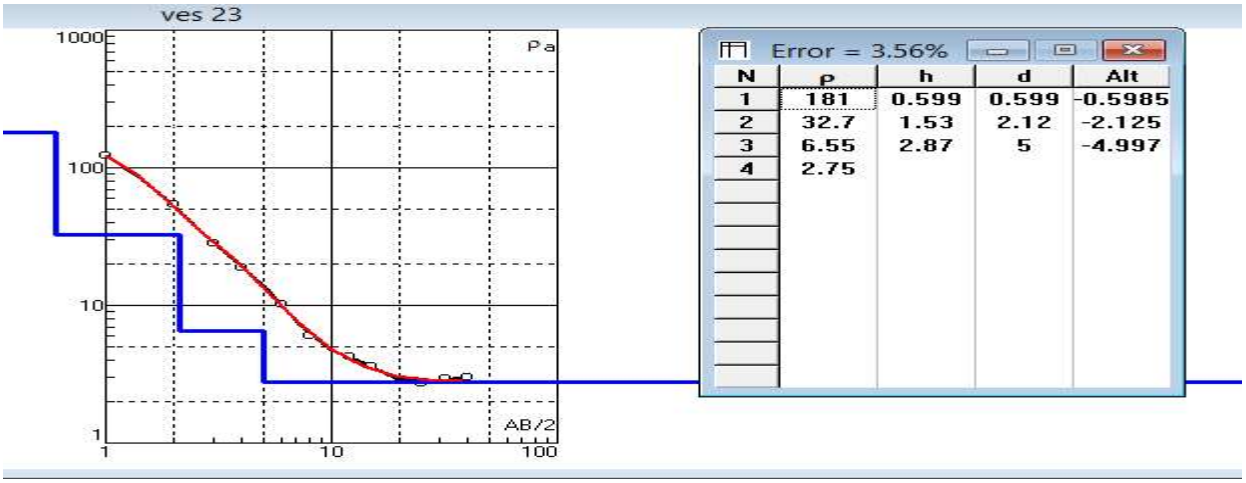


Error = 3.56%

| N | ρ | h | d | Alt |
|---|---|---|---|---|
| 1 | 181 | 0.599 | 0.599 | -0.5985 |
| 2 | 32.7 | 1.53 | 2.12 | -2.125 |
| 3 | 6.55 | 2.87 | 5 | -4.997 |
| 4 | 2.75 | | | |

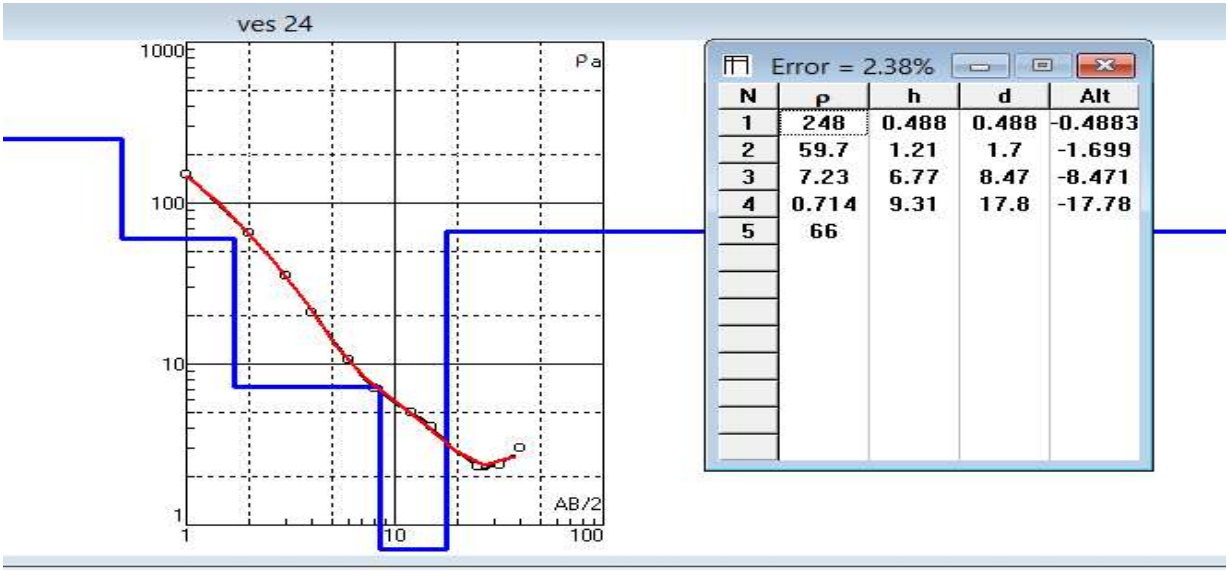


Error = 2.38%

| N | ρ | h | d | Alt |
|---|---|---|---|---|
| 1 | 248 | 0.488 | 0.488 | -0.4883 |
| 2 | 59.7 | 1.21 | 1.7 | -1.699 |
| 3 | 7.23 | 6.77 | 8.47 | -8.471 |
| 4 | 0.714 | 9.31 | 17.8 | -17.78 |
| 5 | 66 | | | |

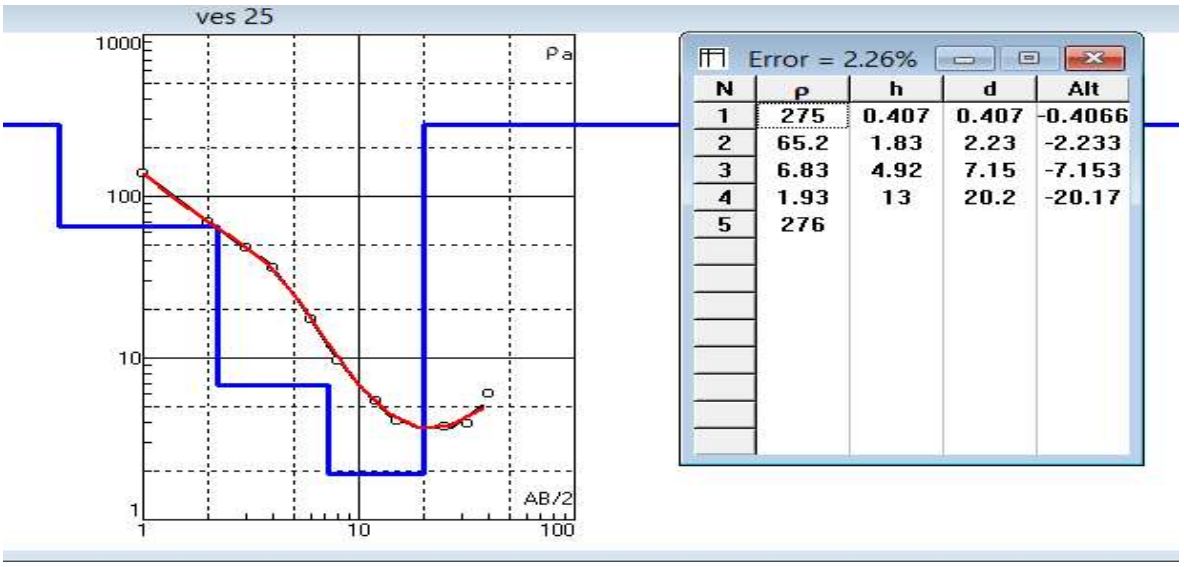
ves 25
1000
100
10
1
ρa
AB/2
1
10
100
Error = 2.26%
N ρ h d Alt
1 275 0.407 0.407 -0.4066
2 65.2 1.83 2.23 -2.233
3 6.83 4.92 7.15 -7.153
4 1.93 13 20.2 -20.17
5 276

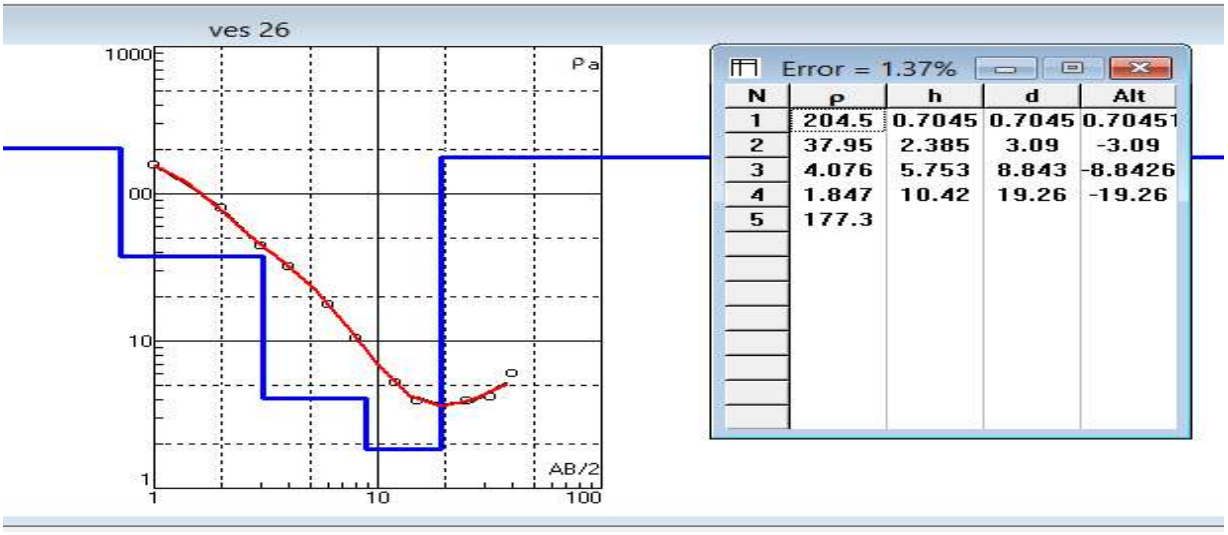
ves 26
1000
00
10
1
ρa
AB/2
1
10
100
Error = 1.37%
N ρ h d Alt
1 204.5 0.7045 0.7045 0.70451
2 37.95 2.385 3.09 -3.09
3 4.076 5.753 8.843 -8.8426
4 1.847 10.42 19.26 -19.26
5 177.3

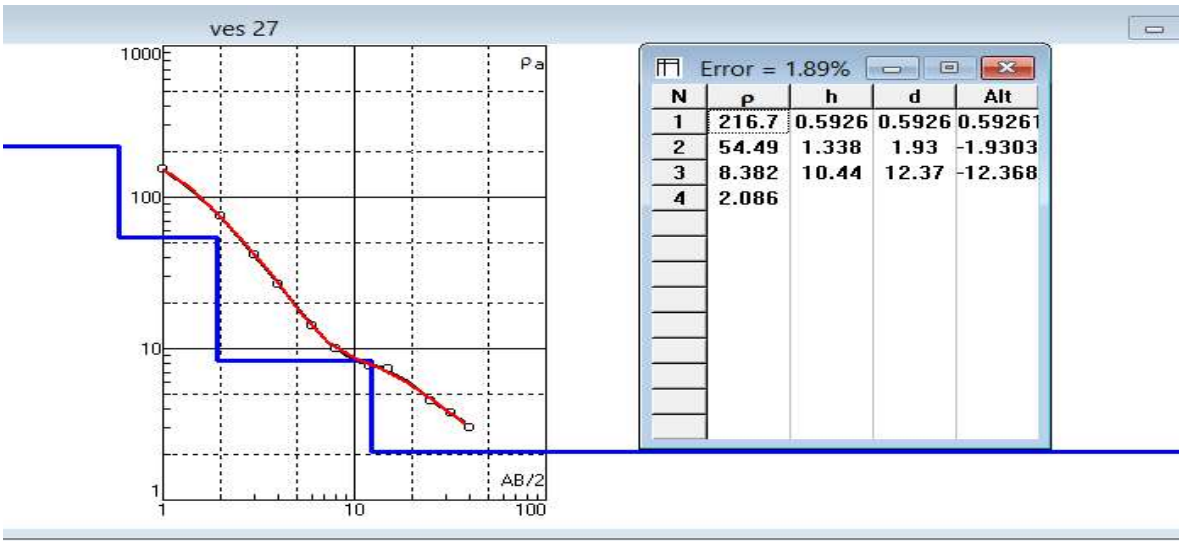


Error = 1.89%

| N | ρ | h | d | Alt |
|---|---|---|---|---|
| 1 | 216.7 | 0.5926 | 0.5926 | 0.59261 |
| 2 | 54.49 | 1.338 | 1.93 | -1.9303 |
| 3 | 8.382 | 10.44 | 12.37 | -12.368 |
| 4 | 2.086 | | | |

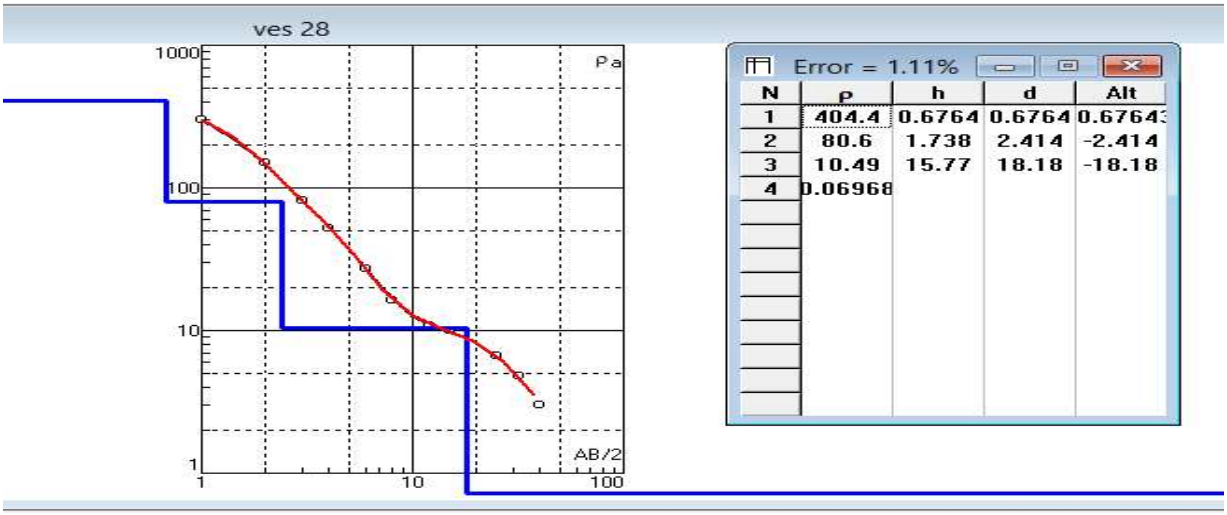


Error = 1.11%

| N | ρ | h | d | Alt |
|---|---|---|---|---|
| 1 | 404.4 | 0.6764 | 0.6764 | 0.67643 |
| 2 | 80.6 | 1.738 | 2.414 | -2.414 |
| 3 | 10.49 | 15.77 | 18.18 | -18.18 |
| 4 | 0.06968 | | | |

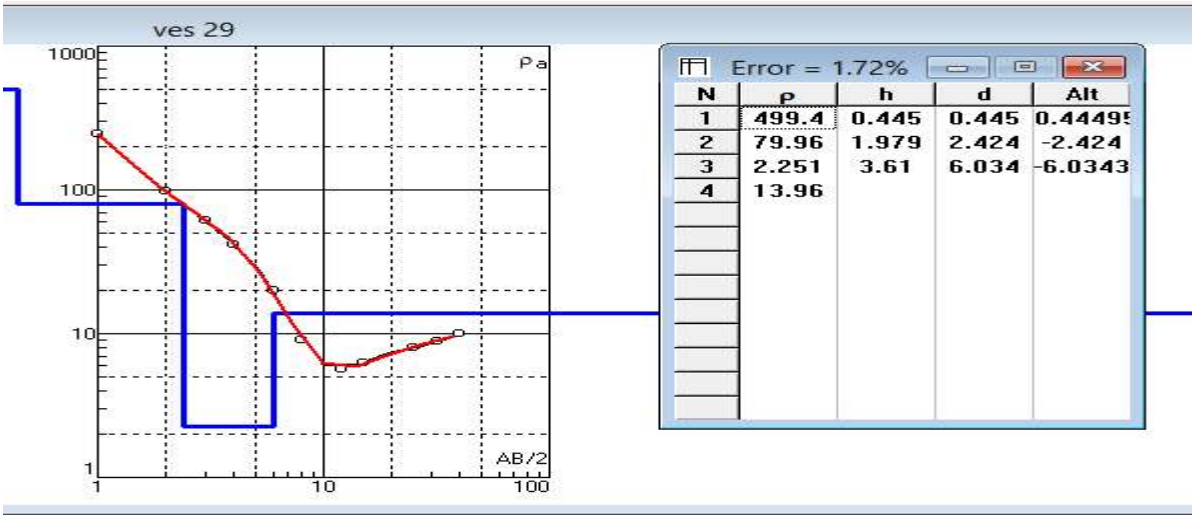


Error = 1.72%

| N | ρ | h | d | Alt |
|---|---|---|---|---|
| 1 | 499.4 | 0.445 | 0.445 | 0.44495 |
| 2 | 79.96 | 1.979 | 2.424 | -2.424 |
| 3 | 2.251 | 3.61 | 6.034 | -6.0343 |
| 4 | 13.96 | | | |

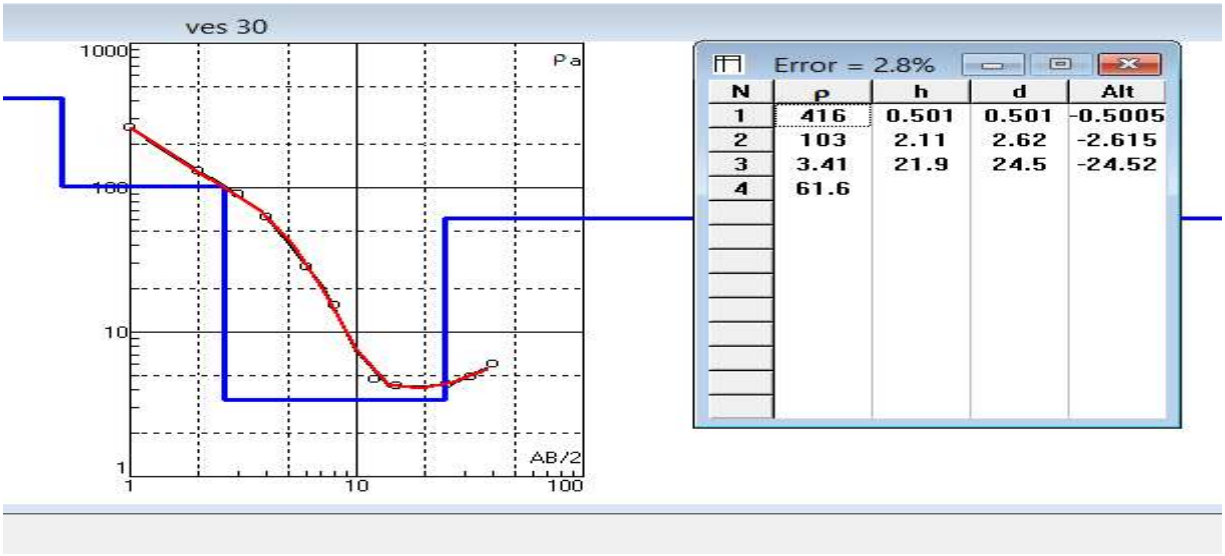


| N | ρ | h | d | Alt |
|---|---|---|---|---|
| 1 | 416 | 0.501 | 0.501 | -0.5005 |
| 2 | 103 | 2.11 | 2.62 | -2.615 |
| 3 | 3.41 | 21.9 | 24.5 | -24.52 |
| 4 | 61.6 | | | |

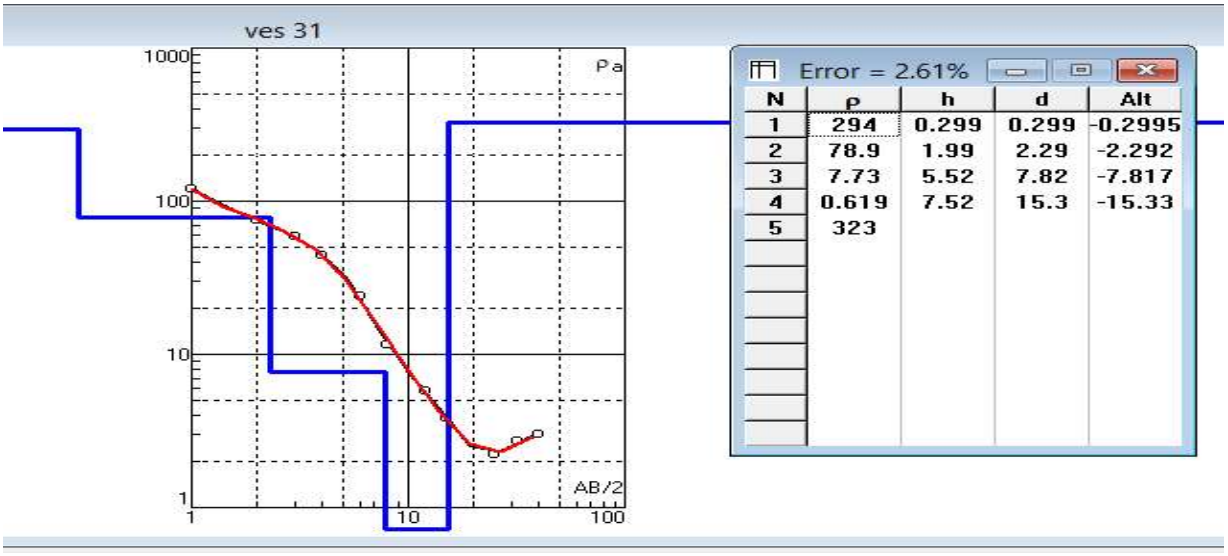


| N | ρ | h | d | Alt |
|---|---|---|---|---|
| 1 | 294 | 0.299 | 0.299 | -0.2995 |
| 2 | 78.9 | 1.99 | 2.29 | -2.292 |
| 3 | 7.73 | 5.52 | 7.82 | -7.817 |
| 4 | 0.619 | 7.52 | 15.3 | -15.33 |
| 5 | 323 | | | |

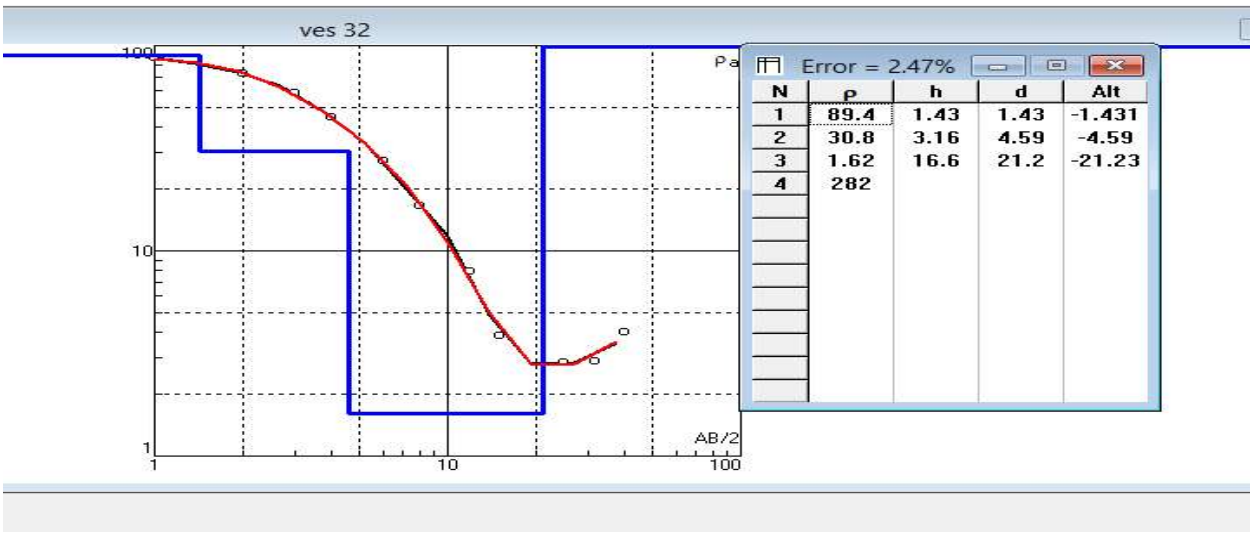


Error = 2.47%

| N | ρ | h | d | Alt |
|---|---|---|---|---|
| 1 | 89.4 | 1.43 | 1.43 | -1.431 |
| 2 | 30.8 | 3.16 | 4.59 | -4.59 |
| 3 | 1.62 | 16.6 | 21.2 | -21.23 |
| 4 | 282 | | | |

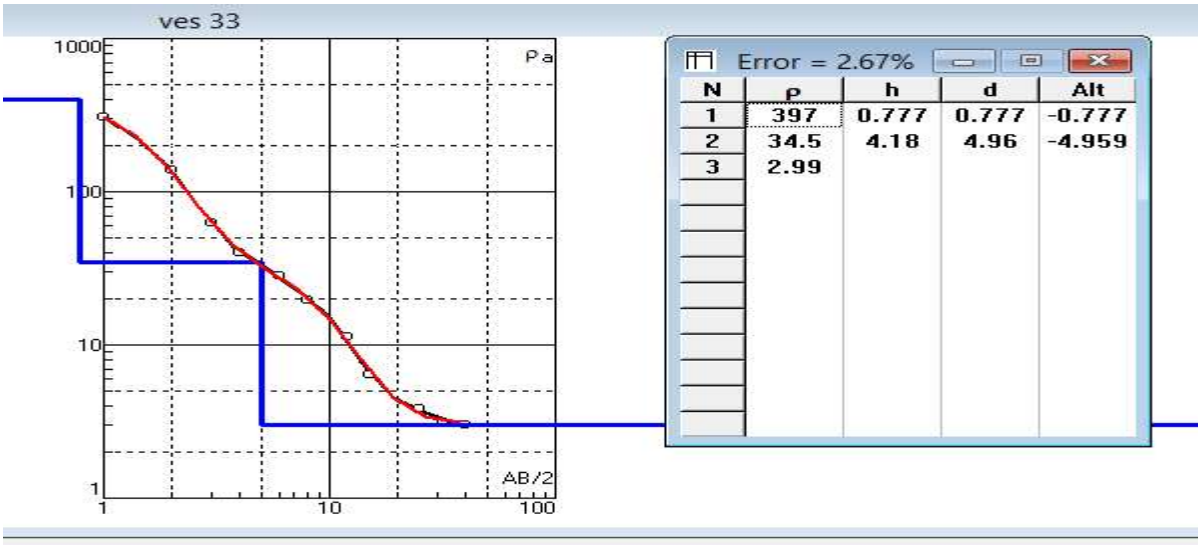


Error = 2.67%

| N | ρ | h | d | Alt |
|---|---|---|---|---|
| 1 | 397 | 0.777 | 0.777 | -0.777 |
| 2 | 34.5 | 4.18 | 4.96 | -4.959 |
| 3 | 2.99 | | | |

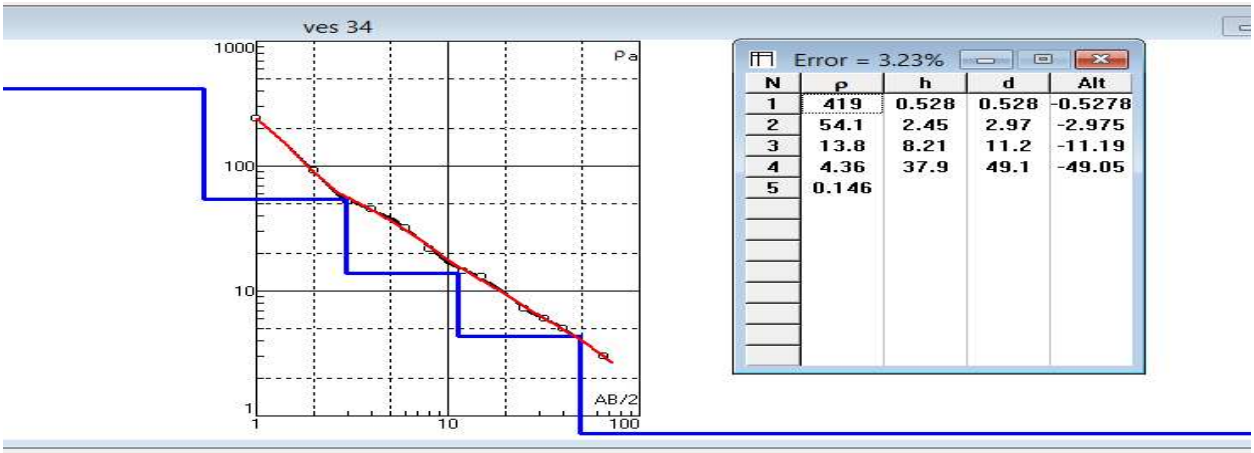


Error = 3.23%

| N | ρ | h | d | Alt |
|---|---|---|---|---|
| 1 | 419 | 0.528 | 0.528 | -0.5278 |
| 2 | 54.1 | 2.45 | 2.97 | -2.975 |
| 3 | 13.8 | 8.21 | 11.2 | -11.19 |
| 4 | 4.36 | 37.9 | 49.1 | -49.05 |
| 5 | 0.146 | | | |

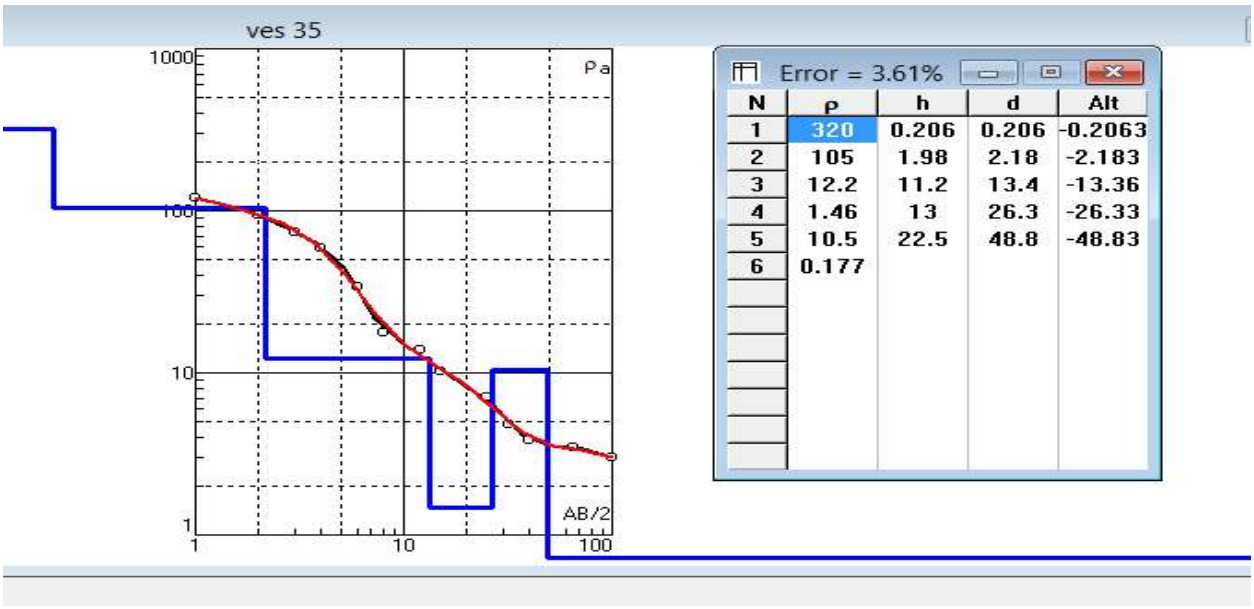


Error = 3.61%

| N | ρ | h | d | Alt |
|---|---|---|---|---|
| 1 | 320 | 0.206 | 0.206 | -0.2063 |
| 2 | 105 | 1.98 | 2.18 | -2.183 |
| 3 | 12.2 | 11.2 | 13.4 | -13.36 |
| 4 | 1.46 | 13 | 26.3 | -26.33 |
| 5 | 10.5 | 22.5 | 48.8 | -48.83 |
| 6 | 0.177 | | | |

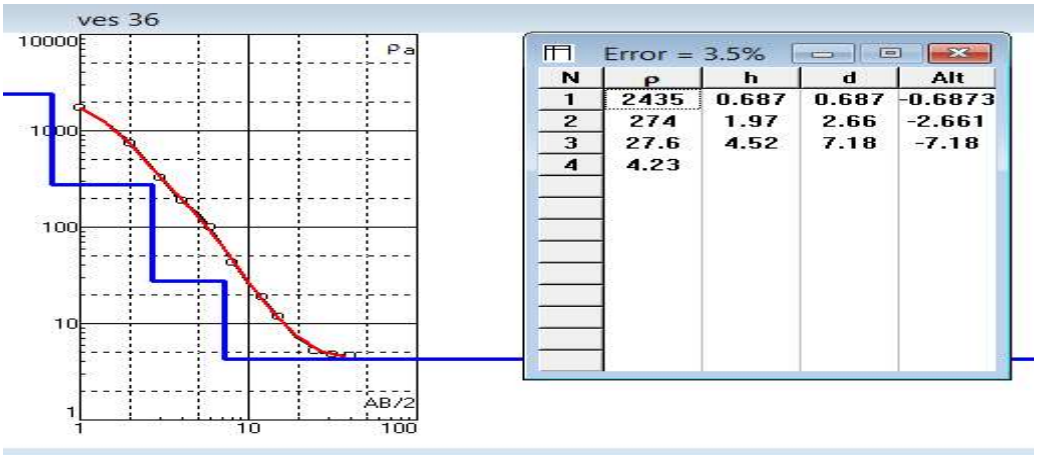


Error = 3.5%

| N | ρ | h | d | Alt |
|---|---|---|---|---|
| 1 | 2435 | 0.687 | 0.687 | -0.6873 |
| 2 | 274 | 1.97 | 2.66 | -2.661 |
| 3 | 27.6 | 4.52 | 7.18 | -7.18 |
| 4 | 4.23 | | | |

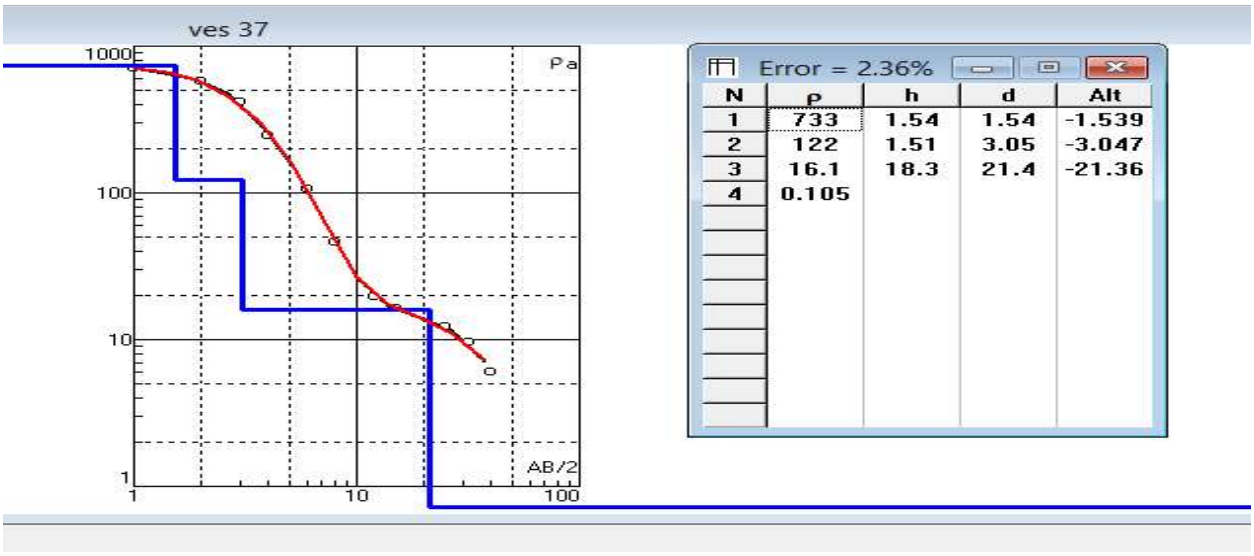


Error = 2.36%

| N | ρ | h | d | Alt |
|---|---|---|---|---|
| 1 | 733 | 1.54 | 1.54 | -1.539 |
| 2 | 122 | 1.51 | 3.05 | -3.047 |
| 3 | 16.1 | 18.3 | 21.4 | -21.36 |
| 4 | 0.105 | | | |

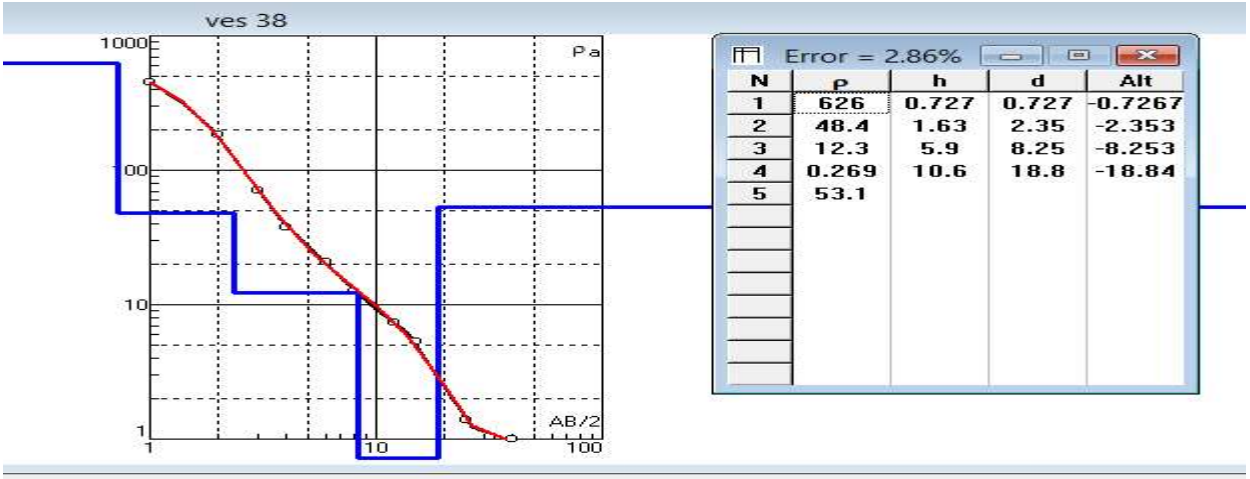


Error = 2.86%

| N | ρ | h | d | Alt |
|---|---|---|---|---|
| 1 | 626 | 0.727 | 0.727 | -0.7267 |
| 2 | 48.4 | 1.63 | 2.35 | -2.353 |
| 3 | 12.3 | 5.9 | 8.25 | -8.253 |
| 4 | 0.269 | 10.6 | 18.8 | -18.84 |
| 5 | 53.1 | | | |

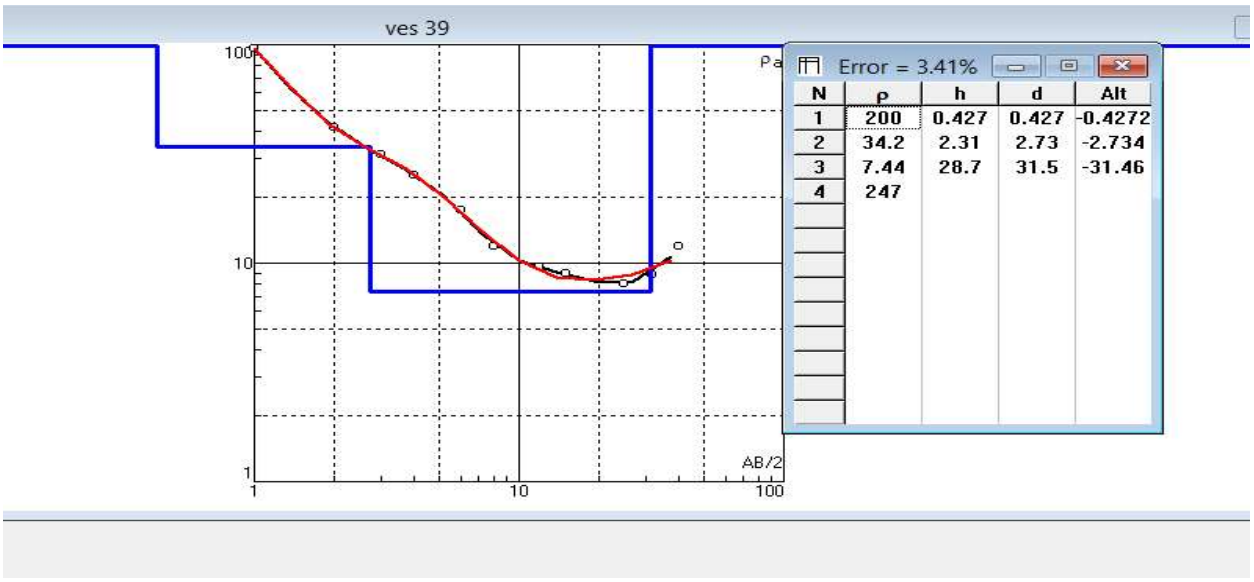
ves 39
Pa
100
10
1
1
10
100
AB/2
Error = 3.41%
N ρ h d Alt
1 200 0.427 0.427 -0.4272
2 34.2 2.31 2.73 -2.734
3 7.44 28.7 31.5 -31.46
4 247

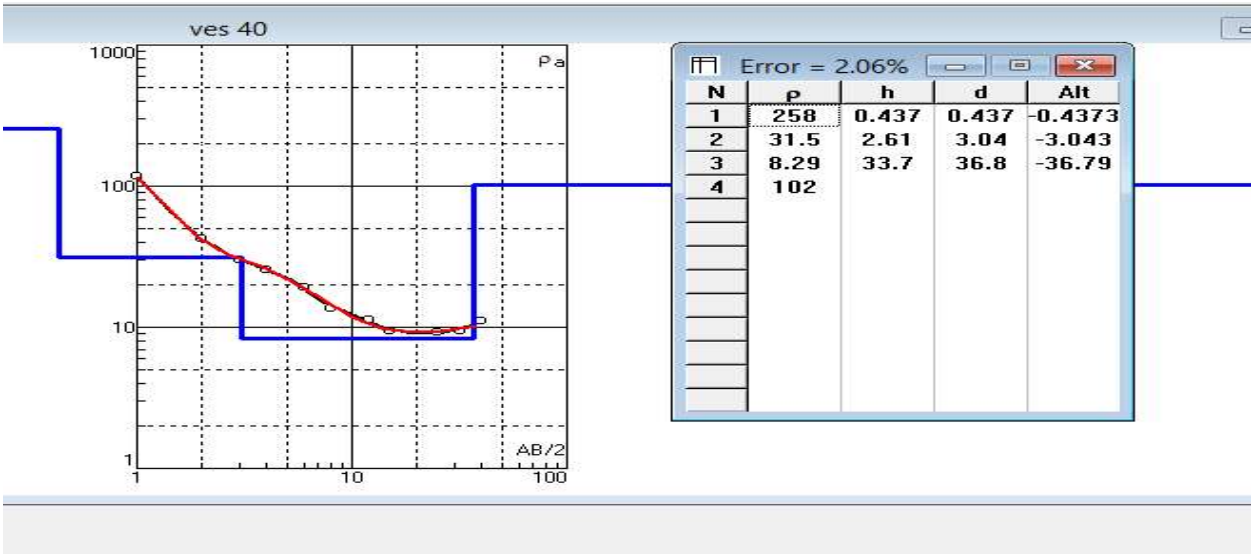
ves 40
Pa
1000
100
10
1
1
10
100
AB/2
Error = 2.06%
N ρ h d Alt
1 258 0.437 0.437 -0.4373
2 31.5 2.61 3.04 -3.043
3 8.29 33.7 36.8 -36.79
4 102

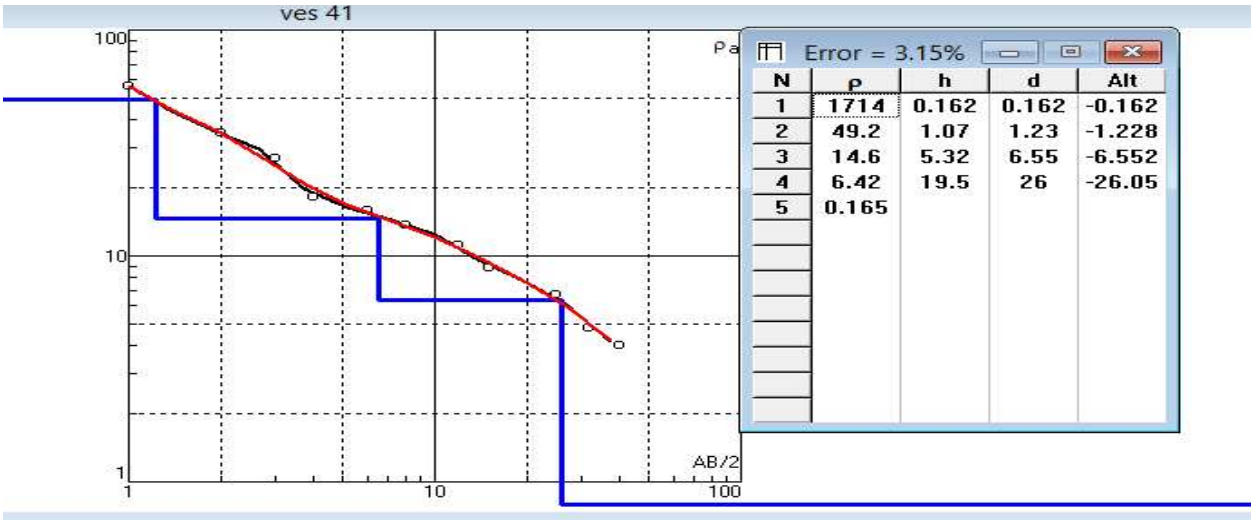


Error = 3.15%

| N | ρ | h | d | Alt |
|---|---|---|---|---|
| 1 | 1714 | 0.162 | 0.162 | -0.162 |
| 2 | 49.2 | 1.07 | 1.23 | -1.228 |
| 3 | 14.6 | 5.32 | 6.55 | -6.552 |
| 4 | 6.42 | 19.5 | 26 | -26.05 |
| 5 | 0.165 | | | |

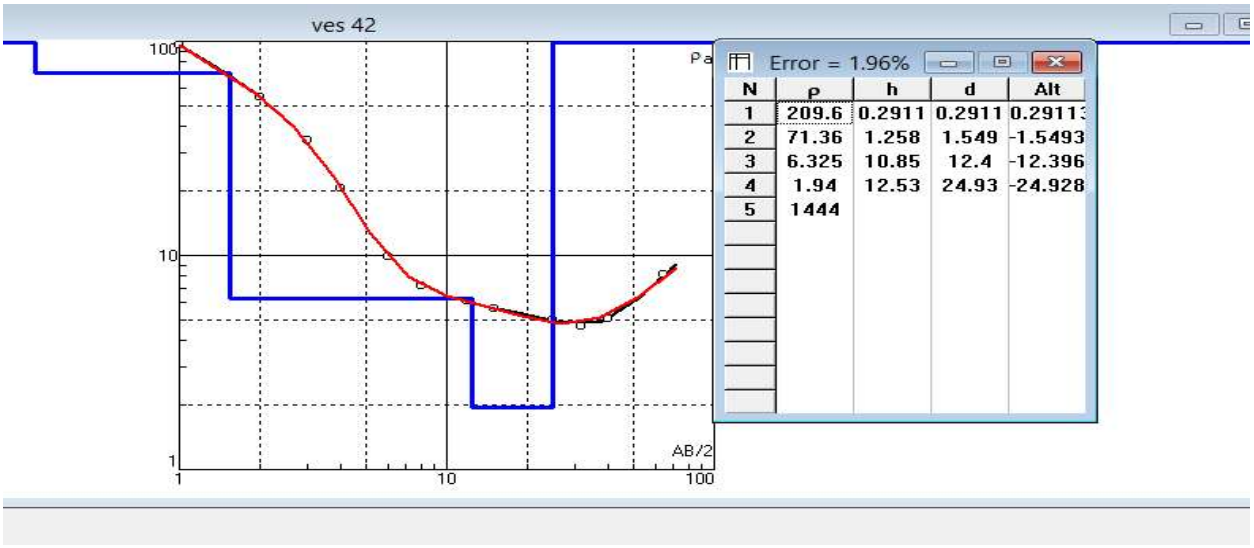


Error = 1.96%

| N | ρ | h | d | Alt |
|---|---|---|---|---|
| 1 | 209.6 | 0.2911 | 0.2911 | 0.2911 |
| 2 | 71.36 | 1.258 | 1.549 | -1.5493 |
| 3 | 6.325 | 10.85 | 12.4 | -12.396 |
| 4 | 1.94 | 12.53 | 24.93 | -24.928 |
| 5 | 1444 | | | |